

Cellular and molecular mechanisms of zebrafish heart regeneration

D I S S E R T A T I O N

zur Erlangung des akademischen Grades

**Doctor rerum naturalium
(Dr. rer. nat.)**

vorgelegt

der Fakultät Mathematik und Naturwissenschaften
der Technischen Universität Dresden

von

Dipl. - Humanbiol. Kristin Schnabel

geboren am 25. Juli 1981 in Forst-Lausitz, Deutschland

Gutachter: Prof. Dr. Michael Brand, Technische Universität Dresden
Prof. Dr. Evelin Schröck, Technische Universität Dresden

Eingereicht am: 22. Juni 2011

Tag der Verteidigung: 09. September 2011

Table of contents

Summary.....	7
Index of Figures and Tables.....	9
Abbreviations.....	12

Introduction

1.1 Heart morphology in zebrafish and mammals.....	14
1.2 Vertebrate heart development.....	17
1.3 Cardiac injury in zebrafish and mammals – different reactions to keep and improve cardiac function.....	19
1.3.1 Heart regeneration in zebrafish.....	19
1.3.2 Mammalian myocardial infarction	23
1.3.2.1 The main response to mammalian heart injury – cardiac hypertrophy.....	23
1.3.2.1 Capacity for “real” cardiac regeneration in mammals.....	24
1.4 The canonical Wnt/ β -catenin signaling pathway and Sox9 transcription factor - potentially involved in zebrafish heart regeneration.....	26
1.4.1 Canonical Wnt signaling.....	26
1.4.1.1 The role of canonical Wnt signaling in heart development and cardiac specification.....	27
1.4.1.2 The role of Wnt signaling in pathological cardiac hypertrophy.....	28
1.4.2 Sox9 transcription factor.....	29
1.4.2.1 The role of Sox9 in heart development	31
1.5 Aims of the thesis.....	32

2.1 Material

2.1.1	<i>Reagents and buffers</i>	33
2.1.2	<i>Chemicals</i>	34
2.1.3	<i>Antibodies</i>	34
2.1.4	<i>Transgenic fish lines</i>	35
2.1.5	<i>Mutant fish lines</i>	35
2.1.6	<i>Primer sequences for identification of jellyfish^{tw3} (sox9a+/- mutant fish)</i>	35
2.1.7	<i>Constructs for generation of mRNA used for injections into embryos</i>	36
2.1.8	<i>Constructs for generation of in-situ hybridization probes</i>	36
2.1.9	<i>Molecular biology kits</i>	37
2.1.10	<i>Technical equipment</i>	37
2.1.11	<i>Microscopes</i>	38

2.2 Methods

2.2.1	<i>Fish maintenance</i>	39
2.2.2	<i>Preparation of poly (A)-mRNA for injection into zebrafish embryos</i>	39
2.2.3	<i>Injection of mRNA or DNA into zebrafish embryos</i>	40
2.2.4	<i>Heat-shock treatment of zebrafish embryos and adult fish...</i>	
2.2.5	<i>Identification of heterozygous mutant masterblind (mbl) and sox9a-/- fish via incrosses and/or PCR (mutant Sox9a+/- fish)</i>	41
2.2.6	<i>DNA extraction from fin clips</i>	42
2.2.7	<i>Ventricular heart resection / heart amputation</i>	43
2.2.7	<i>Cryoinjury at zebrafish hearts</i>	43
2.2.8	<i>Control hearts</i>	44
2.2.9	<i>Intraperitoneal BrdU injection</i>	44

2.2.10	<i>Heart extraction / Head harvest</i>	44
2.2.11	<i>Fixation and processing for sectioning</i>	45
2.2.12	<i>Acid Fuchsin Orange G staining (AFOG) staining</i>	45
2.2.13	<i>Production of Dioxygenin-labeled antisense riboprobes for in situ hybridization</i>	46
2.2.14	<i>RNA in situ hybridization on whole-mount hearts</i>	46
2.2.15	<i>RNA in situ hybridization on heart sections</i>	47
2.2.16	<i>Antibody staining on heart sections</i>	48
2.2.16.1	<i>Sox9 and PCNA antibody staining</i>	49
2.2.16.2	<i>BrdU antibody staining</i>	50
2.2.16.3	<i>Detection of apoptosis</i>	50
2.2.17	<i>Electron microscopy and toluidin blue staining</i>	50
2.2.18	<i>Imaging</i>	51
2.2.19	<i>Total RNA production from embryos and hearts</i>	52
2.2.20	<i>cDNA synthesis</i>	53
2.2.21	<i>quantitative PCR</i>	53
2.2.22	<i>Generation of constructs</i>	54
2.2.23	<i>Microarray expression analysis</i>	54
2.2.23.1	<i>Annotation of the microarray</i>	54
2.2.23.2	<i>Functional annotation of the microarray</i>	55
2.2.23.3	<i>Microarray processing and data analysis</i>	55
2.2.23.4	<i>Statistical analysis of functional and expression annotation based on Panther database</i>	56

3. Results

3.1.1	<i>Is Wnt/β-catenin signaling active during zebrafish heart regeneration?</i>	58
3.1.2	<i>Overactivation or inhibition Wnt/β-catenin signaling</i>	

did not influence heart regeneration.....	63
3.1.2.1 The tools.....	63
3.1.2.2 Does Wnt signaling influence early events in heart regeneration?	65
3.1.2.3 Microarray: Which genes are regulated by Wnt/ β -catenin signaling during heart regeneration? Are Wnt target genes expressed during heart regeneration?.....	68
3.1.2.4 Does Wnt signaling influence proliferation during heart regeneration?	72
3.1.2.5 Long term loss of function and gain of function of canonical Wnt signaling does not influence heart regeneration.....	77
3.1.2.5.1 Is Wnt/ β -catenin signaling required for morphological regeneration and/or wound resolution?	78
3.2.1 The expression pattern and functional role of Sox9a in zebrafish heart regeneration.....	83
3.2.1.1 Analysis of the temporal and spatial Sox9 expression pattern in the injured heart.....	83
3.2.1.2 Which cell types express Sox9a?	88
3.2.2 Is Sox9a necessary for zebrafish heart regeneration?.....	94
3.2.2.1 Is Sox9a required for morphological regeneration and/or wound resolution?	94
3.2.2.2 Interfering with Sox9a-dependent gene expression – consequences on adult heart regeneration zebrafish.....	101
3.3.1 Alternative heart infarct model in zebrafish.....	104
3.3.1.1 The zebrafish heart regenerates after cryoinjury.....	104

3.3.1.2 Characterization of the cellular damage caused by cryoinjury.....	107
3.3.1.3 Organ-wide response of the epicardium to cryoinjury.....	112
3.3.1.4 Induction of cardiomyocyte proliferation after cryoinjury.....	115
3.3.1.5 Sox9 induction after cryoinjury.....	116
3.4.1 Gene expression profiling during zebrafish heart Regeneration.....	118
3.4.1.1 FGF signaling targets and Epithelial - to - mesenchymal transition are presumably activated early during heart regeneration as indicated by the microarray results	123
Discussion	
4.1 No evidence for a role of Wnt/ β -catenin signaling in zebrafish heart regeneration.....	126
4.1.1 Target genes of the Wnt/ β -catenin pathway are not detectable in the first days after ventricular resection.....	126
4.1.2 Overexpression of Wnt/ β -catenin pathway inhibitors has no influence on gene expression in early heart regeneration.....	127
4.1.3 Wnt/ β -catenin signaling does not influence cardiomyocyte proliferation.....	129
4.1.4 Wnt/ β -catenin signaling does not influence the overall extent of heart regeneration.....	130
4.1.5 Wnt/ β -catenin signaling influences mammalian and zebrafish heart development and mammalian cardiac hypertrophy – but does not influence zebrafish heart regeneration.....	131

4.2 Sox9a in zebrafish heart regeneration.....	133
4.2.1 The transcription factor Sox9a is expressed in epicardial, myocardial and endocardial/endothelial cells during early stages of cardiac regeneration.....	133
4.2.2 Sox9a is important for endothelial and myocardial regeneration.....	135
4.2.3 Possible role of Sox9a during heart regeneration	137
4.3 Cryoinjury – an alternative heart injury model in zebrafish.....	139
4.3.1 Epicardium and myocardium respond similarly to cryoinjury and ventricular resection.....	139
4.4 Gene expression profiling of zebrafish heart regeneration verifies known and identifies novel regulated genes.....	141
4.5 General conclusion.....	144
References.....	146
List of Publications.....	158
Erklärung	
Acknowledgements	

Summary

Humans can, if they survived a cardiac injury such as heart infarction, heal this cardiac injury only by scarring and with minimal regeneration of some cardiac cells. Zebrafish, however, can fully regenerate cardiac tissue after surgical resection of up to 20% of the ventricle. Regenerating tissue includes cells of the three cardiac layers, i.e. myocardium, epicardium and endocardium. Thus, zebrafish, with its ability to regenerate damaged heart and as a model enabling genetic manipulations, provides the possibility to study cellular and molecular mechanisms of heart regeneration. Understanding these mechanisms may help develop new therapeutic approaches to improve the situation after a heart injury in humans. Since molecular mechanisms regulating heart regeneration are so far largely unknown, I aimed to identify and analyze molecular signals that are important for cardiac regeneration in zebrafish.

Molecular signals that are crucial during heart development have been suggested to be reactivated during cardiac regeneration. Since Wnt/ β -catenin signaling is crucial for vertebrate heart development, it is likely to be important for zebrafish cardiac regeneration as well.

First, I focused on the functional role of Wnt/ β -catenin signaling in cardiac regeneration mainly by using transgenic fish lines that allow inducible activation or inhibition of the pathway. By using in situ hybridization and expression profiling, I tested whether endogenous Wnt/ β -catenin target genes are detectable in regenerating hearts and screened for activity of the β -catenin responsive reporter in TOPdGFP transgenic fish (Tg(*TOP:GFP*)^{w25}) after ventricular resection. I could not identify endogenous Wnt/ β -catenin targets during the early phase of regeneration up to 7 days post amputation (dpa) using oligoexpression microarrays or in situ hybridization. An injury specific activation of the β -catenin responsive TOPdGFP reporter was not detectable either, suggesting that Wnt/ β -catenin signaling is not active during this early phase of regeneration. The manipulation of Wnt/ β -catenin signaling using transgenic fish lines did not influence cell proliferation or the overall extent of zebrafish heart regeneration. These results suggested that Wnt/ β -catenin signaling has no functional role during entire zebrafish heart regeneration.

Second, I found the transcription factor Sox9a to be upregulated after ventricular resection during the early phase of heart regeneration. Using transgenic reporter fish lines, I detected

Sox9a expression in cardiomyocytes and endothelial cells, part of which were proliferative. Furthermore Sox9a was expressed in some cells of the epicardial layer that activated the expression of developmental genes in the entire heart in response to injury. These results indicated that Sox9a is expressed in cells that were actively involved in the regenerative response.

To gain insight into the functional role of Sox9a, I generated a transgenic fish line where a repressor construct is inducibly expressed, which then interferes with Sox9a target gene transcription. I detected a significant reduction in myocardial and endothelial regeneration after induction of the repressor. These results suggested that Sox9a function is important for regeneration of endothelial and myocardial cells after heart injury.

Third, using oligoexpression microarrays, I performed systematic gene expression profiling of the zebrafish heart regeneration within the first 2 weeks following amputation. I found that known genes, which have previously been shown to be strongly expressed during heart regeneration, as well as novel genes were upregulated after ventricular resection. Some of these genes have been implicated in vertebrate heart development, supporting the idea that cardiac developmental genes are reactivated during heart regeneration. Hence, these results reveal a good starting point for further analysis of the cellular and molecular events occurring within the first days after cardiac injury.

Finally, I developed a cryoinjury method that more closely resembled the injured tissue after human heart infarction. I induced tissue death by exposing the ventricle to dry ice and detected that the zebrafish heart can regenerate upon this cardiac injury similarly as in response to a ventricular resection injury. After cryoinjury, the entire epicardium activated the expression of developmental genes and started to proliferate. I detected also proliferating cardiomyocytes, indicating that similar cellular mechanisms are induced in the epicardium and the myocardium after cryoinjury and ventricular resection. Furthermore, activation of Sox9 expression early after cryoinjury suggested that molecular mechanisms of regeneration are also similar in both injury methods. Thus, cryoinjury provides a useful tool for future studies of zebrafish heart regeneration with more relevance to human cardiac infarction.

I discuss all results with reference to vertebrate heart development and to the response after mammalian heart infarction. Furthermore, the results were put into the context of cellular mechanisms that are present in the process of zebrafish heart regeneration.

Index of Figures and Tables

Figures

Figure 1.1.	The zebrafish and mammalian heart morphology and circulation.....	15
Figure 1.2	Myocardial structure in zebrafish and mammals.....	16
Figure 1.3	Non mammalian vertebrates display an elevated regenerative capacity..	19
Figure 1.4	The zebrafish heart regenerates after ventricular resection.....	20
Figure 3.1.1	Active Wnt/ β -catenin signaling was not reproducibly detectable in TOPdGFP reporter fish during zebrafish heart regeneration.....	60
Figure 3.1.2	Active Wnt/ β -catenin signaling is not detectable using in situ hybridization for <i>axin2</i> mRNA.....	62
Figure 3.1.3	Transgenic lines to inhibit or overactivate Wnt/beta-catenin signaling displayed transgene expression in the heart.....	64
Figure 3.1.4	<i>hand2</i> expression is not regulated by Wnt/ β -catenin signaling.....	67
Figure 3.1.5	Approaches used to identify Wnt/ β -catenin target genes during early heart regeneration using oligoexpression microarray analysis.....	70
Figure 3.1.6	Dkk1 does not significantly interfere with cardiomyocyte and non- cardiomyocyte cell proliferation in the regenerating heart.....	73
Figure 3.1.7	In a second experiment, proliferation of cardiomyocytes was not significantly influenced in hsDkk1GFPxcmlc2:dsRed versus cmlc2:dsRed hearts.....	76
Figure 3.1.8	Inhibition of Wnt/ β -catenin signaling during the entire regeneration process did not influence zebrafish heart regeneration.....	79
Figure 3.1.9	Overactivation of Wnt/ β -catenin signaling did not influence heart regeneration.....	82
Figure 3.2.1	Sox9 expression pattern in zebrafish heart regeneration.....	86
Figure 3.2.2	Sox9a+ cells are proliferating at 3 and 7dpa while Sox9a+ and PCNA+ cells are not (PCNA rarely) detectable in uninjured hearts.....	87
Figure 3.2.3	Sox9a+ is expressed in myocardial cells.....	88

Figure 3.2.4 A subset of endothelial cells, identified in <i>fli1:eGFP</i> or <i>kdrl:GFP</i> fish, express Sox9a at 3 and 7 dpa.....	90
Figure 3.2.5 Epicardial cells labeled in <i>wt1b:GFP</i> fish display Sox9a expression.....	93
Figure 3.2.6 No difference in regenerative capability between Sox9a heterozygous mutants (<i>sox9a+/-</i>) and wild-type siblings.....	95
Figure 3.2.7 Inhibitory construct Sox9a Δ CEngrailed (Sox9aEng) presumably interferes with Sox9a but also Sox9b and Sox10 target genes; Sox8 target genes were not influenced by the repressor.....	97
Figure 3.2.8 Inhibitory function of Sox9aEng construct in TG(<i>hsp70l: dTomato p2A Sox9aΔCEng</i>) transgenic fish (short: <i>hsSox9aEng</i>) on Sox9a target gene expression.....	100
Figure 3.2.9 Induction of <i>sox9aEng</i> transgene impairs endothelial and myocardial regeneration.....	103
Figure 3.3.1 The zebrafish heart regenerates tissue damage after cryoinjury.....	106
Figure 3.3.2 Cryoinjury causes myocardial cell death, inflammatory response, massive changes in tissue morphology and appearance of activated cardiomyocytes at the wound edges.....	109
Figure 3.3.3 Ultrastructural analysis of cryolesioned myocardium reveals cardiomyocyte cell death and an inflammatory response.....	110
Figure 3.3.4 Cryoinjury causes loss of cardiomyocyte specific marker gene expression and upregulation of apoptosis.....	112
Figure 3.3.5 Organ-wide activation of embryonic gene expression and cell proliferation in the epicardium in response to cryoinjury and ventricular resection.....	114
Figure 3.3.6 Activation of myocardial proliferation in response to cryoinjury.....	116
Figure 3.3.7 Activation of Sox9 expression after cryoinjury.....	117
Figure 3.4.1 Scheme of sample collection.....	118
Figure 3.4.2 Most genes are differentially regulated early after amputation.....	121
Figure 3.4.3 Epithelial - to - mesenchymal transition might be activated during heart regeneration.....	124
Figure 3.4.4 Fgf target genes are activated at 3 and 7 dpa	125

Tables

Table 2.1	Antibodies used in this study.....	34
Table 2.2	Primer sequences for identification of <i>jellyfish</i> ^{tw3} (<i>sox9a</i> +/- mutant fish).35	
Table 2.3	Constructs for generation of mRNA used for injections into embryos....	36
Table 2.4	Constructs for generation of in-situ hybridization probes.....	36
Table 3.1.1	Comparisons of expression profiles showed few regulated genes after inhibition of Wnt/ β -catenin signaling using Dkk1GFP or Axin1YFP overexpression in amputated hearts using approach I and no regulated genes using approach II.....	71
Table 3.1.2	Comparisons of amputated and uninjured wild-type hearts showed upregulation of known induced genes in heart regeneration at 7 dpa using approach I and II.....	71
Table 3.4.1	Biological gene annotation from the Panther database according to biological process level I.....	120
Table 3.4.2	Genes known to be upregulated within the first 14 days of heart regeneration.....	122
Table 3.4.3	Novel identified differentially expressed genes during early heart regeneration.....	122

Abbreviations

AFOG	acid fuchsin orange G
CNS	central nervous system
°C	degree celsius
Dig	dioxygenin
Dkk1	Dickkopf 1
DNA	desoxyribonucleic acid
dpa	days post amputation
dpsa	days post sham amputation
dpi	days post injury
EMT	Epithelial - to - mesenchymal transition
et al.	et aliter (Latin “and others”)
fl	full length
g	gramm
GFP	green fluorescent protein
h	hour(s)
HMG	high mobility group
hpa	hours post amputation
hpf	hours post fertilization
hpsa	hours post sham amputation
l	litre
M	molar
MAB	maleic acid buffer
MABT	maleic acid buffer with Tween 20
µg	micro gram
min	minutes
µl	microlitre
mm	millimeter
mM	millimolar
(m)RNA	(messenger) ribonucleic acid
NBT	4-nitroblue tetrazolium chloride
NCS	newborn calf serum
ng	nanogram

PBS	phosphate buffered saline
PBT	phosphate buffered saline with Tween 20
PCR	polymerase chain reaction
PCNA	proliferative cell nuclear antigen
PFA	paraformaldehyde
s	seconds
Sox	Sry (sex-determining region Y) – related box
SSC	saline sodium citrate
Tg	transgenic
RT	room temperature
TCF/Lef	T-cell factor/lymphoid enhancer factor
Wnt	Wingless-type MMTV integration site
w/v	weight / volume
YFP	yellow fluorescent protein

1.1 Heart morphology in zebrafish and mammals

The zebrafish (*Danio rerio*) belonging to the teleost family is an ideal model organism to study heart development and regeneration (Wixon 2000, Hu et al 2001). Embryological studies are facilitated by the external embryonic development after external fertilization. All stages of development are visible due to the transparency of the embryos. The possibility for genetic manipulations allowed enormous insights into molecular cues regulating embryonic development (Glickman and Yelon 2002) and facilitates functional studies of regeneration processes in the adult zebrafish (e.g. Kikuchi et al 2010).

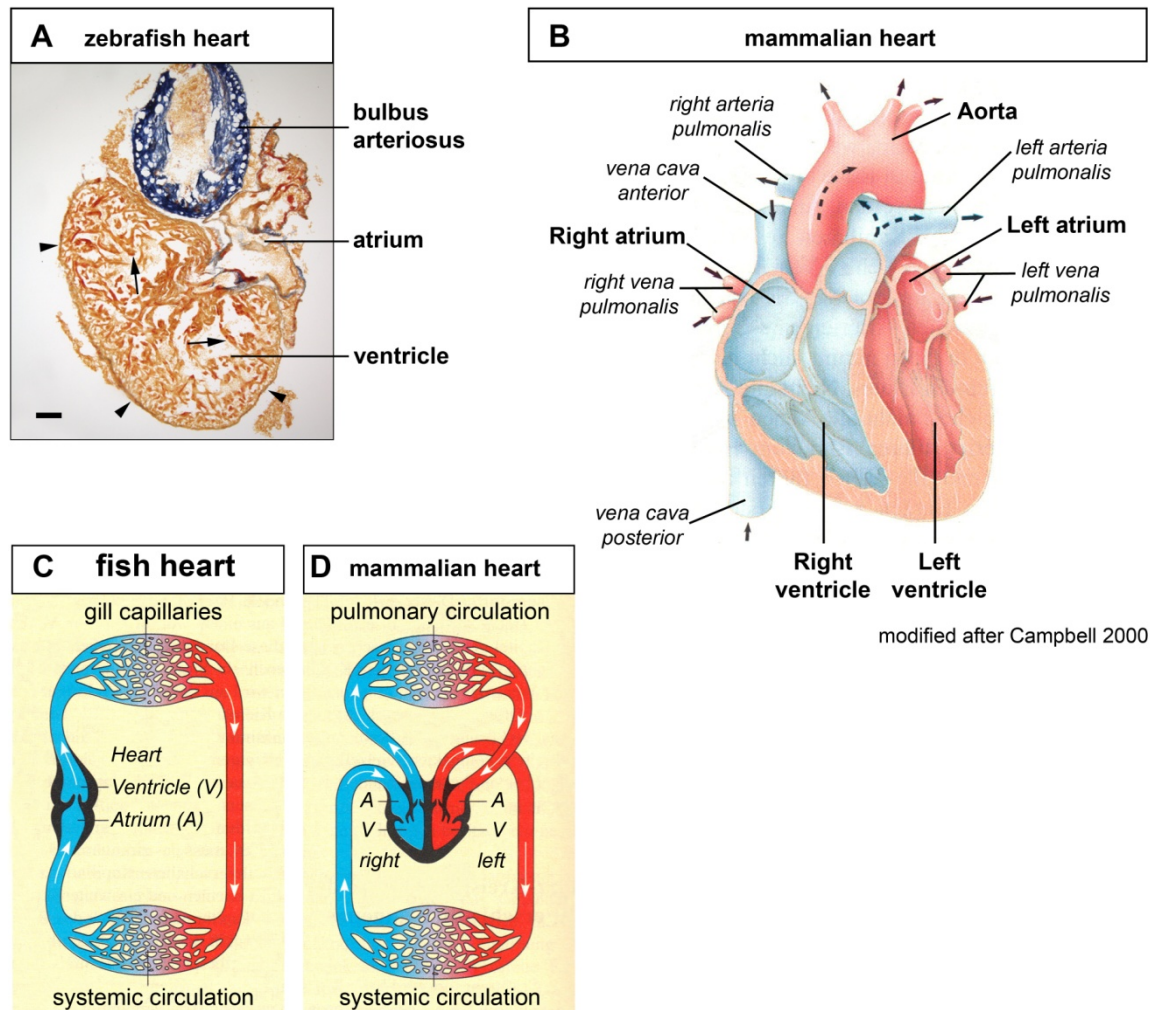
The adult zebrafish heart is covered by the pericardial sac (Hu et al 2001) and is composed of one atrium and one ventricle and therefore represents a two – chambered type of heart (**Fig 1.1A**). The ventricle is connected with the bulbus arteriosus, which serves as outflow tract. The blood returns from the body into the atrium. The atrium pumps it into the ventricle, which pumps it further via the bulbus arteriosus towards the gill arches from where it is distributed into the body (**Fig 1.1A**). Valves between atrium and ventricle and between ventricle and bulbus allow for unidirectional blood flow (Hu et al 2001). In contrast, the mammalian heart is a four – chambered heart with right and left atria and ventricles and the pulmonary circuit is separated from the systemic circuit of the body, which is not the case in the two chambered heart of the zebrafish (**Fig 1.1B**).

Figure next page

1.1. The zebrafish and mammalian heart morphology and circulation

A. A zebrafish heart section is stained in histological Acid fuchsin orange G staining, which stains muscle in orange and collagen in blue. The two chambered zebrafish heart consists of one atrium and one ventricle, which has a longitudinal length of approximately 1-1.5 mm. The bulbus arteriosus is the outflow tract transporting blood to the gill arches. The atrium is characterized by a thin wall of cardiomyocytes whereas the ventricle shows a compact external layer of cardiomyocytes (black arrowheads) and internal cardiomyocytes organized into trabeculae (black arrows). Scale bar is 100 μ m.

B. An illustration of the human heart is shown. The mammalian heart is a four-chambered heart, which consists of left and right atria and ventricles. Different veins transport blood to the heart and arteries transport blood into the pulmonary or systemic circulation. (Modified after Cambell 2000)



modified after Campbell 2000

C. Circulation in fish: Venous blood from the systemic circulation is transported to the atrium. The blood is pumped into the ventricle, which then pumps it into the gill arches, from where oxygenated blood is distributed into the systemic circulation of the body. (Modified after Cambell 2000)

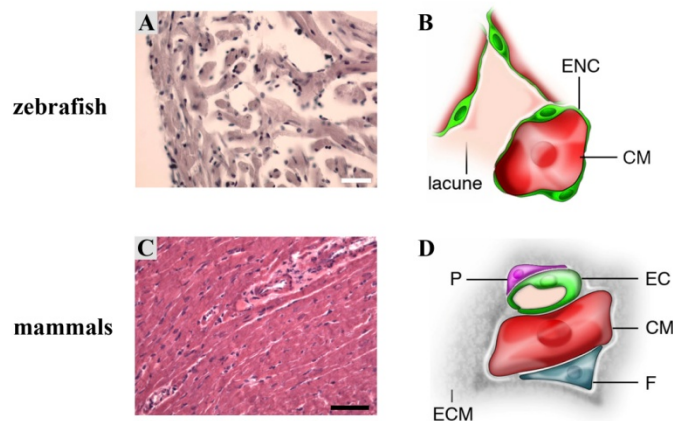
D. Mammalian circulation: Venous blood from the systemic circulation is transported to the left atrium, which pumps it into the right ventricle. The right ventricle pumps the blood via pulmonary arteries into the lungs (pulmonary circuit). Oxygen-rich blood is transported to the left atrium, which then pumps it into the left ventricle. The left ventricle pumps oxygen rich blood via the Aorta into the systemic circulation of the body. (Modified after Cambell 2000)

The zebrafish heart is confined externally by the epicardium (Hu et al 2001), which covers the myocardium. The zebrafish atrium is characterized by a thin wall of cardiomyocytes whereas the ventricle shows a compact external layer of cardiomyocytes and internal cardiomyocytes organized into trabeculae (**Fig 1.1A, Fig 1.2A and B**). Endothelial cells

(the endocardium) surround the myocardial trabeculae and thus form the inner-most layer of the heart (Hu et al 2001) ((**Fig 1.2B**). The epicardium, myocardium and endocardium are also present in mammalian hearts. However, the zebrafish heart structure rather resembles a trabeculated fetal than an adult mammalian heart (Hu et al 2001, Ausoni and Sartore 2009) (**Fig 1.2A**).

In the zebrafish ventricle, coronary vessels, composed of a layer of endothelial cells and pericytes, are only found in the compact myocardial layer and subepicardial space (Hu et al 2001). Compared to mammals, zebrafish hearts have only few cardiac fibroblasts which are exclusively located in the subepicardial space. In contrast, the mammalian heart is provided with a complex coronary network that supports the compact myocardium of atria and ventricles with oxygen and nutrients (**Fig 1.2C and D**). Every single cardiomyocyte is associated with supporting capillaries and fibroblasts (Hu et al 2001, Ausoni and Sartore 2009).

In summary, although the anatomy of the adult zebrafish and mammalian hearts are different both are composed of the same cell types and display a similar basic organization. An important difference is the high number of cardiac fibroblasts in mammals compared to the very few fibroblasts in the zebrafish heart.



modified after Ausoni and Sartore 2009

1.2 Myocardial structure in zebrafish and mammals

A and B. Hematoxylin and eosin staining shows tissue organization in (**A**) zebrafish, which displays a spongy like trabecular internal organization and a compact external layer of cardiomyocytes, while (**B**) rat hearts, display a compact organization of the cardiac muscle.

B and D. Two schematic representations show positional relationships between cardiomyocytes (CM) surrounding endothelial (EC) or endocardial (ENC) cells, fibroblasts (F) and vessel associated pericytes (P). Modified after Ausoni and Sartore 2009.

1.2 Vertebrate heart development

This thesis addresses the regenerative abilities of the adult zebrafish heart. Molecular signals regulating this process are largely unknown, while, in contrast, enormous efforts during the last decades led to the identification of signaling pathways and factors that regulate vertebrate cardiac development. It has been suggested that reactivation of developmental processes and signaling pathways is also important for adult heart regeneration (Lepilina et al 2006, Jopling et al 2010), thus I briefly describe vertebrate heart development.

The complex formation of the vertebrate heart including cardiac specification, heart tube formation and cardiac remodeling processes as well as molecular pathways involved in these developmental steps are well described in several reviews (for reviews see: Stainier 2001, Glickman and Yelon 2002, Brand 2003, Perez-Pomarez et al 2009, Eisenberg and Eisenberg 2006, Eisenberg and Eisenberg 2007). The descriptions mentioned here mainly refer to zebrafish heart development but also information about mammalian systems is added.

The multichambered heart is the first organ that forms and functions during vertebrate development (Stainier 2001). During early stages of gastrulation involuting mesodermal cells migrate to anterior-lateral regions of the vertebrate embryo to build the heart forming field, which is the source for the myocardial and endocardial lineage.

The cardiogenic field in mammals consists of progenitors for the first heart field (FHF) forming the cardiac crescent and progenitors of the second heart field (SHF) lying medially to the crescent (Klaus et al. 2007, Perez-Pomarez et al 2009).

Adjacent tissues such as the anterior endoderm, which is an important regulator of cardiac induction and maintenance, provide signals to regulate cardiogenesis (Brand 2003). Several pathways like BMP and FGF signaling are essential to promote cardiac specification of the mesodermal cells (Brand 2003, Marques et al 2008). Furthermore, Dickkopf 1 (Dkk1) and crescent, which are described as inhibitors of canonical Wnt signaling, positively influence cardiogenesis (Eisenberg and Eisenberg 2007, Brand 2003). The size of the heart field is controlled by restricting factors like noggin.

Myocardial precursors of the paired anterior lateral plate mesoderm further differentiate and migrate towards the embryonic midline. Cardiac progenitors differentiate into

myocardial cells, a process that is regulated by several pathways like FGF and BMP signaling and leads to the expression of genes for contractile proteins (Wang et al 2010, de Pater et al 2009, Marques et al 2008, Klaus et al 2007). Besides these myocardial cells of the working myocardium, precardiac cells give rise to cells of the conduction system as well (Perez-Pomarez et al 2009). The two heart fields fuse and form a linear heart tube, meanwhile the endocardial cells, which likewise migrated to the midline, are forming the inner lining of the myocardial tube (Glickman and Yelon 2002). This simple heart tube is already functional and driving circulation by regular contractions. It successively undergoes complex morphogenetic movements and chamber formation. In addition to cardiac looping, remodeling steps include thickening of the ventricular wall, formation of ventricular trabeculae and cardiac valves, the latter by cells that originate from the endocardial endothelium (Glickman and Yelon 2002, Akiyama et al 2004, Yamagishi et al 2009).

In mammals, cells of the simple heart tube originate from the FHF and contribute later to the left ventricle. Cells of the SHF, likewise migrated to the midline, join with cells of the FHF and later contribute to the right ventricle and outflow tracts (Klaus et al 2007, Perez-Pomarez et al 2009).

Furthermore, two cell populations, originating from the cardiac neural crest and proepicardial epithelium, invade the heart and regulate its morphogenesis (Brand 2003). Cells of the cardiac neural crest migrate into the cardiac outflow tract where they form smooth muscle cells and neurons and additionally contribute to some parts of the developing cardiac valves (Brand 2003, Akiyama et al 2004, Yamagishi et al 2008). Proepicardial cells originate for instance from the lining of the coelom, they migrate to and further onto the surface of the heart, where they give rise to the epicardium. Some epicardial cells undergo epithelial to mesenchymal transition/transformation (EMT) to form epicardial derived cells (EPDCs), which contribute to subepicardial connective tissue and to all cellular components of the coronary vascular system like endothelium, smooth muscle cells and perivascular fibroblasts (Brand 2003, Lie-Venema et al 2007). Additionally, EPDC's have been suggested to function as cardiac stem cells that can differentiate into myocardial cells (van Wijk and van den Hoff 2010). Whether adult epicardial cells can differentiate into myocardial cells remains unknown.

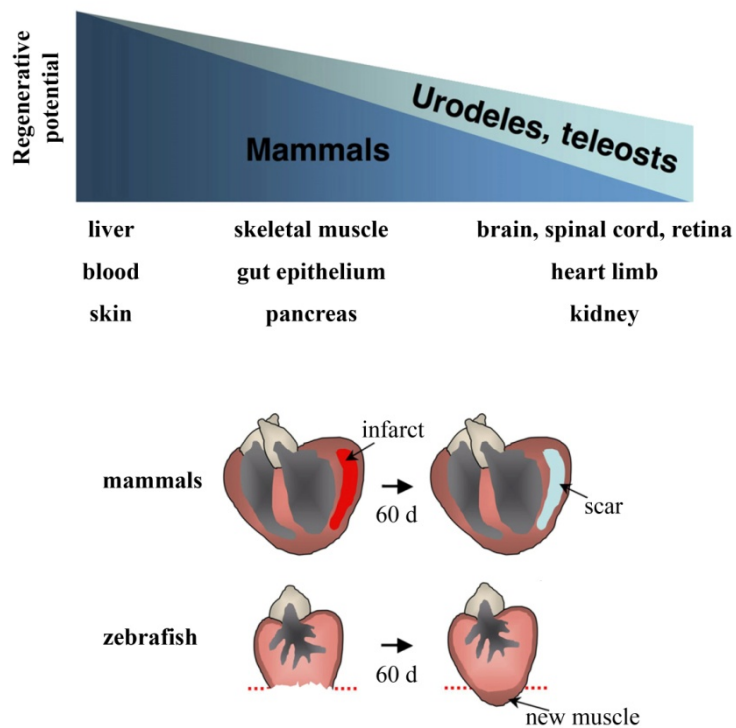
However, there are also different data showing that cells of the sinus venosus, the venous inflow tract of the embryonic heart, are the source for coronary arteries (Red-Horse et al 2010).

1.3 Cardiac injury in zebrafish and mammals – different reactions to keep and improve cardiac function

1.3.1 Heart regeneration in zebrafish

The regenerative capacity varies in response to injuries widely amongst different vertebrate species. Higher vertebrates like mammals can regenerate liver and repair damage to skeletal muscle but display limited regenerative capability for most tissues and organs (Stoick-Cooper et al 2007). In contrast, other vertebrates like fish have a remarkable capacity to efficiently regenerate numerous organs like retina, brain, heart, liver and fins (Qin et al 2009, unpublished observations of V. Kröhne, Poss et al 2002, Kan et al 2009, Knopf et al 2011) (**Fig 1.3**).

Strikingly, adult zebrafish can completely regenerate heart tissue after an enormous injury such as ventricular resection unlike mammals that mainly heal the injured cardiac area by scarring (Cleutjens et al 1999, Ausoni and Sartore 2009, Poss et al 2002) (**Fig 1.3**).



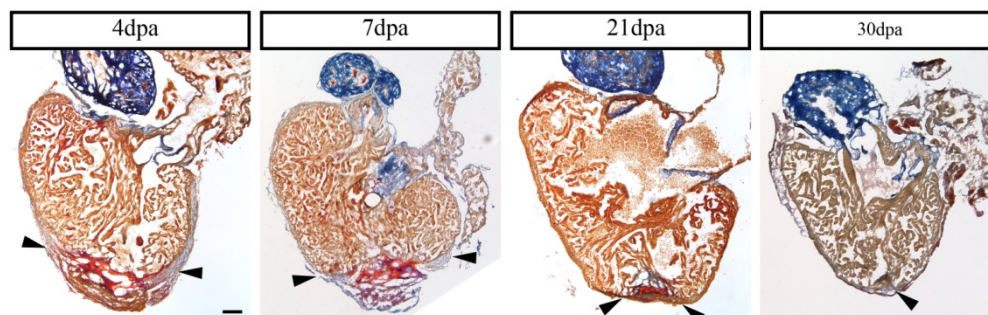
modified after Poss 2007

1.3 Non mammalian vertebrates display an elevated regenerative capacity

Many mammalian tissues like liver, blood, skin, skeletal muscle, gut and pancreas possess a significant regenerative capacity. In contrast, mammalian brain, spinal cord, retina, kidney, heart and limb fail to regenerate. The typical mammalian cardiac injury is a myocardial infarct.

Cardiomyocytes in the affected area undergo cell death and are subsequently replaced by scar tissue. The zebrafish heart regenerates after ventricular resection with little or no scarring and lost cardiac muscle is replaced within weeks. Modified after Poss 2007.

Cardiac injury in zebrafish is experimentally performed by the surgical removal of ~20% of the ventricle at the apex (Poss et al 2002). Only seconds after resection, a blood clot is established and replaced by a fibrin clot within the next 2-4 days. The fibrin clot is subsequently surrounded, penetrated and replaced by new myocardial cells. After 30 days a new wall of cardiac muscle has formed and by 60 days post amputation (dpa) the ventricular size is restored and its shape is mainly reestablished (**Fig 1.4**). Only few or no fibers of collagen-rich connective tissue are detectable in the apical ventricle indicating that no scarring has occurred (Poss et al 2002).



1.4 The zebrafish heart regenerates after ventricular resection

Heart sections were stained using histological Acid fuchsin orange G (AFOG) staining, which stained muscle in orange, fibrin in red and collagen in blue. Fibrin rich wound tissue, detectable at 4 days post amputation (dpa), was removed within 30 days after ventricular resection and a new wall of muscle was formed, while collagen rich scar tissue was absent in the ventricle. Only few collagen fibers were detectable in the regenerated cardiac tissue at 30 dpa (black arrowhead at 30 dpa). The wound border is indicated by black arrowheads (4 - 21 dpa). Scale bar is 100 μ m.

While the cellular mechanisms underlying zebrafish heart regeneration start to be reasonably well understood, little is known about the molecular regulation of the process.

Transcriptional profiling covering the first 14 days of regeneration revealed the induction of secreted molecules especially during early phases of regeneration (Lien et al 2006). Tissue remodeling processes and cell migration are suggested to be important during later phases of cardiac regeneration (Lien et al 2006). Signaling pathways and molecules identified in this transcriptional profile analysis presumably contribute to or confirmed insights into cellular mechanisms that are explained in the following.

The entire epicardial layer induces a developmental gene program only hours after amputation, as indicated by an upregulation of *raldh2* and *tbx18* transcripts that are also critical for cardiac development (Lepilina et al 2006). Further indications for an activation of the epicardium are the proliferation of epicardial cells, morphological changes like the thickening of the epicardium close to the lateral wound edges and the coverage of the wound by the epicardial layer few days after amputation (Lepilina et al 2006). The presence of *tbx18* expressing cells initially in epicardial cells and later in cells of the regenerated myocardial area suggested that epicardial cells invade the regenerating area to revascularize the new muscle (Lepilina et al 2006). Recently, Kim et al (2010) showed the upregulation of EMT markers *snail2* and *twist1b* in the wound of regenerating hearts. Since epicardial cells undergo EMT, invade the myocardium and contribute to vessel formation during cardiac development (Kim et al 2010, Brand 2003), both studies suggested that these cellular processes are recapitulated during zebrafish heart regeneration (Lepilina et al 2006, Kim et al 2010). By overexpressing a dominant negative Fgf receptor Lepilina et al (2006) detected that *tbx18* expressing cells did not integrate into the regenerating tissue and vessel regeneration was strongly impaired in transgenic fish compared to wild-type controls. Moreover myocardial regeneration was limited and collagen-rich scars were formed after long-term inhibition of FGF signaling (Lepilina et al 2006). These results suggested that FGF signaling is crucial for recruitment of epicardial cells and neovascularization of the regenerating myocardium. An impairment of these processes due to FGF inhibition results in limited myocardial regeneration and finally leads to formation of collagen-rich scars (Lepilina et al 2006). Inhibition of PDGF signaling by a chemical inhibitor results in reduced expression of EMT markers and in impaired vessel regeneration after ventricular resection, indicating that PDGF signaling is also important for neovascularization of the regenerating myocardial area (Kim et al 2010). Thus FGF and PDGF signaling have been suggested to regulate revascularization of the new myocardial area, possibly be influencing EMT of epicardial cells; yet whether epicardial cells really

undergo EMT and contribute to new coronary vessels during heart regeneration and how these pathways regulate these processes remains unclear.

During cardiac regeneration, proliferation of cardiomyocytes is detectable starting from 7 dpa and peaks at 14 dpa (Poss et al 2002). As revealed by lineage tracing analysis the vast majority of new cardiomyocytes is generated by proliferation of mature cardiomyocytes (Jopling et al 2010, Kikuchi et al 2010). Thus, Cre induction resulted in myocardial GFP expression, which led to labeling of all differentiated cardiomyocytes before injury. Following ventricular resection and cardiac regeneration the vast majority of new cardiomyocytes displayed GFP expression, indicating that new myocardial cells are generated by mature (GFP positive) cardiomyocytes. Electron microscopy revealed a limited dedifferentiation of cardiomyocytes, which is presumably necessary to reenter the cell cycle (Jopling et al 2010, Kikuchi et al 2010). These data strongly indicate that mature cardiomyocytes generate new cardiomyocytes during zebrafish heart regeneration. Transcripts like *hand2*, *nkx2.5* and *tbx20*, which are crucial for cardiac development, are induced after injury suggesting a progenitor like cell status, presumably of cardiomyocytes (Lepilina A. et al 2006, Kikuchi K. et al 2010). However, activation of developmental genes is also detectable after opening of the pericardial sac and thus their functional role remains to be tested (Wills et al 2007).

Furthermore, it is suggested that mainly subepicardial cardiomyocytes displaying *gata4* expression proliferate and thus contribute to new myocardial cells (Kikuchi et al 2010). The activation of *gata4* regulatory sequences in subepicardial cardiomyocytes is detectable soon after activation of the entire epicardium suggesting that the epicardial layer provides signals for following events like cardiomyocyte proliferation.

Different signaling pathways are described to influence proliferation of cardiomyocytes during cardiac regeneration. DNA synthesis in cultured zebrafish cardiomyocytes was enhanced using PDGF ligand (PDGF-B) application and decreased after applying a chemical inhibitor of PDGF receptor function (Lien et al 2006). Application of the chemical inhibitor also decreased DNA synthesis by 16% in regenerating zebrafish hearts *in vivo*, suggesting that PDGF signaling positively influences myocardial DNA synthesis *in vitro* and *in vivo* (Lien et al 2006).

Studies on the cell cycle regulatory gene *mitotic checkpoint kinase 1*, *mps1*, using a mutant fish line showed enhanced collagen-rich scar formation in mutant fish compared to wild-type heart regeneration (Poss et al 2002). Another cell cycle regulatory gene, *plk1*, is presumably involved in heart regeneration since chemical Plk1-inhibitor treatment results

in reduced regenerative capacity of zebrafish hearts (Jopling et al 2010). Thus cell cycle regulatory genes are involved in heart regeneration; yet it is not clear whether all proliferating cardiac cells depend on expression of these genes.

The endocardial/endothelial layer of the regenerating heart produces signals like retinoic acid (RA) during cardiac regeneration (Kikuchi et al 2011). After inhibition of RA signaling, cardiomyocyte proliferation was strongly reduced indicating that RA signaling is required for injury induced myocardial proliferation (Kikuchi et al 2011). Other signals in heart regeneration like IGF2 are not examined concerning their functional role and the presence of activated Notch signaling is discussed controversially (Lien et al 2006, Raya et al 2004)

In summary, zebrafish can efficiently regenerate cardiac tissue after a ventricular resection. The initial activation of the entire epicardium precedes the induction of proliferation in mature cardiomyocytes leading to new myocardial cells. The proliferative ability of cardiomyocytes is influenced by the activated epicardium and endocardium/endothelium.

1.3.2 Mammalian myocardial infarction

Cardiovascular diseases like chronic heart disease, myocardial infarct and heart insufficiency are the leading causes of death in Germany (Statistisches Bundesamt Deutschland 2009).

A myocardial infarction is a severe, acute form of heart injury. The acute occlusion of a coronary artery causes an ischemia of the myocardial area due to the loss of oxygen and nutrients supply (van de Schans et al 2008). Acute myocardial cell death in the affected area leads to a regional loss of contractile force and an inflammatory response is initiated. If patients survived an acute myocardial infarction, the affected area matures into scar tissue and remaining heart tissue undergoes an extensive remodeling process to compensate for the loss of contractile force (Leri et al 2008, van de Schans et al 2008).

1.3.2.1 The main response to mammalian heart injury - cardiac hypertrophy

Cardiac hypertrophy is a response of the mammalian heart to increased workload, which - dependent on the stimulus - either results in physiological or in pathological hypertrophy (for reviews see: van de Schans et al 2008, Balakumar and Jagadesh 2010, Zelarayan et al 2007, Cleutjens et al 1999). In general, the majority of cardiomyocytes are regarded as

terminally differentiated, which thus do not undergo cell division. However, proliferation of mammalian cardiomyocytes was observed to a very limited extent after heart injury and can be induced experimentally (Laflamme and Murry 2011). The proliferative capacity of mammalian cardiomyocytes and the potential role of cardiac stem cells for generation of new cardiomyocytes are explained below (1.3.2.1).

In contrast to mammals, growth of adult zebrafish hearts is caused by cardiomyocyte hyperplasia rather than hypertrophy (Wills et al 2008). Still, the generation of new mammalian cardiomyocytes is insufficient and thus adult mammalian hearts undergo hypertrophy, which is characterized by the increase in size of individual myocardial cells. Since I am focusing on pathological changes in the adult heart further explanations will refer to pathological hypertrophy of the mammalian heart. Pathological hypertrophy can result from various cardiovascular diseases like hypertension, valvular diseases or myocardial infarction. The initial hypertrophic response reduces increased wall stress and thus has a compensatory function to normalize wall tension and provide required cardiac output. This early beneficial mechanism can have adverse effects since sustained cardiac hypertrophy leads to cardiac decompensation, resulting in heart failure and sudden death (van de Schans 2008). Detectable remodeling processes are, beside the abnormal increase in heart muscle due to enlargement of cardiomyocytes, also proliferation of non-muscle cells and molecular responses like re-expression of embryonic markers as for instance the reactivation of fetal forms of contractile proteins. Numerous molecular processes are involved in cardiac hypertrophic remodeling as reviewed in Balakumar and Jagadeesh (Balakumar and Jagadeesh 2010). The role of the canonical Wnt signaling pathway as one example is further explained below (1.4.1.2).

1.3.2.1 Capacity for “real” cardiac regeneration in mammals

In contrast to mammals, adult zebrafish can efficiently regenerate cardiac injury of considerable size and replace wound tissue by new functional myocardium (Kikuchi et al 2010, Poss et al 2002). It was shown recently that neonatal mice possess the ability to regenerate heart tissue completely after removal by ventricular resection (Porello et al 2011). Beside morphological regeneration, functional restoration was also shown. Similar to zebrafish heart regeneration cardiomyocyte proliferation is induced in response to injury and it is suggested that new cardiomyocytes are possibly derived from mature myocardial cells. This regenerative ability decreased dramatically within a few days after birth and

thus in addition to scar formation the remaining mammalian cardiomyocytes mainly undergo hypertrophy to compensate for myocardial loss (Leri et al 2008).

In the adult mammalian heart endogenous regenerative capacity is limited after injury although to some degree cardiomyocyte regeneration may occur in mammals (Yi et al 2010, van Amerongen et al 2008). Throughout life, new cardiomyocytes are generated to a limited extent in the uninjured mammalian heart indicating a homeostatic turnover of myocardial cells (Yi et al 2010). Thus, different strategies are investigated to enhance cardiac regeneration after injury by inducing regeneration of cardiomyocytes and other cell types necessary for functional myocardium. Several studies suggested the presence of resident stem cells or progenitors in the adult heart, although these cell populations appear to be very rare (Leri et al 2008, Wu et al 2008). The use of multipotent stem cells provides the possibility to regenerate cardiomyocytes as well as cells for coronary vessels and other cardiac cell types (van Amerongen and Engel 2008). Their rare occurrence is an obstacle in the aim to provide enough cells for regeneration of a relatively large area of lost myocardium in an infarcted heart. Furthermore, it is challenging to get a repopulation of the infarct area itself (Leri et al 2008). An important question is whether adult cardiomyocytes or their progenitor cells can be induced to proliferate. So far it was shown that growth factor stimulation and p38 inhibition induce adult cardiomyocyte proliferation, presumably after transient dedifferentiation of the contractile apparatus (Engel et al 2005). Thus, it may be possible to enhance the endogenous regenerative capacity of mammalian cardiomyocytes and other cardiac cells using extracellular factors.

Due to the rare occurrence of stem and progenitor cells in the mammalian heart exogenous cell sources like bone marrow derived cells (BMCs), ES cells or others have been tested for their therapeutic potential (Leri et al 2008, Yi et al 2010). So far, results indicate only marginal positive effects which are presumably due to paracrine effects of injected cells, mainly BMCs (Yi et al 2010, Chien et al 2008, van Amerongen and Engel 2008). ES cells, however, hold the risk of teratoma formation since it is not possible to induce uniform populations of myocytes for injections (Leri et al 2008, Yi et al 2010). Furthermore it is questionable whether injected cells can integrate into the host myocardium and whether myocardial progenitors can achieve a mature state and therefore positively contribute to heart function (Chien et al 2008, Leri et al 2008, van Amerongen and Engel 2008).

To conclude, the mammalian heart might have the potential to regenerate myocardial tissue after injury. Thus identification of cellular mechanisms and signaling molecules that mobilize endogenous cardiac regeneration or enable strategies for the use of exogenous

cell sources is of great importance for therapeutic approaches to improve mammalian heart function. The regenerating model organism zebrafish can help to identify the respective signals and mechanisms.

1.4 The canonical Wnt/ β -catenin signaling pathway and Sox9 transcription factor - potentially involved in zebrafish heart regeneration

As described above, the picture about molecular signals that regulate zebrafish heart regeneration remains incomplete. Presumably, several molecular signals that are important during zebrafish heart development are also reactivated during cardiac regeneration. In this thesis I aimed to examine the function of molecular signals in zebrafish heart regeneration and thus in following introduce the Wnt/ β -catenin pathway and the transcription factor Sox9. I describe their role in heart development and, since it is known the role of Wnt/ β -catenin signaling in pathological hypertrophy of the mammalian heart.

1.4.1 Canonical Wnt signaling

Different Wnt signaling pathways are known and they are referred to as the “canonical” Wnt pathway and as “non-canonical” Wnt pathways, the latter signaling independent of β -catenin. In this work I will only address the “canonical” or β -catenin – dependent Wnt pathway, thus in the following I focus on the signaling mechanism and components of this pathway (for reviews see: MacDonald et al 2009, Clevers 2006, Reya and Clevers 2005, Moon et al 2004).

Canonical Wnt signaling is a crucial regulator of embryonic development but also plays an important role in maintenance and proliferation of adult stem cells of several tissues like the intestine, hair follicles, hematopoietic system and others (Clevers 2006, Reya and Clevers 2005). A misregulation of this pathway leads to severe diseases resulting i.e. in misregulation of bone mass and cancer such as colon cancer (Clevers 2006, Reya and Clevers 2005).

The presence of Wnt ligands and other extracellular molecules affect the initiation of the canonical signaling pathway and ultimately β -catenin dependent target gene transcription.

A stable pool of β -catenin proteins is bound to adherens junctions; but there is also another β -catenin pool, which is cytoplasmic and highly unstable; this pool serves for signaling (Clevers 2006).

In the absence of Wnt ligands, β -catenin is phosphorylated by kinases of a so-called destruction complex, which are the casein kinase 1 (CK1) and the Glycogen synthase kinase 3 α/β (GSK 3 α/β) (Clevers 2006, Moon et al 2004). Phosphorylated β -catenin is recognized by β -TrCP, a component of the E3 Ligase Complex, and thus β -catenin gets ubiquitinated and targeted for proteasomal degradation. Meanwhile Wnt target genes are kept in a repressive state by binding of T-cell factor/Lymphoid enhancer-binding protein (TCF/Lef) and associated co-repressors like Groucho (Clevers 2006, Moon et al 2004).

Activation of the canonical signaling pathway is initiated after binding of Wnt ligands to the Frizzled (Fz) and LDL-receptor related proteins 5/6 (LRP5/6) receptor complex (Clevers 2006, Moon et al 2004). After receptor complex activation, Fz interacts with Disheveled (Dsh), which gets phosphorylated. Furthermore GSK3 β and CK-1 γ phosphorylate LRP, and Axin, a scaffold protein of the destruction complex, is recruited to the receptor complex. The destruction complex dissociates whereupon β -catenin is stabilized and enters the nucleus. There, β -catenin binds to Tcf/Lef, displaces Groucho and promotes transcription of Wnt target genes (Clevers 2006, Moon et al 2004).

The Wnt/ β -catenin signaling cascade can be inhibited by extracellular antagonists. For example the Dickkopf1 (Dkk1) protein binds directly to LRP5/6 and interferes with formation of the Frizzled/LRP complex (Bafico et al 2001, Semenov et al 2008). Soluble Frizzled related proteins (sFRPs) have been suggested to function as extracellular pathway inhibitors, too (Clevers 2006).

1.4.1.1 The role of canonical Wnt signaling in heart development and cardiac specification

The function of canonical Wnt signaling in heart development is discussed controversially in the literature. However, in essence, the timing of activated and reduced Wnt signaling is suggested to be crucial for proper heart development.

The heart is of mesodermal origin and Wnt signaling enhances mesoderm formation in mouse embryonic stem (ES) cells (Ueno et al 2007). In zebrafish it has been shown that Wnt/ β -catenin signaling at pregastrulation stages positively regulates cardiogenesis whereas during gastrulation Wnt signaling inhibits heart formation (Ueno et al 2007). The

same effect with a cardiac promoting function early and an inhibitory function later in differentiation was reproduced in an ES cell system (Ueno et al 2007, Naito et al 2006). These results suggest that canonical Wnt signaling initially induces formation of the mesodermal cardiac progenitor cells but restricts the cardiac field during gastrulation.

The role of Wnt signaling, specifically its inhibitory function on cardiogenesis, is discussed in several reviews (Eisenberg and Eisenberg 2006, Eisenberg and Eisenberg 2007). It is suggested that Dkk1 and crescent, which are known as inhibitors of canonical Wnt signaling, positively regulate specification of cardiac progenitor cells early in development. On the other hand there are studies describing active Wnt/ β -catenin signaling in progenitors of the SHF and the expression of several canonical pathway components in the developing heart (Klaus et al 2007, Kwon et al 2007, Eisenberg and Eisenberg 2006). In this respect Wnt/ β -catenin signaling positively regulates generation and proliferation of Isl1+ progenitor cells of the SHF (Klaus et al 2007, Kwon et al 2007).

Furthermore, canonical Wnt signaling positively regulates expression of early cardiac markers like *tbx5*, *nkx2.5*, *hand2* and *isll* in ES cell culture (Klaus et al 2007, Kwon et al 2007, for some genes also shown by Ueno et al 2007, Naito et al 2006). Kwon et al (2007) also show that β -catenin is required for proliferation of cells that underwent early cardiac commitment *in vivo* (Kwon et al 2007). However, the precise temporal control of Wnt/ β -catenin is important for heart development; yet some data are controversial and thus the role of Wnt/ β -catenin signaling in certain stages of heart development remains to be determined (Ueno et al 2007, Kwon et al 2007, Kwon et al 2008).

Misregulated canonical Wnt signaling also results in defective heart tube formation and cardiac looping in mammals (Klaus et al 2007). Additionally, canonical Wnt signaling is an important regulator of endocardial cushion formation, which are valve precursor structures, in zebrafish (Hurlstone et al 2003).

In summary, the function of Wnt signaling in some developmental time windows is still not fully understood but it seems that exact regulation of canonical Wnt signaling is critical for vertebrate heart development.

1.4.1.2 The role of Wnt signaling in pathological cardiac hypertrophy

The reexpression of a developmental gene program in hypertrophy also led to the suggestion that canonical Wnt signaling, which is critical for cardiac development, can influence pathological hypertrophy (van de Schans et al 2010).

Different pathway components like frizzled-2, Dkk3 or β -catenin were found to be expressed or upregulated in the hypertrophic heart which suggested reactivation of Wnt/ β -catenin signaling (for review see: van de Schans et al 2010; Qu et al 2007).

Furthermore, different studies manipulating the activity of GSK3 β , an inhibitor of the Wnt/ β -catenin pathway, show that decreased kinase activity promotes hypertrophy. In contrast GSK3 β overexpression is a negative regulator of cardiac hypertrophy (reviewed in van de Schans et al 2010, Hadt and Sadoshima 2002). In context of canonical Wnt signaling this kinase promotes destabilization of β -catenin (Clevers 2006), which was also studied in the process of cardiac hypertrophy. β -catenin is stabilized by hypertrophic stimuli such as mechanical aortic constriction, and its overexpression induces hypertrophic growth of cardiomyocytes. Furthermore decreased β -catenin levels were shown to inhibit cardiac hypertrophy (Qu et al 2007). However, studies using another hypertrophic stimulus, drug induced hypertension, produced different data as β -catenin downregulation resulted in hypertrophy, too (reviewed in Zelarayan et al 2007, van de Schans et al 2010). Whether β -catenin function in hypertrophy is different due to application of different protocols, mainly hypertrophic stimuli, remains to be tested (van de Schans et al 2010; Blankestijn et al 2008).

Interestingly, intervention in Wnt signaling using FrzA/sFRP1, an antagonist of the Wnt pathway, results in improved heart function, reduced infarct size and possibly indirectly reduced apoptosis after myocardial infarction (Barandon et al 2003).

The canonical Wnt signaling pathway has been suggested to positively regulate cardiac hypertrophy. However, activation of GSK3 β can be regulated by numerous pathways (Hardt and Sadoshima 2002). Additionally it is suggested that the influence of β -catenin, beside its transcriptional role, is possibly also due to its function in cell-cell-contacts of adherent junctions.

1.4.2 Sox9 transcription factor

Sry-related box (Sox) transcription factors are members of the superfamily of high mobility group (HMG) DNA binding domain containing proteins. Sox factors are characterized by the presence of a similar type of HMG, which allows the sequence specific binding to the minor groove of the DNA. The Sox family consists of 20 Sox genes in mammals and is categorized into 8 subgroups (A-H), which share little conserved sequence outside the HMG box. Sox9 is, as well as Sox8 and 10, part of the subgroup E,

and they share conserved structural domains outside of the HMG domain as well (for review see: Kiefer et al 2007, Wegner 2010). Sox factors can function either as transcriptional activators or as transcriptional repressors.

Sox9 deficiency in humans leads to a severe disease called Campomelic Dysplasia (CD) that is usually lethal within the first year of life (Mansour et al 2002, Mansour et al 1995). CD patients display severe skeletal malformations, a high frequency of male sex reversal, sometimes defects in olfactory tissues, congenital heart diseases and other defects (Mansour et al 2002, Mansour et al 1995). These symptoms indicate that Sox9 is involved in numerous developmental processes. The lethality of heterozygous Sox9 mutant mice confirms the importance of Sox9 for developmental processes such as chondrogenesis (Yan et al 2002, Furuyama et al 2010). It is suggested that mutations in the *sox9* gene either result in haploinsufficiency or cause a dominant negative effect in mammals (Yan et al 2002).

Zebrafish contains two orthologues of the human *SOX9* gene, *sox9a* and *sox9b* (Chiang et al 2001). These Sox9 co-orthologues are expressed in partly overlapping regions during zebrafish development. This different but also overlapping expression is mainly described for the developing brain and cartilages (Yan et al 2005). In the gonads, Sox9a is expressed in testes whereas Sox9b is detectable in the ovaries (Chiang et al 2001). Due to their similar DNA binding and transactivation properties, it is assumed that Sox9a and Sox9b possess a potential functional redundancy (Chiang et al 2001). The combined expression patterns of zebrafish *sox9a* and *sox9b* have been suggested to resemble the *sox9* expression pattern in mouse (Yan et al 2005). Validated target genes for both Sox9 variants are the collagen variants *collagen type II alpha-1a (col2a1a)* and *collagen type XI alpha 2 (col11a2)*, which are expressed in chondrogenic cell lineages during embryonic development (Yokoi et al 2009). Studies of fish mutants for *sox9a* and *sox9b* have so far confirmed the functional relevance of these co-orthologues for development of the skeleton and other organs (Yan et al 2005, Yokoi et al 2009).

Recent studies describe Sox9 function in stem or progenitor cells of several embryonic and adult mammalian tissues (Seymour et al 2007, Kopp et al 2011, Furuyama et al 2010, Scott et al 2010). For example, Sox9 is expressed in and required for maintenance of progenitor cells of the developing and adult pancreas (Seymour et al 2007, Kopp et al 2010, Furuyama et al 2010). Furthermore, Sox9 positive progenitor cells are present during intestinal development and in the adult intestine and liver (Furuyama et al 2010). Hence, Furuyama et al. (2010) suggest that progenitor cells of these Sox9-expressing progenitor

zones contribute to physiological organ maintenance in the adult (Furuyama et al 2010). Others have also shown Sox9 expression in and its requirement for maintaining multipotent neural stem cells of the embryonic and adult central nervous system (Scott et al 2010).

In addition to its expression in adult progenitor cells, Sox9 is also relevant for regenerative processes. After certain types of liver injury, Sox9 positive precursor cells are suggested to function as a source of regenerating cells (Furuyama et al 2010). Furthermore, *sox9a* and *sox9b* expression is present during caudal fin regeneration in zebrafish (Smith et al 2006).

In summary, proper Sox9 function is necessary for the development of numerous organs in mammals and fish. Besides its expression in adult progenitor cells of several tissues Sox9 is presumably also important for processes of regeneration. Thus it is particularly interesting to examine Sox9 function in adult regeneration of tissues that display Sox9 expression or are affected by Sox9 deficiency during development.

1.4.2.1 The role of Sox9 in heart development

The transcription factor Sox9 has an essential role in various tissues such as the heart during vertebrate development (Lincoln et al 2007, Mansour et al 1995, Mansour et al 2002).

Studies in mouse revealed Sox9 expression in valvular and septal regions of the developing heart. Expression of Sox9 was shown in myocardial cells during cardiac development by Rahkonen et al (2003) whereas Lincoln and colleagues (2007) did not detect Sox9 expression in the developing myocardium at several stages. At any rate, a function of Sox9 in myocardial development has not been shown. In contrast, Sox9 function is clearly implicated in cardiac valvulogenesis. In early stages of heart valve development, Sox9 regulates the EMT process that is initiated in endocardial cells to form the endocardial cushions (Akiyama et al 2004, Lincoln et al 2007). During later stages of heart valve development Sox9 is required for proliferation of mesenchymal cells after EMT and for differentiation of heart valve precursors (Lincoln et al 2007). A role of Sox9a or Sox9b in zebrafish cardiac development has not been described so far.

In summary, Sox9 is required for early and late mammalian heart valve development. A functional role in cardiomyocyte development is not described.

1.5 Aims of the thesis

As mentioned above, zebrafish can regenerate lost cardiac tissue after resection of ~ 20% of the ventricle. Molecular mechanisms that regulate zebrafish heart regeneration are largely unknown. Thus, I aimed to identify molecular signals that are important during cardiac regeneration and addressed the following questions:

- Is Wnt/ β -catenin signaling important for zebrafish heart regeneration?
- Is Sox9 activated after ventricular resection and, if so, in which cell types is it upregulated?
- Is Sox9a function necessary for regeneration of cardiac cell lineages?
- Can zebrafish regenerate a heart injury, more specifically cryoinjury, which is associated with widespread cell death?
- Do cellular responses show similarity after cryoinjury and after ventricular resection?
- Which genes are upregulated in response to ventricular resection of the zebrafish heart during the first two weeks?

2.1 Material

2.1.1 Reagents and buffers

E3 medium	5mM NaCl, 0.17 mM KCL, 0.33 mM CaCl ₂ x 2H ₂ O, 0.33mM MgSO ₄ x 7H ₂ O, 0.2 ‰ methylene blue, pH 6,5
PBS	1.7 mM KH ₂ PO ₄ , 5.2 mM Na ₂ HPO ₄ , 150mM NaCl
TAE	40mM Tris acetate, 1mM EDTA
Solutions for Hank's full strength:	
	sol #1.: 8.0g NaCl, 0.4g KCl in dH ₂ O (100ml total Vol)
	sol #2.: 0.358g Na ₂ HPO ₄ (anhydrous), 0.6g KH ₂ PO ₄ in dH ₂ O (100ml total Vol)
	sol #3.: 0.72g CaCl ₂ in dH ₂ O (50ml total Vol)
	sol #4.: 1.23g MgSO ₄ x7H ₂ O in dH ₂ O (50ml total Vol)
	sol #5.: 0.35g NaHCO ₃ in 10ml dH ₂ O
Hank's Premix:	10ml sol #1, 1ml sol #2, 1ml sol #3, 1ml sol #4, 86ml dH ₂ O
Hank's full strength:	9.9 ml Hank's Premix, 0.1ml sol #5
Phosphate buffer (0.1M)	14.24 g Na ₂ HPO ₄ x2H ₂ O, 2.62g NaH ₂ PO ₄ xH ₂ O in 1l ddH ₂ O, pH 7.4
Fixative	4% (hearts) or 2% (heads) (w/v) paraformaldehyde in 0.1M phosphate buffer, pH 7.5
staining buffer	100mM Tris HCL pH 9.5, 50mM MgCl ₂ , 100mM NaCl, 0.1% Tween20
STOP solution	0.05M phosphate buffer pH 5.8, 1mM EDTA, 0,1% Tween
SSC (20x)	300 mM NaCl, 300 mM Na-Citrate, pH 7.0
Salt (10x)	1.95M NaCl, 89mM Tris HCl, 11mM Tris Base, 50mM NaH ₂ PO ₄ xH ₂ O, 50mM Na ₂ HPO ₄ xH ₂ O, 50mM EDTA
Hybridization buffer I	5x SSC, 500 µg/ml type VI Torula yeast RNA(Sigma), 50 µg/ml Heparin, 0.1% Tween, 20, 9mM Citric Acid (Monohydrate), 50% deionized formamide, pH 6.0
50x Denhardt's	1g BSA, 1g Ficoll, 1g PVP (polyvinylpyrrolidone) in DEPC-H ₂ O (total Volume 100ml)
Hybridization buffer II	1x Salt, 50% deionized formamide, 10% (w/v) dextran sulfate, 1mg/ml yeast torula RNA, 1x Denhardt's

Staining buffer	100mM NaCl, 50mM MgCl ₂ , 100mM Tris pH9.5, 0.1% Tween
MAB	100mM Maleic acid, 150mM NaCl
blocking solution II	20% sheep serum (v/v), 2% blocking reagent (w/v), 60% MABT
PEM buffer	80mM Na-PIPES, 5mM EGTA, 1mM MgCL ₂ , pH 7,4
AFOG	1g aniline blue, 2g orange G, 3g acid fuchsin in 200ml dH ₂ O, pH 1.09

2.1.2 Chemicals

Bouin's solution	- Sigma
Phosphomolybdic acid	- Sigma
Cytoseal XL	- Richard Allan Scientific
Trizol	- Invitrogen
BrdU	- Sigma
NBT and BCIP	- Roche

Additional chemicals were, if not indicated otherwise, purchased from AppliChem, Invitrogen, Merck, Roth, Sigma and VWR.

2.1.3 Antibodies

Name	Type	Host	Source	Working dilution
Anti -Dioxygenin AP	polyclonal	sheep	Roche	1:2000 - 4000; 1:5000 (ISH on sections)
Anti – DsRed	polyclonal	rabbit	Clontech	1:200
Anti - Mef2 (c-21):sc313	polyclonal	rabbit	Santa Cruz Biotechnology	1:50
Anti - MF20 (anit - myosin)	monoclonal	mouse	Developmental Studies Hybridoma Bank	1:250
Anti - PCNA (Clone PC10)	monoclonal	mouse	Dako Cytomation	1:5000-10000
Anti - Sox9 a/b (paired)	polyclonal	rabbit	Anaspec	1:500
Anti - GFP	polyclonal	chicken	Abcam	1:1500-2000

Anti - VE-Cadherin	polyclonal	rabbit	H.G. Belting, Affolter M.; Wang et al., 2010	1:1000
Anti-BrdU Clone BU 1/75 (ICR1)	monoclonal	rat	AbD Serotech	1:200

Table 2.1 Antibodies used in this study

2.1.4 Transgenic fish lines

Tg(<i>TOP</i> :GFP) ^{w25}		Dorsky et al., 2002
Tg(<i>hsp70l</i> : <i>dkk1</i> -GFP) ^{w32}		Stoick-Cooper et al., 2007
Tg(<i>hsp70l</i> : <i>axin1</i> -YFP) ^{w35}		generated by Gilbert Weidinger
Tg(<i>hsp70l</i> : <i>wnt8a</i> -GFP) ^{w34}		Stoick-Cooper et al., 2007
Tg(<i>myl7</i> :GFP) ^{fl/+}	- (<i>short</i> : <i>cmlc2</i> :GFP)	Burns et al., 2005
Tg(-5.1 <i>myl7</i> :nDsRed2) ^{f2/+}	- (<i>short</i> : <i>cmlc2</i> :dsRed)	Mably et al., 2003
Tg(<i>wt1b</i> :eGFP) ^{li1}		Perner et al., 2007
Tg(<i>fli1</i> :eGFP) ^{y1}		Lawson and Weinstein, 2002
Tg(<i>kdrl</i> :GFP) ^{la116}		Jin et al., 2005
Tg(<i>hsp70l</i> :dTomato p2a Sox9aΔCEngrailed)		this study
	- (<i>short</i> : <i>hsSox9aEng</i>)	
Tg(<i>dusp6</i> :EGFP) ^{pt6}		Molina et al., 2007

2.1.5 Mutant fish lines

<i>axin1</i> ^{tm13/+} (<i>masterblind</i> (<i>mb1</i>)+/- mutant fish)	Heisenberg et al., 2001
<i>jellyfish</i> (<i>jef</i>) ^{fw37} (<i>sox9a</i> +/- mutant fish)	Yan et al., 2002

2.1.6 Primer sequences for identification of *jellyfish*^{fw3} (*sox9a*+/- mutant fish)

Primer name	Primer sequence
fw1	AAGAAGGACGAAGAGGACAAGTT
rw1	AAATTTTCGATGGACATTTCTGAC
fw3	CACGTCAAGAGACCGATGAAC
rw3	ATGTTTTATGAATCATCCCAAGAAA

Table 2.2 Primer sequences for identification of *jellyfish*^{fw3} (*sox9a*+/- mutant fish)

2.1.7 Constructs for generation of mRNA used for injections into embryos

Plasmid insert	vector	source	Sense (S) Digest/Pol	Weidinger database #; information	used concentration for injection
Sox9aEng	pCS2P+	this study	(S) Asp718, SP6	763; dominant negative	15 ng/ μ l
Sox9afl	pCS2P+	this study	(S) Asp718, SP6	767; full length	12,35 ng/ μ l
Sox9b	pCS2P+	this study	(S) Asp718, SP6	856; full length	11,47 ng/ μ l
Sox8	pCS2P+	this study	(S) Asp718, SP6	854; full length	10,4 ng/ μ l
Sox10	pCS2P+	this study	(S) Asp718, SP6	855; full length	13,14 ng/ μ l
GFP	RN3	Wolke et al., 2002	(S) XbaI, T3	53; full length	7,58 ng/ μ l

Table 2.3 Constructs for generation of mRNA used for injections into embryos

2.1.8 Constructs for generation of in-situ hybridization probes

Plasmid insert	vector	source	Antisense (A) Digest/Pol	Weidinger database #
Sox9a	unknown	Chiang et al., 2001	(A) EcoRI, T7	749
Sox9b	unknown	Chiang et al., 2001	(A) StuI, T7	750
Tb18	PCRII	Lepilina et al., 2006	(A) XhoI, T7	386
dGFP (for TOPdGFP)	pCS2P+	Dorsky et al 2002	(A) EcoRI, T7	326
Axin2	pSport1	Stoick-Cooper et al., 2007	(A) Asp,718	302
Snail2	unknown	Yan et al, 2004	(A) EcoRI, T7	799

Pea3	unknown	Raible and Brand, 2001	(A) NotI, T7	913
------	---------	------------------------	--------------	-----

Table 2.4 Constructs for generation of in-situ hybridization probes

2.1.9 *Molecular biology kits*

RNeasy Mini kit	(Quiagen)
Rneasy Micro kit	(Quiagen)
Wizard Plus SVMini preps	(Promega)
Midi kit	(Quiagen)
QIA quick Gel extraction kit (PCR purification/Gel extraction)	(Quiagen)
mMessage mMachine kit	(Ambion, UK)
I-Sce I kit for DNA injection	(NEB)
SP6, T3, T7 RNA polymerase	(Promega)
ApopTag Red in situ Apoptosis Detection Kit	(Chemicon)
Thermo Script RT-PCR system	(Invitrogen)
Brilliant SYBR Green QPCR Master Mix	(Stratagene)
One-Color Microarray-Based Gene Expression Analysis kit	(Agilent)

Used restriction enzymes were purchased from New England Biolabs (NEB) and the DNA ladder was purchased from MBI Fermentas.

For cloning steps, DNA amplification via polymerase chain reaction (PCR) was performed using Phusion High-Fidelity DNA polymerase (NEB).

2.1.10 *Technical equipment*

Spectrophotometer	- Nano Drop NC-1000 Spectrophotometer, Peqlab
Needle puller	- Flaming/Brown Instruments Model – 97, Sutter
Micromanipulators	- Narishige MN-151
Microinjector	- PV820 Pico-Pump with foot pedal, WPI
Pipette holders	- MPH6S
Preparation of cryosections	- Microm HM 560, Thermo Scientific
Homogenizer	- Polytron PT2100 with PT-DA 2105/2EC knife, Kinematica
Analysis of RNA quality	- Agilent 2100 Bioanalyzer, Agilent technologies

MX3000P real-time PCR instrument	- Stratagene
Forceps	- World Precision Instruments (WPI)
Iridectomy scissors	- WPI
Borosilicate glass capillaries	- WPI
Syringe for intraperitoneal Injections	- 0.1 ml #1710, Hamilton
Syringe for RNA preparation	- Omnifix - F 1 ml, B/Braun
Injection needle	- 30 G ¹ / ₂ BD Microlance, 25G ⁵ / ₈ , B/Braun
Pistil	- Roth
Cryo - molds	- Peel-a way, Polysciences
Customized Agilent 44K microarrays	- Agilent

2.1.11 *Microscopes*

fluorescent stereomicroscope	- Olympus MVX10, LEICA MZ 16FA
stereomicroscopes (for sections)	- Olympus BX61
confocal microscopes	- Leica TCS SP5

2.2 Methods

2.2.1 Fish maintenance

Fish were raised and kept under standard laboratory conditions (Westerfield 2000). Embryos were collected after fertilization, maintained in 1x E3 medium at 28,5°C, and staged using developmental time (hours post fertilization, hpf) and according to morphological criteria (Kimmel et al 1995).

Adult fish used in this thesis were approximately between 6-8 month old and had a body length of ~ 30 mm and a heart size of approximately 1.0-1.5 mm. Used fish lines, described in this study were of AB, Wik, TL or Gol background.

2.2.2 Preparation of poly (A)-mRNA for injection into zebrafish embryos

Up to 10 µg DNA of the expression vector, which contains the desired insert was linearized using ~ 40 units of the appropriate restriction enzyme (**Table 2.3**) for 1.5 h at 37°C in a total volume of 100 µl. The expression vector was cleaved after the poly (A) signal sequence to allow mRNA transcription that contains the stabilizing poly (A) signal. Complete linearization of the DNA was checked by electrophoresis with an agarose gel. The linearized DNA was purified via PCR purification kit (Quiagen) and the desired mRNA was produced by *in vitro* transcription with SP6, T7 or T3 polymerase using the mMessage mMachine kit (Ambion, UK). A reaction mix (total volume 20 µl) containing 500 ng – 1 µg of the DNA, 2 µl reaction buffer, 10 µl 2x Nucleotide Mix + Cap analog and 2 µl enzyme mix was incubated for 1 h (for T7 and T3) or 2h (for SP6) at 37°C. The DNA template was digested by incubating with 1 µl DNase I for 20 min at 37°C. RNeasy kit (Qiagen) was used to purify the mRNA, whose concentration was determined with a UV-spectrophotometer and the quality was checked on a gel. Finally the mRNA was stored at -80°C.

2.2.3 Injection of mRNA or DNA into zebrafish embryos

Borosilicate glass capillaries were pulled with a needle puller (Flaming/Brown/Sutter Instruments) to produce injection needles, whose sharp tips were generated using fine forceps under the microscope. The needle was carefully filled with the mRNA or DNA solution using a microloader tip (Eppendorf); all liquid was collected in the tip of the needle without air bubbles to avoid an injection of air bubbles. The injection needle was held by a micropipette holder, which was fixed to a micromanipulator. The drop size released by every needle was adjusted to 1 nl by placing a drop of the injection solution into mineral oil, measuring the volume by the scale bar of a stage micrometer, and modulating the ejection pressure. An applied low constant back pressure ensured that the injection solution did not stream back into the needle.

Injection solutions, which contained either DNA to generate transgenic fish or mRNA to test expression constructs in zebrafish development, were prepared.

Before injections, mRNA stock solutions were thawed on ice, diluted to the desired concentration (**Table 2.3**) with RNase free water and kept on ice.

For DNA injection an injection mix was prepared (total volume 20 μ l), which contained the desired DNA concentration (60ng/ μ l were used), 2 μ l 10x I-Sce I buffer without MgCl₂ (Roche), 2 μ l 50mM MgCl₂, 1 μ l 0.5% phenol red (Sigma), filled to the total volume with DNase free water. The injections mix was kept on ice prior to injection. Immediately before injection 2 μ l of I-Sce I enzyme was added to the DNA solution.

After spawning, embryos were collected in petri dishes with E3 medium and placed in depressions of injection petri dishes, which were produced using a custom made mold. The DNA or mRNA solution was injected directly into the cytoplasm of one-cell stage embryos, which were kept in E3 solution at 28.5°C after injections.

DNA injected embryos were raised to adulthood, crossed with wild-type fish and the progeny were screened for the presence of the transgene using for instance heat-shock experiments. Transgenic progeny were raised to establish transgenic fish lines.

2.2.4 Heat-shock treatment of zebrafish embryos and adult fish

Heterozygous transgenic fish lines used in this thesis (see 2.1.4), which inducibly activate transgene transcription, showed expression of the transgene after heat-shock application during embryonic development or in adult zebrafish.

Zebrafish embryos were allowed to grow to the desired developmental stage at 28.5° and were heat-shocked by directly incubating them in 40°C E3 medium to induce transgene expression. The embryos in the warm E3 medium were incubated for 1h at 37°C and afterwards transferred to 28.5°C. Transgenic embryos of the TG(*hsp70l*:dTomato p2a Sox9aΔC*Eng*railed) fish line were screened for nuclear dTomato expression using a fluorescent stereomicroscope and for function of the Sox9a*Eng* transgene by screening for developmental defects.

Adult zebrafish were heat-shocked by heating the water temperature from 27°C to 37°C within 3 – 10 min. The heat-shock temperature at 37°C was kept for 1 h and dropped afterwards to 27°C within approximately 30 min. The heat-shock was repeated if desired according to the applied heat-shock protocol within 12 or 24 h. To identify transgenic adult fish, the heat-shocked fish were screened for expression of GFP, YFP or dTomato (see 2.1.4) using a fluorescent stereomicroscope.

2.2.5 Identification of heterozygous mutant masterblind (mbl) and sox9a^{-/-} fish via incrosses and/or PCR (mutant Sox9a^{+/-} fish)

Heterozygous masterblind mutant fish *axin1^{tm13/+}* (*masterblind*) were identified by incrosses with siblings and progeny were screened for homozygous mutant phenotypes (Heisenberg et al 2001).

Heterozygous *jellyfish^{tw37}* (*sox9a+/-* mutant) fish were identified either by incrosses with siblings, followed by screening of the progeny for homozygous mutant phenotypes, or by sequencing of the respective genomic region that contains the point mutation (Yan et al 2002). For sequencing DNA generated from fin clips of adult zebrafish and the genomic sequence, which spans the point mutation, was amplified using a first PCR with primer pair one (fw1 + rw1). 2 µl of this PCR product (1.PCR with primer fw1 + rw1) was used for amplification in a second PCR with primer pair two (fw3 + rw3) (**Table 2.2**). 2ng of the PCR product after both PCR rounds was sequenced using primer fw3. The PCR reaction mix used for one PCR (total volume 25 µl): 2.5 µl 10x buffer, 2.5 µl 10x dNTPs, 0.5 µl sense Primer (10pmol/µl), 0.5 µl antisense Primer (10pmol/µl), 2 µl DNA template, 17 µl water, 0.1 µl Taq polymerase enzyme (NEB). The temperature protocol used for both PCR rounds: 94°C for 2 min; 35 cycles of: 94°C for 20 s, 57°C for 30 s, 68°C for 15 s; finally 8°C for cooling.

2.2.6 DNA extraction from fin clips

Fish were anesthetized with 0,02 % Tricaine (MS-222) and half of the caudal fin was cut using a scalpel. The fish was returned to holding tanks and the fin was placed in a reaction tube filled with 20 µl water. 100 µl NaOH (50mM) was added to the tube, which was then heated to 95°C for 20 min. After cooling to 4°C and adding 12 µl Tris HCL (1M, pH 8.0) to neutralize the reaction mix, the sample was centrifuged and the supernatant containing genomic DNA served as template for PCR reactions.

2.2.7 Ventricular heart resection / heart amputation

Fish were anesthetized with 0,02 % Tricaine (MS-222) and transferred to a moist sponge for surgery. The fish was placed upside down and held steady with blunt forceps. After visually locating the posterior medial margin of the heart straight iridectomy scissors were used to puncture the skin and the silvery pericardial sac. Subsequently, an incision was made through both the skin and pericardium starting from the junction of the pericardium and peritoneum and reaching anteriorly for about 2/3 of the length of the heart. The incision was spread open laterally using fine forceps and curved iridectomy scissors were pressed gently onto the belly of the fish to expose the ventricle. The end of the apex was held with the fine forceps. A small piece of the ventricle was removed right below the ends of the fine forceps using the curved iridectomy scissors. The bleeding of the injured ventricle stopped within seconds. With small pieces of cellulose the blood was prevented from flowing into the gills. After surgery the fish were returned to holding tanks. To revitalize the fish a pipette was used to vigorously squirting water over the gills until the fish started to breathe regularly.

2.2.7 Cryoinjury at zebrafish hearts

Fish were anesthetized with 0,02 % Tricaine (MS-222) and transferred to a moist sponge for surgery. The fish was placed upside down and held steady with blunt forceps. After visually locating the posterior medial margin of the heart straight iridectomy scissors were used to puncture the skin and the silvery pericardial sac. Subsequently, an incision was made through both the skin and pericardium starting from the junction of the pericardium and peritoneum and reaching anteriorly for about 2/3 of the length of the heart. The incision was spread open laterally using fine forceps to expose the ventricle. Small pieces of dry ice were formed into a conical shape with a length of ~20 mm, one end with a diameter of ~ 2 mm and the other end with a pointed tip. The pointed tip of the dry ice cone was applied to the posterior apex of the

ventricle for 10 s to cause the cryoinjury. After surgery the fish were returned to holding tanks. To revitalize the fish a pipette was used to vigorously squirt water over the gills until the fish started to breathe regularly.

2.2.8 Control hearts

Control hearts were either derived from untreated fish or sham amputated hearts were used, in which I only opened the pericardial sac but left the heart proper untouched. Both types of controls are not considered injuries of the heart proper, thus control hearts are referred to as uninjured.

To perform sham amputation, fish were anesthetized with 0,02 % Tricaine (MS-222), transferred to a moist sponge and placed upside down. Straight iridectomy scissors were used to puncture the skin and the silvery pericardial sac and an incision was made through both the skin and pericardium. After this, the fish were returned to holding tanks.

2.2.9 Intraperitoneal BrdU injection

BrdU was dissolved in Hank's full strength to a concentration of 6.25 $\mu\text{g}/\mu\text{l}$. Fish were anesthetized with 0,02 % Tricaine (MS-222) and transferred to a moist sponge for injection. The fish was placed upside down and intraperitoneal injections into the abdominal cavity anterior to the paired pelvic fins were performed. 20 μl of the BrdU solution were injected using an injection needle (size 30G1/2) and a syringe (100 μl ; Hamilton). After injection the fish was returned to holding tank and if necessary it was revitalized by squirting water of the gills using a pipette.

2.2.10 Heart extraction / Head harvest

Fish were anesthetized with 0,02 % Tricaine (MS-222) and transferred to water containing crushed ice to euthanize the fish. The dead fish was transferred to a moist sponge, the cavity containing the heart was opened using iridectomy scissors, the heart including the ventricle, the bulbus arteriosus and parts of the atrium was extracted and subsequently transferred to the fixative (4% PFA, 0.1M phosphate buffer, pH 7.5) for fixation at 4°C overnight.

For extraction of heads, the zebrafish were anesthetized with 0,02 % Tricaine (MS-222) and transferred to water containing crushed ice to euthanize the fish. The head and adjacent tissue that includes the heart were removed using a scalpel and immediately transferred to the fixative (2% PFA, 0.1M phosphate buffer, pH 7.5) for fixation at 4°C overnight.

2.2.11 Fixation and processing for sectioning

Fixed hearts were washed for 3 times (10 min) with washing buffer (0,1M phosphate buffer pH 7.4, 4% sucrose) and incubated in 30% sucrose solution (0,1M phosphate buffer pH 7.4, 30% sucrose) for 5 h or overnight at 4°C. Hearts were embedded in Tissue Tek in cryo-molds, frozen and sectioned into 14 µm cryosections. Sections on glass slides were stored at -80°C.

Fixed zebrafish heads were washed for 3 times (20 min) with 0.1M phosphate buffer and transferred for decalcification and cryoprotection to 20% sucrose (w/v), 20% EDTA (w/v) in 0.1M phosphate buffer (pH 7.5) and incubated overnight at 4°C. Subsequently heads were transferred to 7,5% gelatin (w/v), 20% sucrose (w/v) in 0.1M phosphate buffer (pH 7.5) and after incubating the tissue for 30 min at 37°C it was frozen in cryo-molds and sectioned into 14 µm cryosections. Sections on glass slides were stored at -80°C.

2.2.12 Acid Fuchsin Orange G staining (AFOG) staining

Heart sections on glass slides were thawed and dried at RT for 2 h. After incubation in dH₂O for 5 min the sections were incubated in Bouin's solution for 2 h at 60°C and subsequently in

Bouin's solution for 1 h at RT. Sections were rinsed in water for around 30 min and after that they were incubated for 4.5 min in 1% phosphomolybdic acid. After rinsing them in dH₂O for 5 min, the slides were placed in AFOG solution (1g aniline blue, 2g orange G, 3 g acid fuchsin in 200 ml dH₂O, pH 1.09) for 4.5 min and subsequently rinsed again in dH₂O for 2 min. Heart sections were dehydrated by incubating the slides twice in 95% EtOH for 5 min, followed by two incubations in 100% EtOH (each 5 min) and Xylene. Slides were mounted with Cytoseal XL.

2.2.13 *Production of Dioxygenin-labeled antisense riboprobes for in situ hybridization*

10 µg of the plasmid DNA containing the sequence for the desired riboprobe was linearized using 40 units of the appropriate restriction enzyme (**Table 2.4**) for 1.5 h at 37°C in a total volume of 100 µl. Complete linearization was checked by running 1µl of the digested DNA on an agarose gel. The linearized plasmid DNA was purified using PCR purification kit (Qiagen) and the desired riboprobes were produced. 1 µg of the template DNA was mixed with 2 µl dioxygenin-labeled NTPs (Roche), 4 µl 5x transcription buffer (Promega), 0.5 µl RNase inhibitor (RNasin, 40U/µl, Promega), 2 µl 0.1M DTT and 2 µl of the respective RNA Polymerase and the reaction mix was incubated for 2 h at 37°C. The plasmid DNA (template) was removed by addition of 1 µl DNaseI (Promega) and incubation at 37°C for 20 min. After purification using the RNeasy kit and elution in 30 µl RNase free water, the RNA probe was checked on a gel and stored in 100 µl hybridization buffer I at -20°C.

2.2.14 *RNA in situ hybridization on whole-mount hearts*

Fixed whole mount hearts were rinsed 3 times in PBT, dehydrated using incubation steps in 25%, 50%, 75% MetOH / PBT and 100% MetOH (each 5 min) and stored at -20°C for at least

overnight. Afterwards, hearts were rehydrated using incubation steps in 75%, 50%, 25% MetOH / PBT (each 5 min), which was followed by four washes in PBT. For tissue permeabilization, the hearts were incubated in proteinase K (10 µg/ml in PBT) for 30 min at RT. The digestion was stopped by two washes in PBT and refixation (in 4% PFA, 0.1M phosphate buffer, pH 7.5) for 20 min. Subsequently hearts were rinsed five times in PBT and prehybridized with prewarmed hybridization buffer I for 2-6 h at 67°C. The probe was diluted (1:250) in hybridization buffer I and after heating the probe mix to 67°C it was added to the hearts. After hybridization overnight at 67°C the probe mix was removed and the hearts were washed with hybridization buffer I at 67°C for 20 min. Subsequently, hearts were washed with 50% SSCT 2x/ 50% formamide (3 x 20 min), SSCT 2x (twice for 20 min), SSCT 0.2x (4 x 30 min) and finally once with PBT for 5 min at RT. After incubation in blocking buffer (5% heat-inactivated sheep serum, 10mg/ml BSA in PBT) for 2h at RT under slow agitation, the hearts were incubated in anti-Dig antibody containing solution (preabsorbed; 1:2000-1:4000 in PBT + 2mg/ml BSA) for 24 h at 4°C. Subsequently, the samples were rinsed twice in PBT and washed 6 – 8 times with PBT during the next 3 h at RT. For equilibration the hearts were washed 3 x 5 min in staining buffer and meanwhile the last wash, the samples were transferred to a 24 well plate. Subsequently, staining solution that contained NBT/BCIP according to manufacturer's instructions in staining buffer was prepared and added to the samples. The staining reaction was performed for several hours at RT or overnight at 4°C and stopped using two washes in PBT and STOP solution. The hearts were further washed twice in 100% EtOH (each 15 min) under slow agitation, one incubation in 50% EtOH (5 min) and 4 washes in PBT (each 5 min). Finally the samples were kept in 80% glycerol/ 20% STOP.

2.2.15 RNA in situ hybridization on heart sections

The probe mix containing 2.5 µl of the desired probe diluted in 500 µl hybridization buffer II was heated to 70°C for 10 min to denature the probe. Heart sections on glass slides were

thawed at RT for 1h and placed in a humidified chamber, which was prepared using a filter paper wetted with 1x salt/ 50% formamide. After adding the probe mix onto the slides, coverslips were used to prevent drying of the sections. Subsequently, samples in the humidified chamber were incubated for overnight at 67°C.

For washing steps on the next day, coverslips were removed and slides were washed 4 times in washing solution (1x SSC, 50% formamide, 0.1% Tween 20) at 67°C for 1 x 15 min and 3 x 30 min. Slides were further washed 3 x 30 min in MABT (MAB, 0.1% Tween 20) at RT. After washing steps, blocking solution II was added onto the slides and samples were incubated for 2-3 h in the humidified chamber, which was prepared using a filter paper wetted with PBS. The blocking solution II was removed and the samples were incubated in anti-Dig antibody solution (anti-Dig antibody 1:5000 in blocking solution II) for overnight at 4°C. On the next day, several washes with MABT (5 x 20 min) were performed and subsequently sections were equilibrated twice for 10 min in staining buffer. The staining solution, which contained NBT/BCIP according to manufacturer's instructions in staining buffer, was prepared and added onto the sections. The staining was checked using a stereomicroscope and the staining reaction was stopped according to the staining intensity with several washes in PBT (at least 10 x within 6 hours) and mounted in 70% glycerol/ 30% PBS. If additional antibody staining was performed slides were not mounted, instead antibody staining reactions were started.

All incubations were performed in a humidified chamber, while all washes were performed in coplin jars.

2.2.16 *Antibody staining on heart sections*

Most antibody staining were performed using PEM buffer, which is described in the following, while for few cases like GFP antibody staining after in situ hybridization for *tbx18*

PBT buffer (PBS, 0.1% Tween20) instead of PEM buffer were used with the same incubation times.

At first, heart sections on glass slides were thawed at RT for about 1h and thereafter rehydrated using PEMTx (PEM, 0.2% Triton – X 100). For blocking of unspecific binding sites, sections were incubated in NCS-PEMTx blocking solution (10% newborn calf serum, 1%DMSO in PEMTx) for at least 1 h at RT. Subsequently sections were incubated in primary antibody diluted in NCS-PEMTx (for appropriate dilution see **Table 2.1**) at 4°C overnight. On the next day sections were washed 3 x 20 min with PEMTx and incubated with the secondary antibody from the Alexa class of fluorophores diluted 1:1000 in NCS-PEMTx for 45 min at RT. After this the sections were washed 3x 20 min.

For costaining with antibodies that detect Sox9, PCNA or BrdU, I continued with protocols described in 2.2.16.1 and 2.2.16.2.

If the antibody staining procedure was finished, the sections were incubated for 10 min in Dapi (4ug/ml (w/v) Dapi in PEM) and washed again 3 x 20 min in PEMTx. Finally sections were incubated in PEM and mounted in 70% glycerol/PEM.

All incubations were performed in a humidified chamber, while all washes were performed in coplin jars.

2.2.16.1 Sox9 and PCNA antibody staining

Antigen retrieval treatment was used to detect PCNA or Sox9 proteins. Sections were incubated in 10mM sodiumcitrate buffer, pH 6 for 10 min at 85°C. Subsequently sections were washed 3 x 20 min in PEMTx and incubated in blocking solution NCS-PEMTx for 1 h at RT. Staining was continued with the primary antibody described above.

2.2.16.2 *BrdU antibody staining*

Sections, stained before for another primary antibody, were incubated in 2M HCL for 30 min at RT. Subsequently, sections were washed 3 x 20 min with PEMTx and incubated in blocking solution NCS-PEMTx for 1h at RT. Thereafter, sections were treated with the primary antibody as described above

2.2.16.3 *Detection of apoptosis*

TUNEL staining was performed on 14 µm cryosections using the ApopTag Red *in situ* Apoptosis Detection Kit (Chemicon) according to manufacturer's instructions. Briefly, PFA-fixed hearts were sectioned and after incubation in PBS, sections were post fixed in Ethanol:Acetic acid (2:1) at -20°C for 5 min. After several washes in PBS, sections were incubated in Equilibration buffer and subsequently in a solution containing TdT Enzyme and reaction buffer for 1 h at 37°C. The reaction was stopped with Stop/Wash buffer and several washes in PBS and slides were incubated in antidioxigenin-rohdamine conjugate containing solution for 30 min. The staining was finished by several washes in PBS and incubation in Dapi solution. Slides were mounted in 70% glycerol, PBS.

2.2.17 *Electron microscopy and tuloidin blue staining*

(Experiments of this part were performed by Thomas Kurth. Imaging and analysis of EM pictures were done by Thomas Kurth. Analysis and imaging of tuloidin blue stained sections were done by Kristin Schnabel and Thomas Kurth.)

For semi-thin sections and electron microscopy, zebrafish hearts were fixed in modified Karnovsky's fixative (2% glutaraldehyde + 2% paraformaldehyde in 50 mM HEPES, (Karnovsky 1965, Kurth et al 2010) at 4°C overnight, and washed 2x in 100 mM HEPES and 2x in PBS. For light microscopy the samples were embedded in the methacrylate Technovit

7100 (Heraeus-Kulzer). They were transferred to a microwave-assisted tissue processor (Leica-EM AMW) and processed according to the following protocol: PBS (2x 3 min at 35°C, 15 W), 1% OsO₄ in PBS (30 min at 50°C, 25 W, pulse: 10 s MW on, 50 s MW off), PBS (4 min at 37°C, 15 W), 2x water (4 min at 37°C, 17 W), 30%, 50%, 70%, 95% and 2x 100% ethanol (5 min each at 37°C, 15 W / 11 W), Technovit 7100:ethanol (1:1) (15 min at 37°C, 11 W), Technovit 7100:ethanol (2:1, 3:1) (20 min each at 37°C, 11 W), pure resin (20 min at 37°C, 11 W). After the AMW run, samples were transferred to fresh Technovit resin overnight, and finally embedded. 2 µm sections were mounted on glass slides and stained with 1% toluidin blue 0.5% borax.

For electron microscopy, the specimens were postfixed with 1% OsO₄/water for 2 h on ice, washed with PBS and water, and *en bloc* contrasted with 1% uranyl acetate in water. The samples were then washed several times in water, dehydrated in a graded series of ethanol, infiltrated in epon 812 (epon/ethanol mixtures: 1:3, 1:1, 2:1, 3:1 1.5 h each, pure epon overnight, pure epon 3 h), and embedded in flat embedding molds. Ultrathin sections were collected on formvar-coated slot grids, stained with lead citrate and uranyl acetate according to Venable and Coggeshall (1965), and analyzed on a FEI Morgagni 268 at 80 kV.

2.2.18 Imaging

In general, sections stained with AFOG histological staining or by in situ hybridization were analyzed using Olympus upright microscope. Immunohistochemistry was analyzed using Leica SP5 confocal microscopes. Fluorescent stereo microscope was used for embryo imaging.

2.2.19 Total RNA production from embryos and hearts

Total RNA was produced from regenerating and uninjured adult zebrafish hearts or from zebrafish embryos at different developmental stages.

Zebrafish embryos were dechorionated using forceps and placed in 500 μ l Trizol in a 2 ml reaction tube. Embryos were thoroughly homogenized using a Polytron homogenizer at 4°C. 300 μ l Trizol were added, the suspension was mixed, incubated for 5 min at RT and stored at -80°C.

Heart were extracted and the lower half containing the apex or regenerating tissue was collected in a 1.5 ml reaction tube, which was placed immediately in liquid nitrogen. For each time point 6-8 hearts were collected into the collection tube, which was always stored in liquid nitrogen. Subsequently the tube was placed on dry ice and hearts were homogenized using a pestil. 500 μ l Trizol were added and heart pieces were further homogenized using a 1 ml syringe (used injection needle: first 25G5/8, second 30G1/2). 300 ml Trizol were added and after incubating the suspension for 5 min at RT, the sample was stored at -80°C.

After thawing the samples, remaining cell debris was pelleted at 4°C and RNA containing supernatant was transferred to a fresh tube. 215 μ l chloroform was added, the sample was mixed, incubated for 10 min at RT and centrifuged at 13000 x g for 15 min (4°C) to separate the aqueous from the organic phase. The aqueous RNA containing phase (upper phase) was transferred to a fresh tube, mixed with 2 μ l glycogen (2mg/ml glycogen solution, Roche) and after that mixed with 400 μ l isopropanol to precipitate the RNA. After centrifugation (13000 x g for 30 min, 4°C), the isopropanol was poured off and subsequently the pellet was washed with 70% EtOH and centrifuged again (13000 x g for 10 min, 4°C). EtOH was removed and after drying the RNA pellet was resuspended in 17 μ l RNase free water.

To remove genomic DNA, the sample was incubated with 1 μ l DNase I, 2 μ l 10x DNase I reaction buffer (both Invitrogen) for 15 min at RT according to manufacturer's guidelines. The DNase was inactivated using 2 μ l 25 mM EDTA and incubation at 65°C for 10 min. The

resulting RNA samples were purified using RNeasy Micro kit (Qiagen). The RNA concentration and quality were checked using a UV-spectrophotometer and a Bioanalyzer (Agilent).

2.2.20 *cDNA synthesis*

cDNA was synthesized using the Thermo Script RT-PCR system of Invitrogen. The reaction mix contained 50 ng total RNA, 0.5 μ l random hexamers, 0.5 μ l oligo (dT) primers, 10mM dNTP mix and was adjusted to 12 μ l with RNase free water. RNA and primer were denatured by incubating the sample for 5 min at 65°C. A reaction mix out of 4 μ l 5x cDNA Synthesis buffer, 1 μ l 0.1M DTT, 1 μ l RNaseOUT, 1 μ l RNase free water and 1 μ l ThermoScript RT was added to the denatured RNA/primer mix. cDNA was synthesized by incubating the reaction mix at 25°C (10 min) followed by an incubation at 50°C (50 min). The reaction was terminated by heating to 85°C (5 min). Addition of 1 μ l RNase H and incubation at 37° for 20 min was used to remove the template RNA. The resulting cDNA sample was stored at -20°C

2.2.21 *quantitative PCR*

The Brilliant SYBR Green QPCR Master Mix (Stratagene) was used for quantitative PCR according to manufacturer's instructions that are recommended for use in Mx3000P PCR machines. The amplification protocol for short target was changed to 95°C for 10 min and 40 cycles with 95°C 30s, 58°C 30s, 72°C 30s. The dissociation protocol of the MX3000P real-time PCR instrument (95°C 1 min, 55°C 30s, with fluorescent measurement up to 95°C 30s) was used.

2.2.22 Generation of constructs

Vector NTI software (Invitrogen) was used to plan cloning steps. Genes, gene fragments and fusion constructs were cloned/generated according to standard protocols described in Sambrook and Russel (2001) and by using commercial kits according to manufacturer's instructions (see 1.1.9).

A cDNA library of regenerating hearts and developing embryos at different stages was used to amplify full length cDNA of zebrafish (zf) *sox9a* (NM_131643), *sox9b* (NM_131644), *sox8* (NM_001025465), *sox10* (NM_131875), which was followed by subcloning into pCS2P+ vector for synthesizing RNA for injection into zebrafish embryos. Additionally, a C-terminal deletion construct of *sox9a* (*sox9aΔC*) that still contains the complete N-terminus including the HMG domain and additional protein-protein interaction domains (aa 1 - aa 264 of NM_131643) was amplified and fused with the sequence of the Engrailed transcriptional repressor domain (Leung et al., 2003). The resulting fusion construct *sox9aΔCEngrailed* (abbr: *sox9aEng*) was likewise cloned into pCS2P+ vector for *in vitro* RNA synthesis and injection into zebrafish embryos.

The repressor *sox9aEng* was cloned into Bluescript II vector, which contains an I-SceI meganuclease site, to generate transgenic zebrafish. This vector also contained the Hsp70I promoter (Halloran et al 2000) for heat-shock inducible expression of the downstream *nuclear dTomato* (Clontech) and the *sox9aEng*, which were separated by a *p2a* sequence to allow translation of separate proteins from a single open reading frame (Provost et al 2007).

2.2.23 Microarray expression analysis

2.2.23.1 Annotation of the microarray

Customized Agilent 44K microarrays that provide a nearly genome wide coverage were created in collaboration with Herman Spink at the University of Leiden (Netherlands). Probe

sequences used in the microarray were mapped against 5 separate transcript datasets (NCBI, RefSeq, Ensembl, ZFIN (Sprague et al 2006), Unigene and NCBI nucleotide records relating to *Danio rerio*) using BLAST (Altschul et al 1990) while a maximum of 2 mismatches was accepted. Additional mapping was performed against the ZFISH8 genome assembly and the Ensembl release 54 genomic annotations. This mapping accepted 3 mismatches and assigned probes that were located 1,250 bases 3' or 5' of an annotated gene. For combining the assignments, all transcripts were mapped to the ZFISH8 genome assembly using Spidey (Wheelan et al 2001). After this, transcripts were assigned to genes based on their genomic locations. Over-representation calculations were performed using the unified gene IDs.

2.2.23.2 Functional annotation of the microarray

The functional annotation was received from the following sources: NCBI RefSeq (Wheeler et al 2005) was used for gene descriptions; InterProScan (Zdobnov and Apweiler, 2001) from EBI was used to annotate functional domains; molecular function and biological process data were obtained from both the Panther Ontology (via iprscan, (Zdobnov and Apweiler, 2001) and Gene Ontology ((Ashburner et al 2000) via NCBI RefSeq annotations). Additional information was retrieved from the NCBI Entrez system by automated data mining. Inparanoid 2.0 (Remm et al 2001) was used to determine orthologues in *Homo sapiens* with a 95% confidence cut-off. ZFIN was also used to retrieve gene expression data, which were incorporated based on the unified gene IDs.

2.2.23.3 Microarray processing and data analysis

RNA samples of regenerating and control hearts were generated according to experimental protocols described in section (3.1.2.3 Fig 3.1.5 A and B, 3.4 Fig 3.4.1). All microarray experiments were performed with three independent biological samples.

To produce C3-labeled cRNA, 200ng of each RNA sample was processed using the “One-Color Microarray-Based Gene Expression Analysis” - kit (Agilent) according to manufacturer’s instructions in collaboration with the MPI-CBG DNA Array Facility (Dresden). Arrays were hybridized with C3-labeled cRNA, scanned and expression data was generated with feature extraction software (FE Version 10.1.1.1, Protocol GE1-v5_95_Feb07, FE Grid 015645_D_F_20061219) by the MPI-CBG DNA Array Facility (Dresden). Quality control reports were checked by the Facility and if necessary, hybridization of samples was repeated.

Data were analyzed using Partek Genomic Suite 6.4 (Partek Incorporated, St.Louis, U.S.A.). After importing feature extraction data into Partek, the data was normalized according to quantile normalization. Expression data of all samples were analyzed statistically using One-way ANOVA (Eisenhart, 1947) and the Partek “Contrast” feature (Tamhane and Dunlop, 2000) was used for the respective pairwise comparisons. For correction of the p-values the False Discovery Rate (FDR) was calculated.

Genes differentially regulated at either of the examined time points after ventricular resection (2, 4, 7, 14 days post amputation (dpa)) versus control hearts were used for hierarchical clustering based on similarity of their expression pattern. Hierarchical clustering of the genes was carried out according to Pearson’s dissimilarity and average linkage using Partek.

2.2.23.4 Statistical analysis of functional and expression annotation based on Panther database

(Statistical analysis of this part was done by Charles Bradshaw)

The remapped array, based on the unified gene IDs, was used as functional background to statistically analyze for instance the occurrence of all annotations terms. For each of the annotation terms, such as Panther Process or Panther Function, the probability of occurrence

of each term was calculated based on the occurrence of a term in the functional background library. P - values of occurrence of a term within the genes identified on a given array were calculated based on a hypergeometric distribution (cumulative probability mass function). After ranking of the p-values, it was determined which terms were overrepresented. Data presented in this study refer to analysis of the biological process level I, defined according to the Panther database.

3.1.1 Is Wnt/ β -catenin signaling active during zebrafish heart regeneration?

How signaling pathways regulate heart regeneration in zebrafish remains largely unknown. Therefore I aimed to identify molecular signals that are crucial for the regeneration process. Wnt/ β -catenin signaling, the so called canonical Wnt pathway, is potentially interesting as it is critical for vertebrate cardiac development (Clevers 2006, Eisenberg and Eisenberg 2006). In addition, Wnt signaling is activated and essential for zebrafish fin and liver regeneration in zebrafish (Stoick-Cooper et al 2007), leading to the assumption that Wnt pathway might have an important role during heart regeneration. This idea is supported by the fact that the β -catenin responsive reporter activity in transgenic Tg(*TOP:GFP*)*w25* (in short: TOPdGFP fish), in which 4 TDF/Lef binding sites drive the expression of GFP, is upregulated at the amputation plane at 3 days after surgery (**Fig 3.1.1 A**) (Stoick-Cooper et al 2007). Thus I characterized the domains of active Wnt/ β -catenin signaling in the regenerating heart and used loss-of-function and gain-of-function approaches to examine the necessity of that pathway for the regeneration process.

Heart injuries were performed using ventricular resections. Furthermore, during my experiments, I used either hearts of untreated fish or sham amputated hearts, in which I only opened the pericardial sac but left the heart proper untouched. Both types of controls are not considered injuries of the heart proper, thus controls are referred to as uninjured. However, Wills et al (2008) have shown that opening of the pericardial sac can lead to induction of certain cardiac genes; thus, in some experiments sham amputation was performed as a control, which is then also indicated in the figure legend.

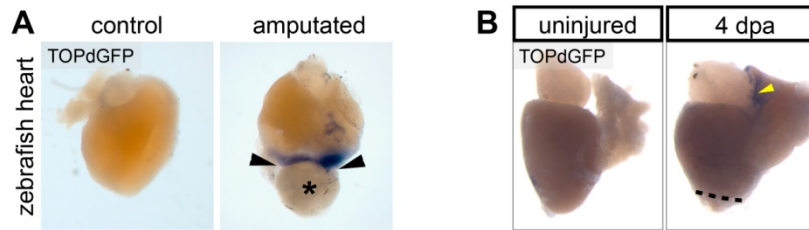
To test the potential role of Wnt/ β -catenin signaling in heart regeneration, I first examined the regions of active signaling in non-regenerating and regenerating hearts of TOPdGFP fish. Specifically, I analyzed hearts at 3, 4 and 7 days post amputation (dpa) and compared them to the corresponding uninjured control hearts.

Upregulation of GFP at the amputation plane of TOPdGFP fish hearts could however not be reproducibly detected by whole mount RNA in situ hybridization at 4 dpa and 7 dpa in comparison to the uninjured controls (**Fig 3.1.1B** and data not shown). After prolonged staining, a weak signal was detected on the surface of the heart, presumably marking the epicardium but not the myocardium (**Fig 3.1.1B**).

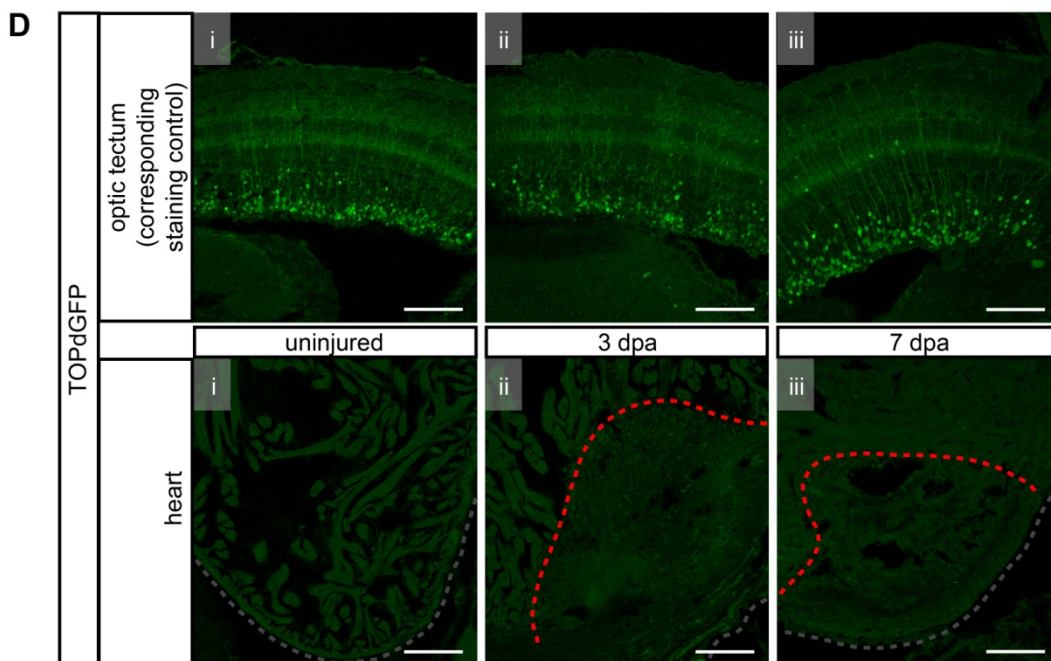
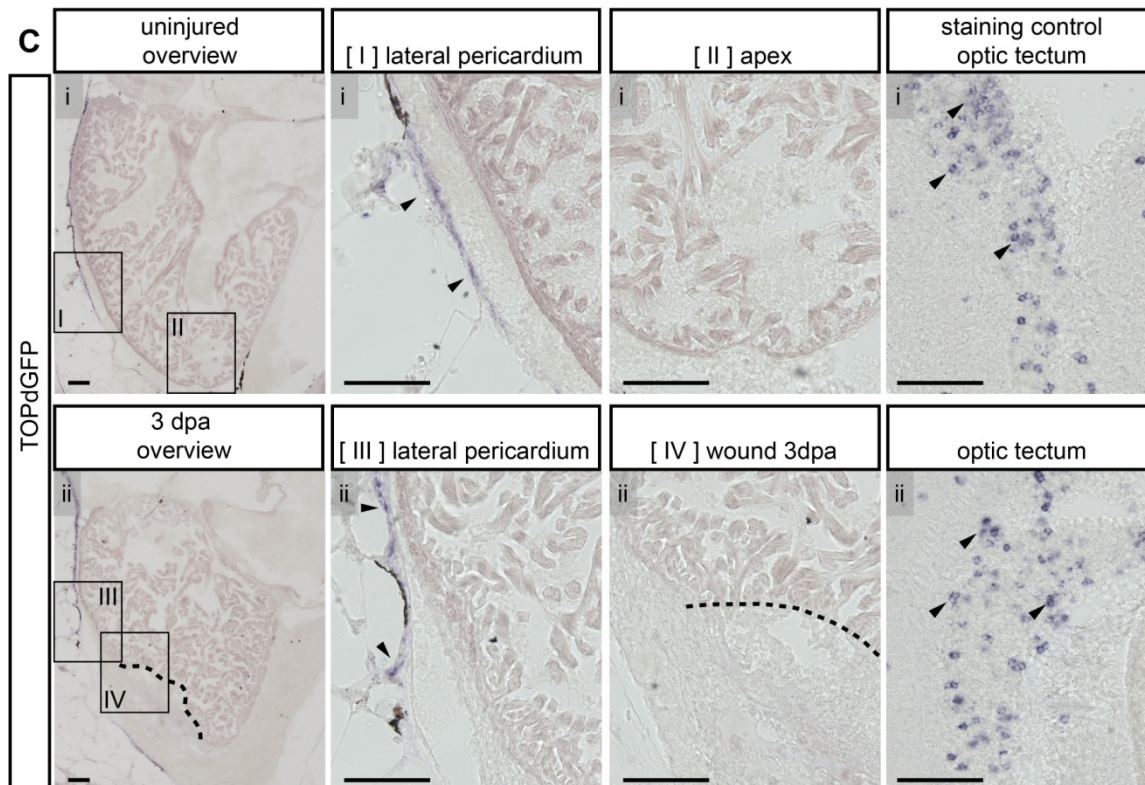
Smith and colleagues previously showed that whole mount in situ hybridization on adult tissue has a limited capacity to detect internal expression domains such as certain central parts of a regenerating fin (Smith et al 2008).

To overcome this limitation and to examine regions with potential active Wnt/ β -catenin signaling in TOPdGFP transgenic fish, I performed in situ hybridization on sections of 3 and 7 dpa hearts and with uninjured hearts as control (**Fig 3.1.1C** and data not shown). Since Wnt/ β -catenin signaling has been shown to be active mostly in neuronal cells of the optic tectum (Nyholm et al 2007; unpublished observations of J. Kaslin), sections of optic tectum from amputated (ii) and uninjured (i) fish to test *gfp* antisense RNA probe quality, tissue preparation and staining procedures. GFP positive cells were clearly detected in the paraventricular layer of the optic tectum in the zebrafish telencephalon, confirming the reliability of the applied protocols. TOPdGFP expression, however, was not detectable in the wounded ventricle (**Fig 3.1.1C**). In contrast, the pericardial sac of amputated as well as uninjured hearts showed TOPdGFP expression which thus indicates non-regeneration specific staining (**Fig 3.1.1C**). The pericardial sac strongly adheres to the wound edges of regenerating hearts; thus it might be possible that the TOPdGFP staining in amputated hearts as observed by Stoick-Cooper et al (2007) results from pericardial sac tissue attached to the extracted heart.

Likewise, no GFP protein expression could be detected by anti-GFP antibody staining in the ventricle of TOPdGFP hearts at 3 dpa and 7 dpa, while it was readily detected in the optic tectum of the brain, which was used as a positive control for active Wnt/ β -catenin signaling (**Fig 3.1.1D**).



Stoick-Cooper et al 2007



3.1.1 Active Wnt/ β -catenin signaling was not reproducibly detectable in TOPdGFP reporter fish during zebrafish heart regeneration.

A. In situ hybridization on whole mount TOPdGFP hearts (control and at 3 days post amputation (dpa)) performed by Stoick-Cooper et al (2007) shows *gfp* RNA expression and thus active β -catenin signaling at the amputation plane. Amputation plane in the 3 dpa heart is indicated by black arrowheads. (Modified from Stoick-Cooper et al 2007).

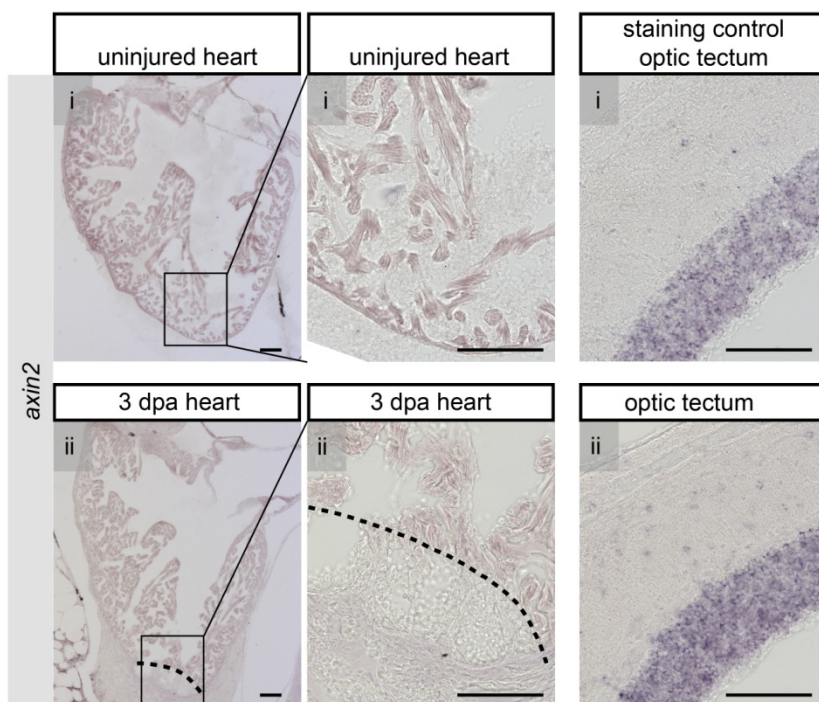
B. Hearts of sham amputated (uninjured control) TOPdGFP fish and at 4 dpa stained for *gfp* expression using whole mount in situ hybridization. Expression of *gfp* at the amputation plane (black dashed line) is not detectable. Weak *gfp* signal can be seen at heart surface (yellow arrowhead). All examined time points n=5 hearts each.

C. TOPdGFP reporter is active in pericardium of uninjured (i) and amputated (ii, 3 dpa) fish. Ventricular apex and wound area (insets II and IV) do not show *gfp* expression as assayed by in situ hybridization. Pericardium (black arrowheads in insets I and III) and corresponding optic tectum (black arrowheads in optic tectum) of the same fish show *gfp* mRNA expression in both uninjured and injured hearts. Scale bars are 100 μ m. 3 dpa n= 3 fish, uninjured n = 3 fish (further tested but not shown: 4 dpa n = 15 hearts, uninjured = 15 hearts; 7dpa n = 6 hearts, uninjured n = 5 hearts)

D. Antibody staining shows GFP expression in the optic tectum of TOPdGFP fish but not in corresponding hearts at 3 dpa and 7 dpa at the wound border (indicated by red dashed line). Uninjured heart (i), heart at 3 dpa (ii) and 7dpa (iii) and corresponding optic tectum of the same fish are shown. Ventricle outline is indicated by gray dashed line. Scale bars are 100 μ m. n = 3 fish; 7dpa n = 8 hearts (further tested but not shown: 4 dpa n = 3 hearts, uninjured = 5 hearts)

While I could not detect TopdGFP expression both at the RNA and protein level in injured hearts, I wondered whether endogenous putative direct Wnt/ β -catenin target genes might be upregulated in response to heart injury. I thus assayed the expression of *axin2* and *lef1*, which have been described to be directly regulated by the canonical Wnt pathway in several systems (Clevers 2006, Skokowa and Welte 2007, Jho et al 2002). *axin2* mRNA was not detected with in situ hybridization on amputated hearts during early regeneration (3, 4 and 7 dpa) (**Fig. 3.1.2** and data not shown). In contrast, *axin 2* was present in the optic tectum, which served again as positive control for active Wnt signaling (**Fig.2**). Furthermore, I analyzed the expression pattern of *lef1* mRNA on sections of amputated and uninjured hearts at 3 dpa using in situ hybridization. Sections of the optic tecum were used as positive control and showed *lef1* mRNA expression pattern in regions of active Wnt signaling. However, a staining of *lef1* mRNA was not detectable in the amputated as well

as uninjured ventricle (data not shown). Additionally I tested the expression level of *lef1* mRNA at multiple time points (2 dpa, 4 dpa, 7 dpa and 14 dpa) with quantitative PCR (qPCR) and did not detect a reproducible amputation specific upregulation of its expression (data not shown).



3.1.2. Active Wnt/ β -catenin signaling is not detectable using in situ hybridization for *axin2* mRNA.

axin2 staining is absent in the uninjured or amputated heart at 3 dpa but is present in corresponding positive controls, the optic tectum of the same fish. Uninjured heart (i) and heart at 3 dpa (ii) are shown.

Wound plane is indicated by black dashed line. Scale bars are 100 μ m. 3 dpa n = 2 fish, uninjured n = 2 fish (further tested but not shown: 4 dpa n = 14 hearts, uninjured = 13 hearts; 7 dpa n = 4 hearts, uninjured n = 4 hearts)

In conclusion, an amputation specific upregulation of Wnt signaling in the heart was not detectable in the TOPdGFP reporter line. Induction of endogenous Wnt targets (*axin2*, *lef1*) as a readout for activated Wnt signaling was not seen - neither at 3 nor at 7 days post amputation. Thus transcripts of Wnt/ β -catenin target genes were not detectable mainly by in situ hybridization. However, using in situ hybridization method I could detect other transcripts in the heart (see 3.2.1.1), indicating that this method works in zebrafish hearts. Hence, Wnt/ β -catenin target genes (TOPdGFP, *axin1*, *lef1*) are not expressed in the regenerating zerbafish heart.

3.1.2 Overactivation or inhibition Wnt/ β -catenin signaling did not influence heart regeneration

3.1.2.1 The tools

My failure to detect evidence for activated Wnt/ β -catenin signaling in the injured ventricle could potentially be due to silencing of the TopdGFP reporter in the myocardium, or due to the characteristics of the tissue which lower the signal-to noise ratio of in situ and immunofluorescence in the heart muscle compared to brain tissue. Thus my negative data do not allow me to exclude a potential role of Wnt/ β -catenin signaling in heart regeneration. Thus I tested whether other Wnt target genes are activated and whether Wnt/ β -catenin signaling has a functional role during heart regeneration and by using transgenic and mutant fish lines to interfere with the pathway during the regeneration process. Overexpression of negative modulators like Dkk1 (secreted inhibitor of Wnt/ β -catenin signaling) or Axin1 (component of the β -catenin destruction complex) allows inhibition of the canonical Wnt signaling pathway (Stoick-Cooper et al 2007; Kagermeier-Schenk et al – in revision). Therefore I used the heterozygous transgenic fish lines hsDkk1GFP (Tg(*hsp70l:dkk1*-GFP)w32) and hsAxin1YFP (Tg(*hsp70l:axin1*-YFP)w35) in which a heat-shock inducibly activates the respective negative modulator (Stoick-Cooper et al 2007; Kagermeier-Schenk et al – in revision). In addition to loss of function studies Wnt gain of function tests were performed. To activate β -catenin signaling, I used heterozygous hsWnt8a-GFP (Tg(*hsp70l:wnt8a*-GFP)w34) fish enabling heat-shock inducible overexpression of Wnt8a (Stoick-Cooper et al 2007). The influence on the Wnt/ β -catenin pathway is detectable on the transcriptional level as indicated by microarray studies in the Weidinger laboratory. Inhibition or overactivation of Wnt/ β -catenin signaling using the respective transgenic fish line causes the downregulation or upregulation of Wnt target genes in embryos (Kagermeier-Schenk et al – in revision). An ectopic overactivation of Wnt signaling is also observed in masterblind (*axin1*^{tm13/+}) mutant fish that are deficient for Axin1, an essential component of the β -catenin destruction complex (Heisenberg et al 2001). Due to the lethality of homozygous masterblind mutants, I used heterozygous mutants to analyze adult heart regeneration.

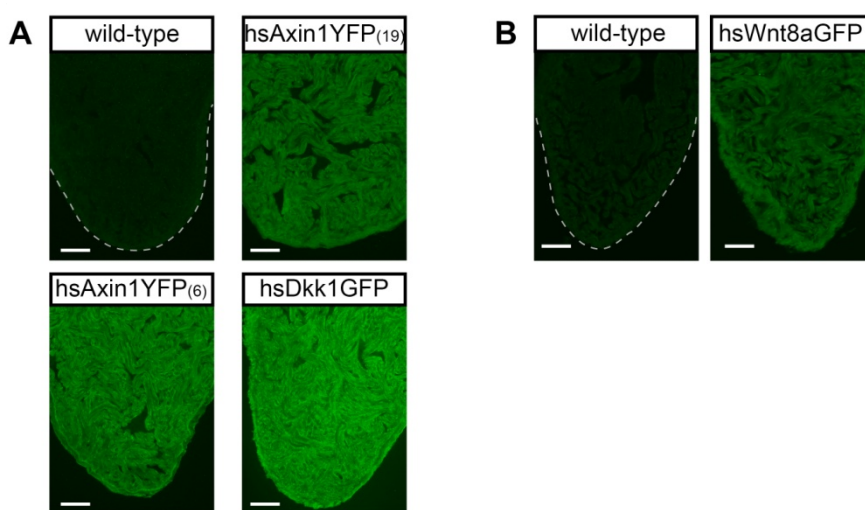
First I checked all transgenic fish lines that were used in this study for expression of the respective transgene after heat-shock in the adult heart. Therefore I heat-shocked

transgenic as well as wild-type fish and explanted the hearts two hours after induction. To detect the transgene I performed antibody staining for the C-terminally fused fluorescent molecules GFP and YFP.

While GFP or YFP staining was absent in wild-type sibling fish I detected a strong induction of Dkk1GFP in hsDkk1GFP fish (**Fig 3.1.3A**). Furthermore I tested two hsAxin1YFP fish lines with different YFP intensities and detected higher expression levels of Axin1YFP in line number 6 hsAxin1YFP⁶ compared to line number 19 hsAxin1YFP¹⁹ as reflected by strength of fluorescence. Intriguingly, I observed decreased survival rate for line 6 after application of heat-shocks for a longer period. This effect was not evident in transgenic fish of line 19. Thus I used the two different hsAxin1YFP fish lines for differential experimental purposes. In general I used hsAxin1YFP⁶ for short term experiments to provide a strong induction of Axin1YFP while the hsAxin1YFP¹⁹ fish line was used in long term loss of function studies.

Finally, I tested hsWnt8a-GFP fish and detected a very weak induction of Wnt8aGFP after a single heat-shock (data not shown). To induce higher Wnt8a-GFP levels I applied a second heat-shock after 12 hours and extracted the heart two hours after the second heat-shock. In contrast to wild-type I detected a strong expression of Wnt8aGFP in the transgenic heart, indicating that Wnt8aGFP protein accumulated after a second induction (**Fig 3.1.3B**).

Since induction of the transgenes could be shown in the heart, I used the transgenic fish lines for Wnt loss and gain of function studies.



3.1.3 Transgenic lines to inhibit or overactivate Wnt/beta-catenin signaling displayed transgene expression in the heart.

A. Wild-type fish and transgenic fish of hsAxin1YFP⁶ (hsAxin1YFP line 6), hsAxin1YFP¹⁹ (hsAxin1YFP line 19) and hsDkk1GFP (hsDkk1GFP) were heat-shocked. Hearts were extracted 2 hours after the heat-shock and sections were stained for YFP and GFP expression using anti-GFP antibody staining. YFP and GFP induction is detectable in all transgenic lines with lowest expression of YFP in hsAxin1YFP line 19, a stronger YFP signal in hsAxin1YFP line 6 and a very strong GFP signal in hsDkk1GFP hearts. Gray dashed line indicates outline of the wild-type ventricle, which shows no GFP signal. Scale bars are 100 μ m.

B. Wild-type and hsWnt8a-GFP (hsWnt8aGFP) fish were heat-shocked twice (the second heat-shock after 12 hours (h)). Hearts were extracted 2 h after the second heat-shock and sections were stained for GFP expression. GFP signal was absent in wild-type hearts but present in hsWnt8aGFP hearts. Gray dashed line indicates outline of the wild-type ventricle, which shows no GFP signal. Scale bars are 100 μ m.

3.1.2.2 Does Wnt signaling influence early events in heart regeneration?

Some of the earliest events described in zebrafish heart regeneration are the appearance of cells at the amputation plane that express transcription factors involved in heart development such as *hand2*, *nkx2.5*, *tbx20* and *tbx5* (Lepilina et al 2006). Furthermore *tbx18* and *raldh2*, expressed in the developing embryonic epicardium, are also activated in the epicardium of amputated hearts but are absent in uninjured hearts (Kraus et al 2001; Lepilina et al 2006). However signaling pathways that regulate these early events in heart regeneration are so far unknown.

Wnt/ β -catenin signaling has been described to promote the expression of early cardiac genes in embryonic stem cells (Kwon et al 2007). Thus I tested whether Wnt/ β -catenin signaling is required for the expression or maintenance of these early genes during heart regeneration.

Therefore I amputated heterozygous transgenic fish of the hsDkk1GFP fish line and their wild-type siblings and additionally used uninjured control hearts of sham amputated fish. The transgene was induced 6 hours before amputation or sham amputation. Starting 24 hours after surgery I applied additional heat-shocks every 12 hours until 7 dpa to provide high Dkk1GFP expression levels during the first phase of regeneration (**Fig 3.1.4A**). I performed qPCRs on the apical half of the hearts and compared amputated Dkk1GFP

induced hearts with amputated wild-type hearts for mRNA levels of cardiac marker genes. I did not detect a significant difference in the expression levels of *nkx2.5*, *tbx20*, *tbx5*, *raldh2* and *tbx18* (data not shown) while *hand2* expression was significantly decreased in Dkk1 expressing amputated hearts (**Fig 3.1.4B**). Although statistically not significant, I detected a reduced expression of *hand2* also in sham amputated Dkk1GFP induced hearts compared to sham amputated hearts of wild-type siblings (**Fig 3.1.4B** uninjured controls), indicating that *hand2* expression is dependent on b-catenin signaling also in uninjured hearts.

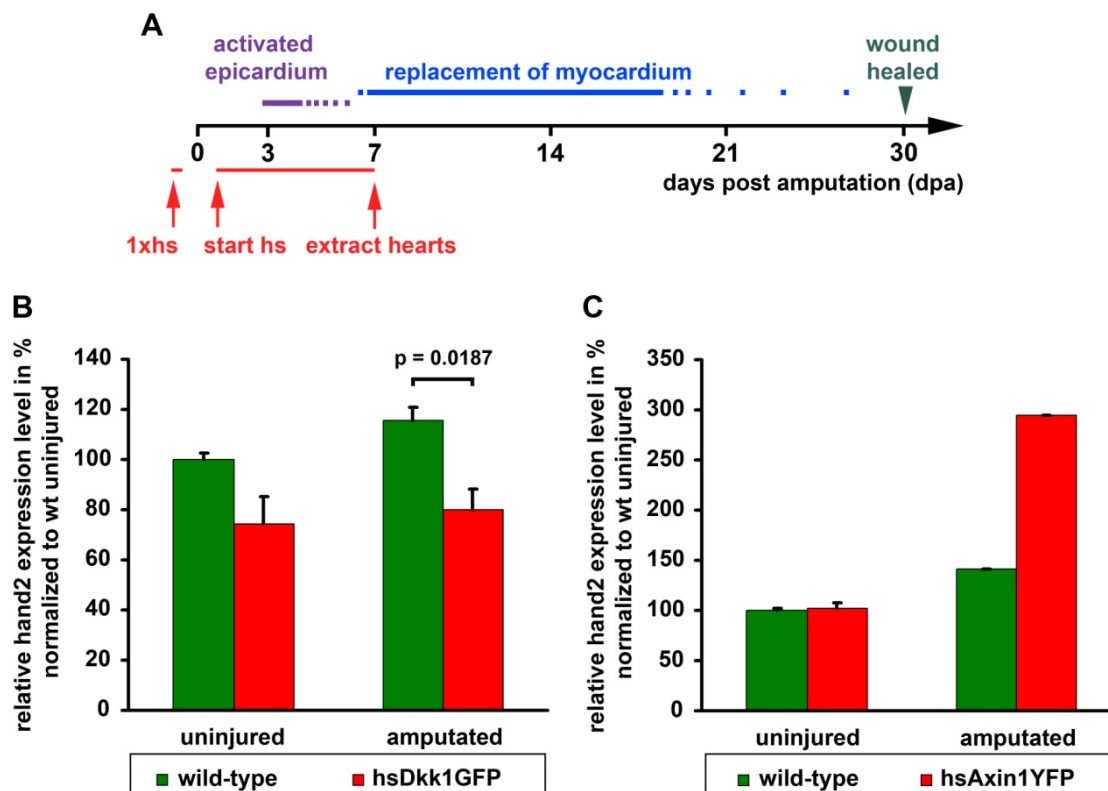
Interestingly, there is only a small increase in *hand2* transcription comparing wild-type amputated versus wild-type sham amputated hearts (**Fig 3.1.4B**). This small difference is probably due an induction of *hand2* in sham amputated fish relative to hearts of untreated fish. Upregulation of *hand2* mRNA (although at low levels) is detectable after opening of the pericardial sac, which is performed for sham amputation (Wills et al 2008). Thus a strong upregulation of *hand2* mRNA comparing amputated versus sham amputated hearts is not expected.

Since *hand2* expression starts at 3 dpa, I also tested whether Wnt signaling is important for the initiation of *hand2* transcription using amputated hearts of hsDkk1GFP and wild-type siblings. Heat-shocks were applied every 12 hours starting one day after amputation, to provide Dkk1 expression during the onset of *hand2* induction. I extracted the regenerating hearts at 4 dpa and assayed for *hand2* expression using in situ hybridization on sections. However, I did not detect any significant difference in the *hand2* expression pattern of amputated, wild-type hearts compared to amputated, Dkk1GFP expressing hearts, suggesting that Wnt signaling is not necessary for *hand2* expression at this stage (data not shown).

To verify the influence of Wnt signaling on *hand2* expression at 7 dpa I used hsAxin1YFP⁶ fish and their wild-type siblings using the experimental setup as described and qPCR for analysis (**Fig 3.1.4A**). However, I did not detect a reduction in *hand2* mRNA levels in amputated Axin1YFP expressing fish, which is in contrast to results in Dkk1GFP expressing fish (**Fig 3.1.4C**). Moreover amputated hearts of transgenic fish showed a markedly increased *hand2* expression compared to amputated wild-type siblings. Thus these results do not confirm a negative influence of reduced Wnt signaling on *hand2* transcription levels as observed after Dkk1GFP induction.

Concluding, I did not detect any consistent requirement of of β -catenin signaling for the expression level or pattern of several marker genes during early heart regeneration.

Dkk1GFP induction did not influence the onset of *hand2* expression (4 dpa). At 7 dpa, *hand2* mRNA was significantly downregulated by Dkk1GFP expression, but not using Axin1YFP. Together these data suggest that inhibition of Wnt/ β -catenin signaling does not influence cardiac marker gene expression during zebrafish heart regeneration.



3.1.4 *hand2* expression is not regulated by Wnt/ β -catenin signaling.

A. Transgenic TG(hsDkk1GFP) and TG(hsAxin1YFP)⁶ fish and the respective wild-type siblings were amputated or sham amputated, which was used as uninjured control, 6 hrs after heat-shock. Starting at 1 dpa heat-shocks were applied every 12 hrs. Hearts were extracted at 7 dpa in the early stage of heart regeneration.

B. Significant reduction of *hand2* expression was detectable after induction of Dkk1GFP in amputated hearts of transgenic fish compared to wild-type hearts. In contrast, *hand2* upregulation was detected after induction of Axin1YFP in amputated hearts of transgenic fish compared to wild-type hearts (C.). Expression levels were determined with quantitative PCR. *hand2* expression levels of each group were normalized to wild-type uninjured. Uninjured samples of this experiment were sham amputated fish. Student's t-test was used for statistics (B and C). n = 6 hearts for each group

3.1.2.3 Microarray: Which genes are regulated by Wnt/ β -catenin signaling during heart regeneration? Are Wnt target genes expressed during heart regeneration?

Although I did not detect an amputation specific upregulation of certain Wnt/ β -catenin target genes, it is possible that other Wnt/ β -catenin target genes are induced during heart regeneration. Using microarray technology, I aimed to identify Wnt/ β -catenin target genes that are regulated in response to heart amputation.

As described before, the induction of Dkk1GFP has a negative influence on *hand2* mRNA expression at 7 dpa, thus I chose this stage to analyze direct and indirect Wnt/ β -catenin target genes.

To influence Wnt/ β -catenin signaling I again used the transgenic fish lines hsDkk1GFP and hsAxin1YFP⁶. I concentrated on identifying target genes that are positively regulated by canonical Wnt/ β -catenin signaling and hence appear as downregulated when the pathway is inhibited. For all experiments, I amputated heterozygous transgenic fish and wild-type siblings whereas I used uninjured transgenic fish and wild-type siblings as control groups. I assayed for direct and indirect target genes using two experimental approaches (**Fig 3.1.5A** and **B**).

First, to enrich the data for putative direct target genes I amputated transgenic hsDkk1GFP and hsAxin1YFP and the respective wild-type fish and applied a single heat-shock at 7 dpa. I extracted the hearts 6 hours after the heat-shock to minimize accumulation of indirect targets in the analysis. (approach I, **Fig 3.1.5A**).

Second, to identify genes whose expression is generally dependent on Wnt signaling, and especially indirect target genes, I applied the first heat-shock 6 hours before the amputation and the following heat-shocks every 12 hours, starting at 24 hours after the amputation, to provide high expression levels of the transgene during the regeneration time of 7 days. In this approach I used hsDkk1GFP fish and their wild-type siblings. Hence with this method, it is expected to obtain a pool of direct as well as indirect target genes accumulating due to constant inhibition of Wnt/ β -catenin signaling and its potential long term influence on indirect target genes and pathways (approach II, **Fig 3.1.5B**).

I prepared total RNA from the lower half of the heart containing the apex and only used the samples of high RNA quality as determined by using the Agilent Bioanalyzer. The respective samples were hybridized on a customized zebrafish 4x44K expression oligomicroarray and analyzed for quality of hybridization using the quality control reports.

I applied a statistical evaluation and filtering of the data according to different criteria, as explained below.

First I applied very low stringency in filtering criteria using a p-value cutoff of 0.15 and a fold change of less than -1.2. Despite the low stringency, I could detect only very few genes positively regulated by Wnt/ β -catenin signaling after heart amputation (**Table 3.1.1**). Comparing Axin1 overexpressing amputated hearts with amputated wild-type hearts I could only identify a single gene, which, according to functional gene annotation criteria defined by the Panther database, encodes for a protein of the Lipoxygenase family.

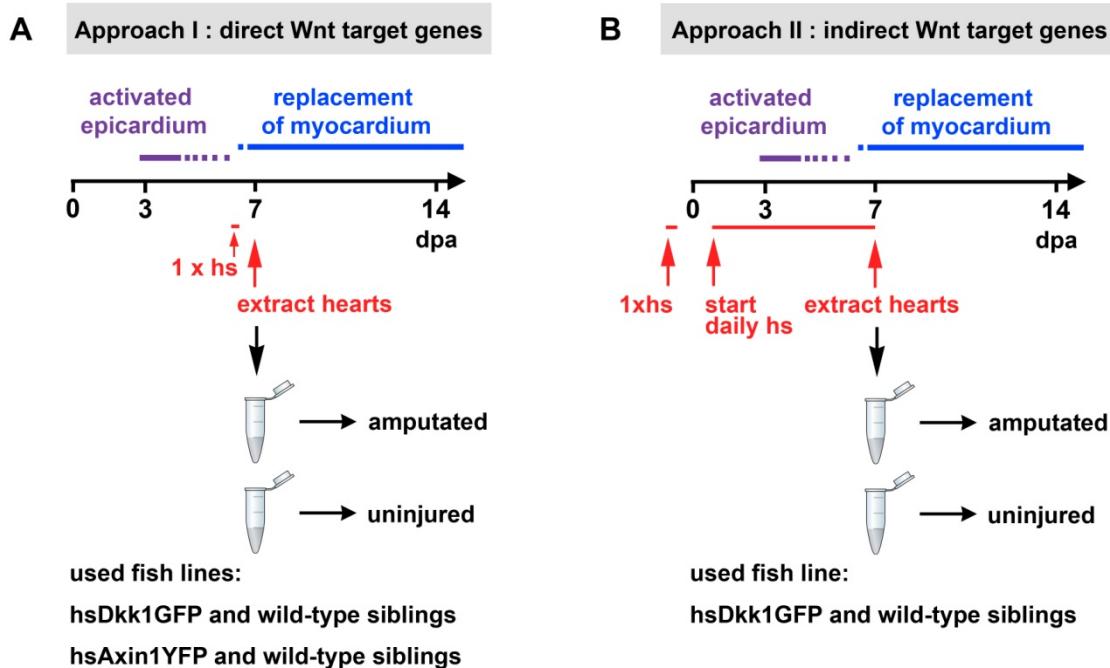
Furthermore, comparing Dkk1 overexpressing and wild-type amputated hearts, I found 15 genes with reduced expression levels. Notably, the gene that was negatively regulated by Axin1 overexpression was not found among these 15 genes.

Due to the very low stringency criteria applied for these comparisons, only genes whose expression is regulated by both Dkk1 and Axin1 overexpression were assumed to represent Wnt/ β -catenin target genes. Since there is no overlapping target gene, which is regulated by both Axin1 and Dkk1 overexpression, I conclude that direct Wnt/ β -catenin target genes were not detectable in regenerating hearts.

Using approach II, I could not detect any significantly regulated target genes either. Notably, *hand2* mRNA, which I showed to be downregulated by Dkk1 overexpression in Q-PCR (**Fig 3.1.4B**) was not significantly regulated in the array data. However, this discrepancy was not due to minor quality of the microarray data, as explained below.

To test the reliability of the applied methods I used the wild-type data of the same array experiment. I analyzed amputation specific genes that are regulated in regenerating wild-type fish hearts (7dpa) compared to uninjured wild-type hearts. Using stringent filtering criteria with a p-value cutoff 0.05 and a fold change greater than 1.5, I detected amputation specific upregulation of more than 300 genes in the analyzed experimental groups either treated with one heat-shock (approach I) or with daily heat-shocks during the regeneration time of 7 days (approach II). Analyzing the wild-type array data, I could identify published amputation specific genes, such as *mdka*, *mmp14a*, *mmp14b* and other genes by using both approaches (**Table 3.1.2**) (Lien et al 2006). From these results I conclude that the microarray worked with respect to technical performance. Still, I could not detect any direct or indirect Wnt/ β -catenin target gene in the first 7 days of heart regeneration.

In conclusion, using even very nonstringent criteria, I could not identify any direct or indirect Wnt/ β -catenin target genes during early regeneration of the zebrafish heart in response to ventricular resection.



3.1.5. Approaches used to identify Wnt/ β -catenin target genes during early heart regeneration using oligoexpression microarray analysis.

Different treatments were applied to identify direct Wnt/ β -catenin target genes using approach I (A.) and indirect target genes using a series of heat-shocks in approach II (B.) For approach I hsDkk1GFP and hsAxin1YFP⁶ and the respective wild-type siblings were used (either amputated or uninjured). For approach II hsDkk1GFP and wild-type siblings (amputated or uninjured) were used. Approach I (A.): One heat-shock was applied 6 hrs before heart extraction at 7 dpa. Approach II (B.): One heat-shock was applied 6 hrs before amputation. Serial heat-shocks with 2 heat-shocks per day started at 1 dpa and hearts were extracted 6 hrs after the last heat-shock at 7 dpa. All time points in triplicates, for each sample $n = 8$ hearts. Uninjured samples of this experiment are untreated fish.

Table Wnt target genes

Target genes of Wnt/β-Catenin signaling expressed at 7 dpa by comparing 7 dpa transgenic vs. 7 dpa wild-type		
	number of genes	names of regulated genes (significantly downregulated: $p \leq 0.15$; Fold Change ≤ -1.2)
direct target genes of approach I.:		
hsAxin1YFP vs. wild-type	1	family*: LIPOXYGENASE
hsDkk1GFP vs. wild-type	15	genes: rnf146, ercc1, mapk1, tll1, os9, med4, LOC100002736, zgc:153165 families*: AQUAPORIN, ZINC FINGER PROTEINS, Draculin, IMMUNOGLOBULIN LIGHT CHAIN, 5'->3' EXORIBONUCLEASE, CELL DEATH ACTIVATOR CIDE, XAP-5 PROTEIN-RELATED
indirect target genes of approach II.:		
hsDkk1GFP vs. wild-type	0	

*protein family names are indicated if transcripts were not gene-annotated

Table 3.1.1: Comparisons of expression profiles showed few regulated genes after inhibition of Wnt/ β -catenin signaling using Dkk1GFP or Axin1YFP overexpression in amputated hearts using approach I and no regulated genes using approach II.

The comparison of Dkk1GFP overexpressing hearts with wild-type hearts showed 15 downregulated genes in amputated samples using approach I and 0 downregulated genes using approach II. In the comparison Axin1YFP overexpression and wild-type of approach I showed 1 downregulated gene, which is not regulated by Dkk1GFP overexpression. Family names of protein families (in capital letters) are given according to functional gene annotation criteria defined by the Panther database, if the gene name of regulated transcript was not annotated. Filtering criteria $p \leq 0.15$; $FC \leq -1.2$.

Table Regeneration specific genes

Differentially regulated genes expressed 7 dpa by comparing 7 dpa wild-type vs. uninjured wild-type	
7 dpa wild-type vs. uninjured wild-type	examples of regulated genes (significantly upregulated: $p \leq 0.05$; Fold Change ≥ 1.5)
Approach I.:	
wild-type siblings of hsAxin1YFP:	mdka, mmp14a, mmp14b, cxcl12a, pdgfa, anxa1a, tbx18, vegfc, bactin2
wild-type siblings of hsDkk1GFP:	mdka, mmp14a, mmp14b, cxcl12a, pdgfa, anxa1a, tbx18, vegfc, bactin2
Approach II.:	
wild-type siblings of hsDkk1GFP:	mdka, mmp14a, mmp14b, cxcl12a, anxa1a, tbx18

Table 3.1.2: Comparisons of amputated and uninjured wild-type hearts showed upregulation of known induced genes in heart regeneration at 7 dpa using approach I and II. Amputated wild-type hearts (7 dpa) were compared to control wild-type hearts (uninjured). Wild-type samples for this comparison were derived from amputated and control wild-type siblings of hsAxin1YFP and hsDkk1GFP fish, as described in Fig 3.1.5, which were treated according to approach I or II. Table shows examples of upregulated genes in this oligoexpression microarray, which have previously been shown by others to be expressed at 7 dpa in regenerating hearts. Filtering criteria $p \leq 0.05$; $FC \geq 1.5$.

(The complete list of regulated genes is available from Dr. Gilbert Weidinger (e-mail: gilbert.weidinger@biotec.tu-dresden.de) upon request.)

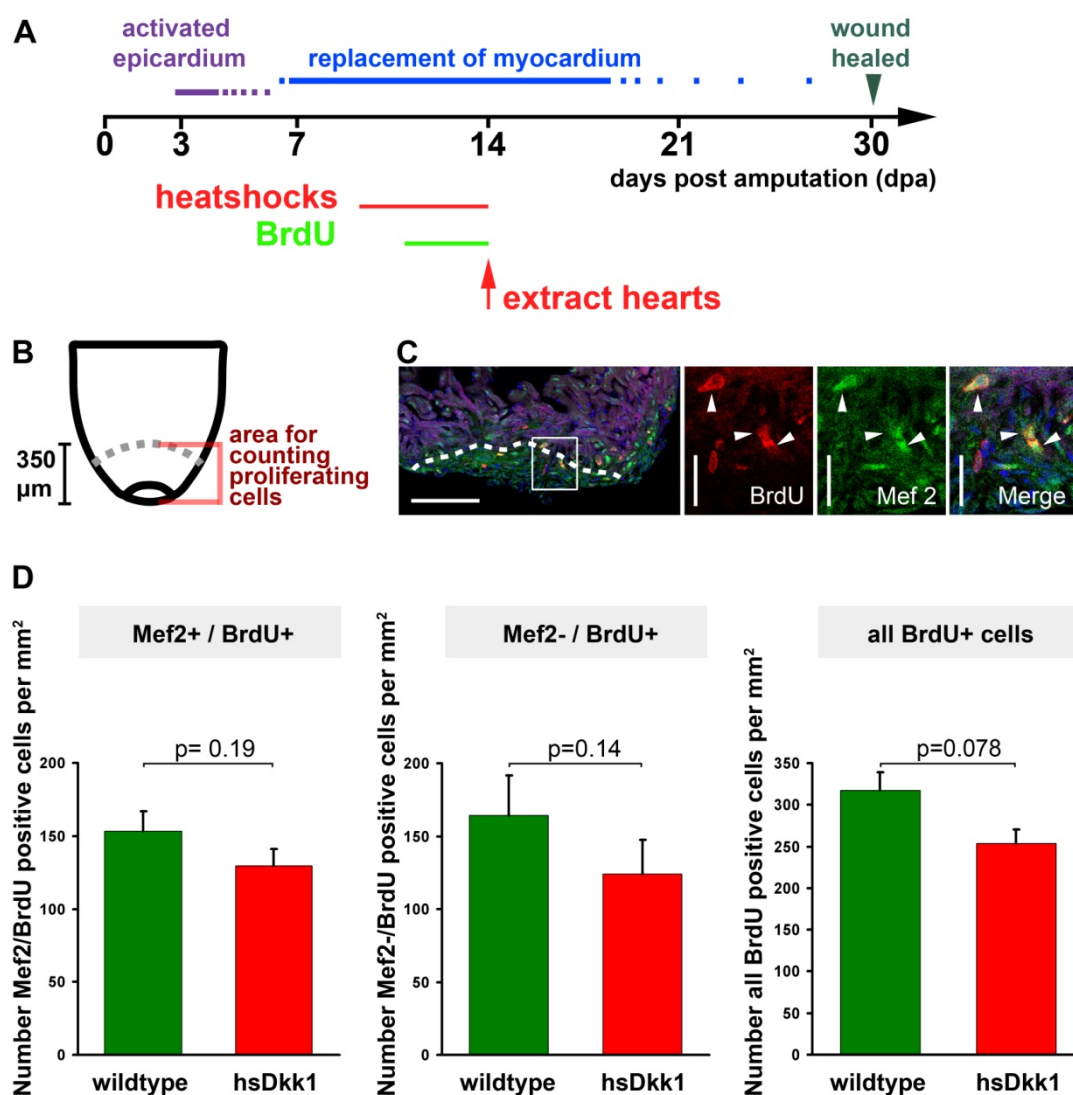
3.1.2.4 Does Wnt signaling influence proliferation during heart regeneration?

During zebrafish heart regeneration proliferation of various cell types is markedly increased. Others could show that proliferation of cardiomyocytes is initiated at 7 dpa and peaks at around 14 dpa (Poss et al, 2002).

Besides its general role in promoting the cell cycle, the Wnt/ β -catenin pathway is described to positively regulate proliferation of early cardiac cells even after their commitment to the cardiomyocyte lineage (for review Davidson G. and Niehrs C. 2010; Kwon et al 2007).

Thus, I analyzed whether Wnt/ β -catenin signaling influences proliferation during heart regeneration. I amputated heterozygous transgenic hsDkk1GFP fish and their wild-type siblings and started heat-shocks twice a day at day 9 post amputation to inhibit β -catenin signaling. Proliferating cells were labeled using 5-bromo-2'-deoxyuridine (BrdU) incorporation with injections of BrdU solution once a day starting at 11 dpa until 13 dpa (**Fig 3.1.6A**). This experimental setup allows the detection of all proliferating cells within 3 days under Wnt loss of function conditions. The hearts were extracted at 14 dpa and analyzed using antibody stainings to detect Mef2, a nuclear marker for cardiomyocytes (Lepilina et al 2006, Hinitz and Hughes 2007), and BrdU (**Fig 3.1.6C**). On all sections showing a wound area, I quantified the following cell populations: “the total number of all proliferating cells” (all BrdU+), “proliferating cardiomyocytes” (Mef2+/BrdU+) and “all cycling non-myocardial cells” (Mef2-/BrdU+) (**Fig 3.1.6B-and D**). Poss et al (2001) reported increased cardiomyocyte proliferation in the area close to the wound and few proliferating cardiomyocytes within the wound. Thus, the cell populations were counted in a defined area around the wound (up to 350 μ m distance from the apex, including the

wound tissue and the wound edges) (**Fig 3.1.6B**). This corresponds to roughly one third of the size of the ventricle. The cell number was normalized to the size of the selected area. For each cell population (Mef2⁺/BrdU⁺ cells, Mef2⁻/BrdU⁺ cells and all BrdU⁺ cells) I detected less proliferating cells after induction of Dkk1GFP compared to wild-type. The differences, however, between Wnt loss of function and wild-type are statistically not significant for any of the examined groups (**Fig 3.1.6D**), suggesting that cell proliferation during heart regeneration is not influenced by Wnt/ β -catenin signaling.



3.1.6 Dkk1 does not significantly interfere with cardiomyocyte and non-cardiomyocyte cell proliferation in the regenerating heart.

A. To examine proliferation stages, hsDkk1GFP and wild-type siblings were heat-shocked from day 9 - 14 post amputation, BrdU was injected from 11-13 dpa once per day and hearts were extracted at 14 dpa.

B. Scheme of a ventricle at 14 dpa. Area for counting proliferating cells contains wound tissue and the wound edges. The border considered area is indicated by a gray dashed line, which is 350 μm distant to the apex.

C. Example of cardiomyocytes of a 14 dpa wild-type heart positive for Mef2 and BrdU. Proliferating cardiomyocytes (Mef2⁺/BrdU⁺) are indicated by white arrowheads. Wound border is indicated by a white dashed line. Scale bar in overview is 100 μm and 25 μm in magnification.

D. Proliferating cardiomyocytes (Mef2⁺/BrdU⁺), proliferating non-myocardial cells (Mef2⁻/BrdU⁺) and all proliferating cells (all BrdU⁺) were counted in the area around the wound to compare TG(hsDkk1GFP) fish and wild-type siblings. There is no significant reduction of proliferation in any of these groups after Dkk1GFP induction. Wild-type n = 5 hearts (29 sections); transgenics n = 5 hearts (33sections). Student's t-test was used.

Although described to be expressed in cardiomyocytes (Lepilina et al. 2006) Mef2 is expressed in other cell lineages as well (Potthoff and Olson 2007). To reliably detect nuclei of myocardial cells only I used the reporter fish line Tg(-5.1myl7:nDsRed2)^{f2/+} cmcl2:dsRed which expresses a nuclear dsRed controlled by the *cardiac myosin light chain 2* promoter (Lepilina et al 2006, Mably et al 2003).

I amputated double heterozygous transgenic fish hsDkk1GFP x cmcl2:dsRed and cmcl2:dsRed siblings as control group and performed the experiment as described above (**Fig 3.1.6A**). I performed antibody stainings to detect dsRed and BrdU (**Fig 3.1.7B**) and counted several cell populations including “the total number of all proliferating cells” (all BrdU⁺), “proliferating cardiomyocytes” (dsRed⁺/BrdU⁺), and “all cycling non-myocardial cells” (dsRed⁻/BrdU⁺) in different areas, which are the wound area (1 in **Fig 3.1.7A**), the wound edges (2 in **Fig 3.1.7A**) and both areas together (3 in **Fig 3.1.7A**). The wound area is demarcated from the surrounding wound edge tissue by significantly lower tissue autofluorescence.

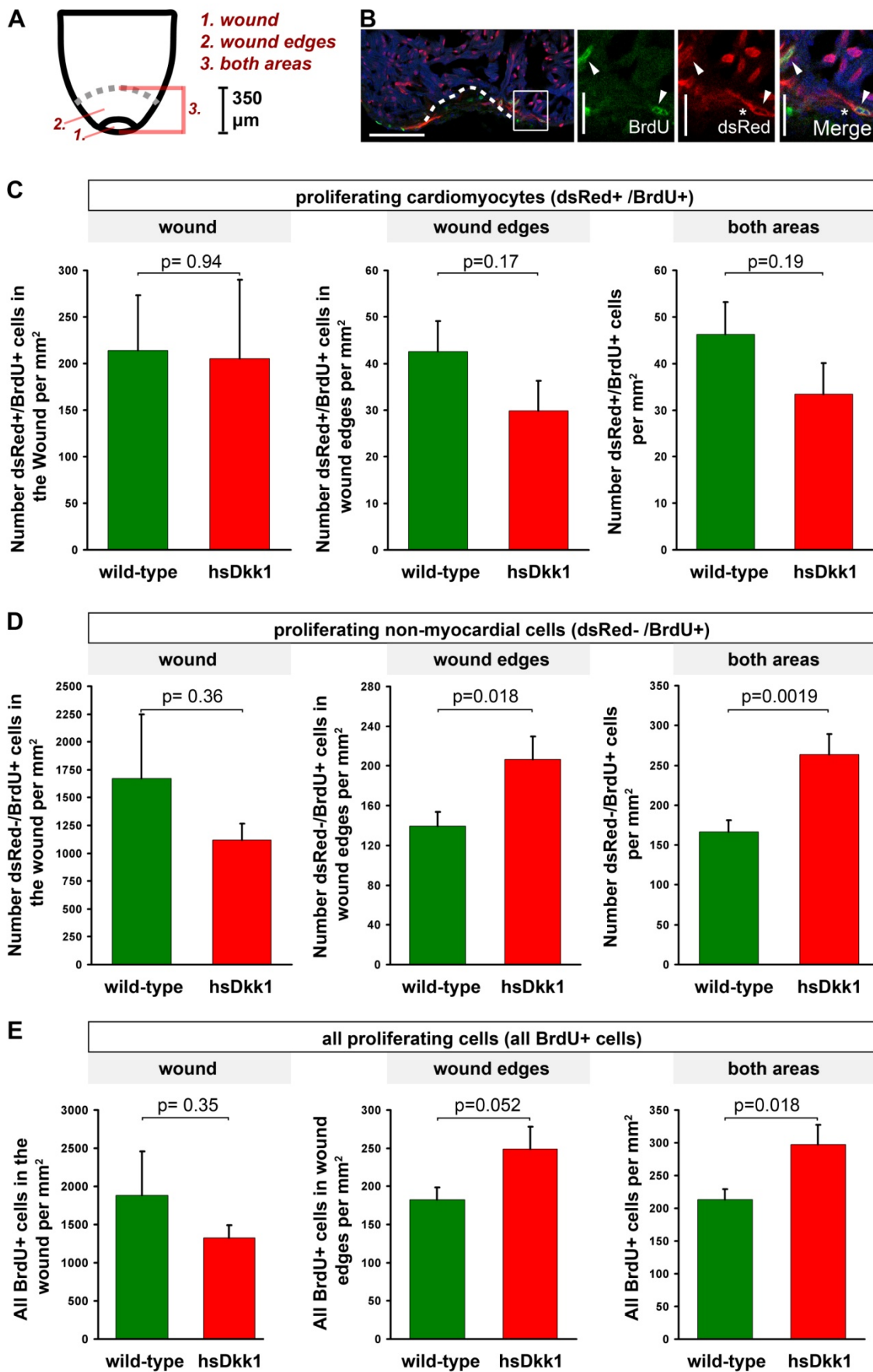
Dkk1 expression compared to wild-type control had no influence on myocardial proliferation in the wound area (**Fig 3.1.7C**) and only a slight, but not significant, reducing influence on cardiomyocyte proliferation at the wound edges (**Fig 3.1.7C**). Accordingly, also the total amount of proliferating cardiomyocytes in both examined areas was not

significantly influenced by an inhibition of Wnt signaling (**Fig 3.1.7C**), suggesting that myocardial proliferation is not regulated by Wnt/ β -catenin signaling.

Compared to wild-type control, Dkk1 expression did not significantly influence proliferating non-myocardial cells in the wound (**Fig 3.1.7D**), and surprisingly resulted in significantly more proliferating non-myocardial cells in the area of the wound edges (**Fig 3.1.7D**). The latter effect influences the total amount of proliferating non-myocardial cells in the combined examined areas (**Fig 3.1.7D**) and thus, a significant increase of cycling cells is detectable after Dkk1GFP expression compared to wild-type in this examined group (**Fig 3.1.7D**). In contrast to the latter data my previous results using Mef2 staining showed a (non-significant) reduction of cycling non-myocardial cells (compare **Fig 3.1.7D third graph** with **Fig 3.1.7D second graph** Mef2-/BrdU+), indicating that an influence (neither a positive nor a negative) of Dkk1 expression on proliferating non-myocardial cells is not reproducible.

Considering all proliferating cells, the number of cycling cells in the wound was not significantly reduced after Dkk1 expression compared to wild-type (**Fig 3.1.7E**) while the wound edges and thus the combination of both areas show an increase in proliferation after Dkk1GFP induction when compared to wild-type (**Fig 3.1.7E**). Both latter results are explained the high amount of cycling non-myocardial cells in Dkk1 expressing hearts. The increase in proliferating cells after Dkk1GFP induction is again contradictory to my previous results, which showed a (non-significant) reduction of dividing cells in transgenic fish (compare **Fig 3.1.7D “all cells”** with **Fig 3.1.7E third graph**), indicating that Wnt/ β -catenin signaling does not reproducibly influence cell proliferation during heart regeneration.

In conclusion, I cannot detect any significant negative or positive influence on cardiomyocyte proliferation after inhibition of Wnt/ β -catenin signaling. Effects of Wnt/ β -catenin signaling on other proliferating cells (mainly non-myocardial cells) are not reproducible, which all together suggests that Wnt/ β -catenin signaling is not important for cell proliferation during heart regeneration.



3.1.7 In a second experiment, proliferation of cardiomyocytes was not significantly influenced in *hsDkk1GFPxcmc2:dsRed* versus *cmc2:dsRed* hearts.

A. Proliferating cells were counted in different areas: wound area (1.), the wound edges delimited by gray dashed line, which is 350 μm distant to the apex (2.) and both areas together (3.) were chosen as shown in the schema of a ventricle. The same treatment protocol as described in 6.A was applied for this experiment.

B. Heart section of *cmc2:dsRed* fish at 14 dpa shows cells positive for dsRed and BrdU. Proliferating cardiomyocytes (dsRed+/BrdU+) are indicated by white arrowheads. Cytoplasmic dsRed staining is detectable in newly differentiated cardiomyocytes (*) while older cardiomyocytes show nuclear dsRed signal. Wound plane is indicated by a white dashed line. Scale bar in overview is 100 μm , in magnification 25 μm .

C. Proliferating cardiomyocytes (dsRed+/BrdU+) were counted in the wound area (left graph), in the wound edges (middle graph). Numbers of dsRed+/BrdU+ cells in both areas are combined in the right graph. Differences in proliferating cardiomyocytes in wild-type versus *Dkk1* overexpressing hearts are not significant.

D. Proliferating non-myocardial cells (dsRed-/BrdU+) were counted in the wound area (left graph), in the wound edges (middle graph 2.). The right graph shows the number of dsRed-/BrdU+ cells in both areas. In the wound edge area and in the total area there are significantly more proliferating non-myocardial cells after *Dkk1GFP* induction.

E. All proliferating cells (dsRed+/BrdU+ and dsRed-/BrdU+ cells) in the wound area (left graph), in the wound edges (middle graph) and in both areas together (right graph) are combined to test for a putative influence of Wnt signaling on proliferation in general. Differences in proliferating cells in the wound area and wound edges are not significant. After *Dkk1GFP* overexpression there are significantly more proliferating non-myocardial cells detectable in the total area.

In G., H. and I.: wild-type n = 11 hearts (32 sections); transgenics n = 10 hearts (29 sections); Student's t-test was used.

3.1.2.5 Long term loss of function and gain of function of canonical Wnt signaling does not influence heart regeneration

While I found that Wnt/ β -catenin signaling appears to play no major detectable role in early stages of regeneration and in later proliferative phases, it might be regulating processes required for successful morphological myocardial regeneration, eg. wound tissue removal and remodelling or for neovascularization. I thus examined its influence on the

overall extent of histological heart regeneration which might include so far disregarded events in regeneration and might also provide a sensitive readout for small additive defects. To test whether Wnt/ β -catenin dependent signaling has a role during later stages of regeneration, Wnt/ β -catenin was continuously inhibited or over-activated using heat-shock inducible fish lines.

3.1.2.5.1 Is Wnt/ β -catenin signaling required for morphological regeneration and/or wound resolution?

To inhibit Wnt signaling I used heterozygous transgenic fish of the hsDkk1GFP and hsAxin1YFP¹⁹ fish line and their wild-type siblings as control. I performed amputations and applied heat-shocks (one heat-shock every 24 hours) during the whole regeneration time starting after a recovery time of 1 day post amputation.

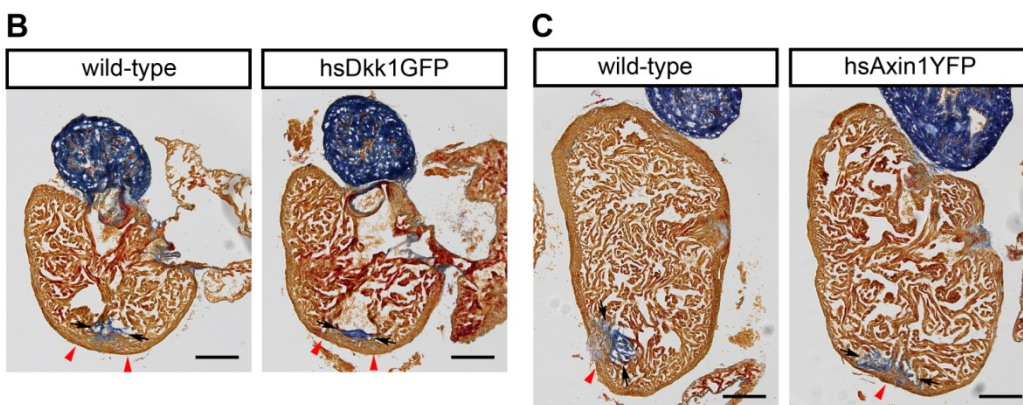
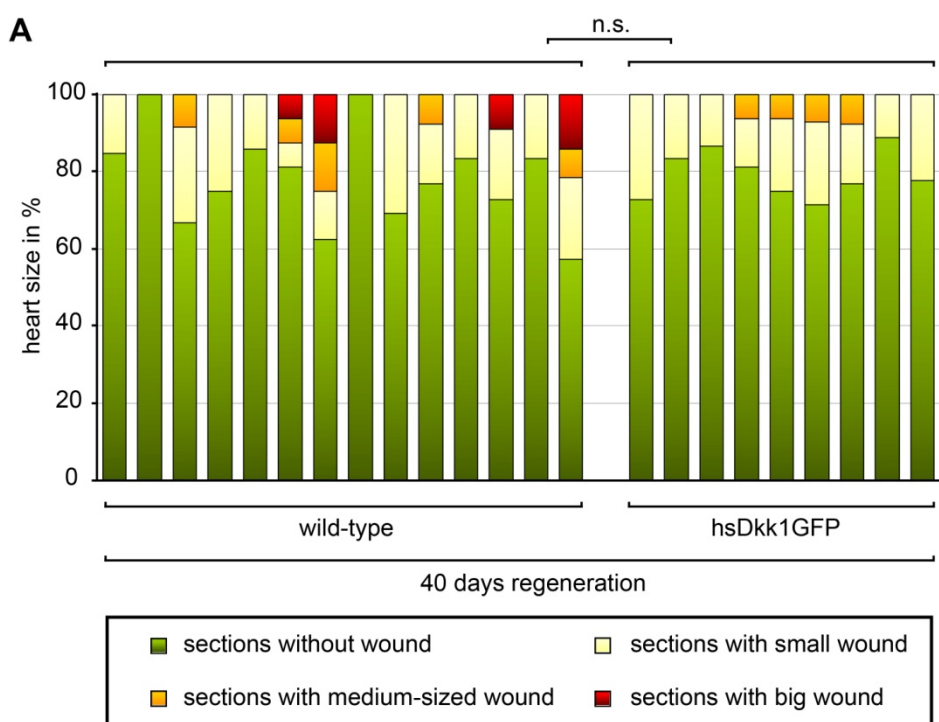
I did not apply more frequent, e.g. every 12 hours, heat-shocks to provide higher levels of the inhibitory transgene, because I detected negative influences on the regenerative process in wild-type controls using frequent heat-shocks (data not shown). A constant expression of the transgene was provided with 1 heat-shock per day, as assayed by GFP or YFP fluorescence using stereomicroscopy (data not shown).

Wild-type and transgenic fish were heat-shocked for 40 after amputation. For analysis I stained heart sections with histological Acid-Fuchsin-Orange-G staining (AFOG, **Fig 3.1.8B and C**) which marks fibrin in red, collagen in blue and muscle in orange (Poss et al 2002). I assayed for size of the remaining wound area and collagen rich scars using light microscopy and assessed the extent of regeneration of each heart in the wild-type and transgenic group according to wound size and enrichment of scar tissue. I classified stained sections of examined hearts according to severity the following way: “sections without a wound”, “sections with a small wound “, "sections with a medium-sized wound” and “sections with a big wound area”.

After initial promising results of a pilot experiment with only few fish I performed this experiment 3 times more with a higher number of fish. As a result, I could not detect a difference in the progress of regeneration regarding wound size and enrichment of scar tissue in the comparison of wild-type versus transgenic fish with inhibited Wnt/ β -catenin signaling in 3 out of 3 experiments (**Fig 3.1.8A** and data not shown). Analysis of the stained sections showed that wound recession as indicated by removal of fibrin as well as histological regeneration especially in the external myocardial layer (**Fig 3.1.8B and C**)

was visible in both the control and the group of transgenic fish. However, obvious scarring events, as indicated by accumulation of collagen, were also present in both groups (**Fig 3.1.8B and C**). Since non-heat-shocked injured wild-type and transgenic fish show an improved regenerative result at this time point (40 dpa) (data not shown) I suspect that the impairment in heart regeneration in amputated wild-type fish is due to negative influences of the heat-shock treatment.

However, there is no difference detectable in regenerative progress of transgenic compared to wild-type fish, suggesting that inhibition of Wnt signaling by Axin1 or Dkk1 overexpression does not impair zebrafish heart regeneration.



3.1.8 Inhibition of Wnt/ β -catenin signaling during the entire regeneration process did not influence zebrafish heart regeneration.

hsDkk1GFP fish and wild-type siblings were amputated and heat-shocked for 40 days (**A,B**). **A**. Heart sections were stained with Acid-Fuchsin-Orange G (AFOG) which stains muscle in orange, fibrin in red and collagen in blue to assess the progress of regeneration. Sections of each heart were sorted into different groups: “sections without a wound”, “sections with a small wound”, “sections with a medium-sized wound” and “sections with a big wound area”. No significant difference is detectable in the comparison of 40 dpa TG(hsDkk1GFP) with wild-type siblings. **C**. hsAxin1YFP fish and wild-type siblings were heat-shocked for 36 days after amputation.

B. and **C**. Sections shown of each genotype are representative samples stained with AFOG. Regenerated muscle fibers of the external myocardial layer are indicated by red arrowheads. Collagen depositions in the wound area are indicated by black arrows. Scale bars are 200 μ m. Pictures correspond to medium sized wounds.

A.-C. hsDkk1GFP n = 9, wild-type n = 14 (in the presented experiment; Experiment was repeated with similar result); hsAxin1YFP n = 12, wild-type n = 18. Qui square test.

In order to over-activate Wnt/ β -catenin signaling and test whether this pathway can improve heart regeneration I used two approaches.

First, a Wnt signaling gain of function phenotype is present in homozygous embryos of the mutant fish line masterblind (mbl), in which the negative Wnt regulator Axin1 is mutated (Heisenberg et al 2001). Since homozygous fish are embryonic lethal I used heterozygous adult fish, which are expected to have minor changes in β -catenin signaling, and wild-type siblings for cardiac amputation.

Second, it is also possible to over-activate wnt signaling via induction of the Wnt8a ligand in hswnt8a-GFP fish. I amputated heterozygous transgenic animals and wild-type siblings and applied heat-shocks every 24 hours after a recovery time of 1 day post amputation. As assayed by fluorescence using stereomicroscopy transgenic fish showed a constant Wnt8aGFP expression at several time points during regeneration (data not shown).

I extracted hearts from both Wnt gain-of-function regimes at 21 dpa and performed analysis as described by using AFOG staining on sections and classification via light microscopy (**Fig 3.1.9A, B, D** and data not shown).

Analyzing the regenerative status using the qualitative assessment of wound size introduced above in both transgenic hswnt8a-GFP fish and wild-type fish I detected no significant difference in the progress of regeneration (**Fig 3.1.9A and B**). I also measured

the wound area in relation to the heart size; while *wnt8* expressing fish had slightly smaller wound, this difference was statistically not significant (**Fig 3.1.9C**). Comparing mutant *masterblind* and wild-type fish I could not detect a significant difference in the progress of regeneration regarding wound size and enrichment of scar tissue either (**Fig 3.1.9D** and data not shown).

Conclusively, I could not detect any effect on morphological heart regeneration after inhibition or induction of Wnt/ β -catenin signaling during the process of heart regeneration.

Figure next page

3.1.9 Overactivation of Wnt/ β -catenin signaling did not influence heart regeneration.

A.-C. hsWnt8aGFP fish and wild-type siblings were amputated and heat-shocked for 21 days.

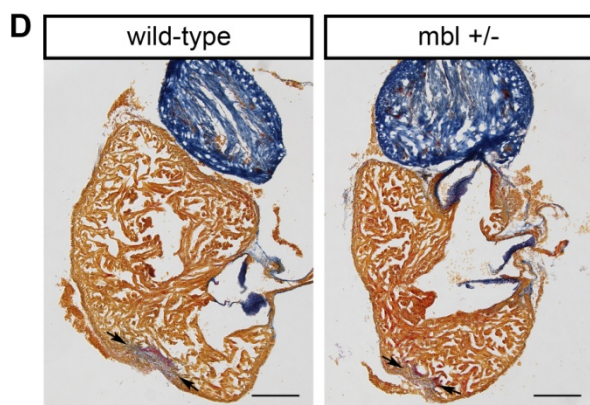
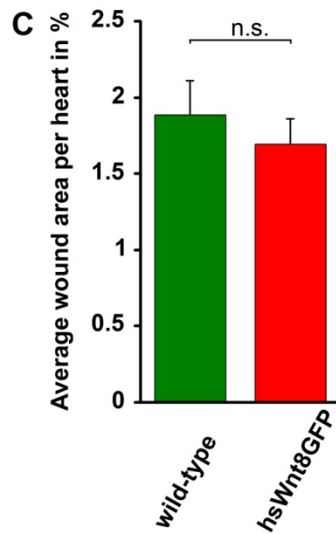
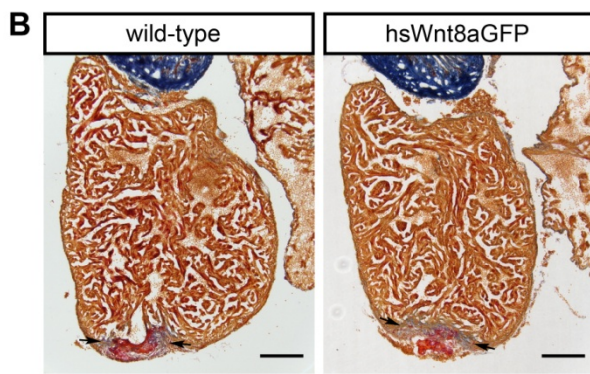
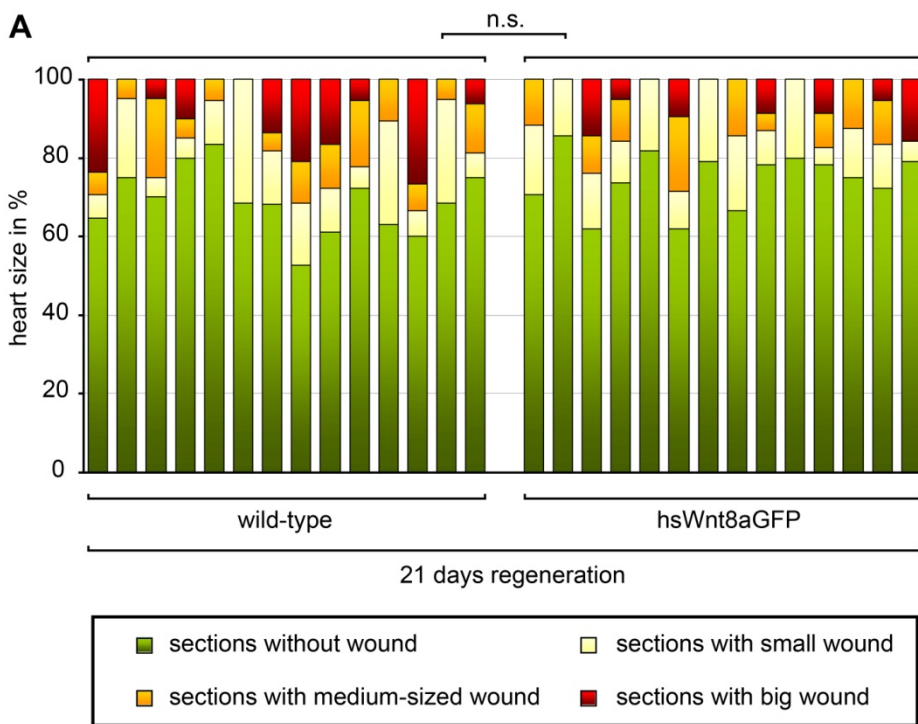
A. There is no significant difference in progress of regeneration between hsWnt8aGFP fish and wild-type siblings using sorting criteria as described in 7.A. Qui Square test was used.

B. Heart sections of wild-type and Wnt8aGFP overexpressing hearts were stained with AFOG. Sections shown of each genotype are representative samples. Wound area is indicated by black arrows.

C. Measurement of wound area and ventricle area on heart sections of hsWnt8aGFP fish and wild-type siblings (experiment in A and B) stained with AFOG. There is no significant difference in wound size at 21 dpa between transgenic and wild-type hearts. Student's t-test was used.

D. Masterblind heterozygous mutants (*mbl*^{+/-}) and wild-type siblings could regenerate for 21 days. Heart sections of wild-type and *mbl* mutant hearts were stained with AFOG. Sections shown of each genotype are representative samples. Wound area is indicated by black arrows.

A.-D.: hsWnt8aGFP n = 14, wild-type n = 14; *mbl*^{+/-} n = 7, wild-type n = 11. (in the presented experiments; Both experiment were repeated with similar results.) Scale bars are 200 μ m.



3.2.1 The expression pattern and functional role of Sox9a in zebrafish heart regeneration

Several transcription factors are known to be upregulated in zebrafish heart regeneration (Lien et al 2006). However, whether these transcription factors have a functional role in the regeneration process largely remains unknown.

Beside its regenerative capability, the zebrafish heart also shows few proliferating cells during homeostatic growth (Wills et al 2008). Using antibody staining on heart sections of untreated fish, Jan Kaslin found very few cells expressing Sox9 (2 cells per section), a transcription factor that is required for maintenance of stem/progenitor cells in several tissues such as the embryonic and adult central nervous system (Scott et al 2010). Thus I performed anti-Sox9 antibody stainings on amputated hearts and detected the transcription factor Sox9 to be upregulated during heart regeneration. Lincoln et al (Lincoln et al 2007) have shown a role of Sox9 in valve formation of the developing mouse heart and its expression was also shown in the regeneration process of the caudal fin (Smith et al 2006). However, expression of Sox9 during heart regeneration has not been shown so far. Thus I intended to test whether Sox9 has a functional role during heart regeneration.

3.2.1.1 Analysis of the temporal and spatial Sox9 expression pattern in the injured heart

As mentioned before, I performed heart injuries using ventricular resection. As control, I used either hearts of untreated fish or sham amputated hearts, in which the pericardial sac was opened but the heart was not touched. Both types of controls are not considered injuries of the heart proper, thus control hearts are referred to as uninjured. However, the induction of certain cardiac genes was detected after opening of the pericardial sac (Wills et al 2008); therefore I used sham amputated hearts in some experiments, which is then also mentioned in the figure legend.

Two paralogs of *sox9*, *sox9a* and *sox9b*, are present in the zebrafish genome (Chiang et al 2001). To identify the spatial expression pattern of both paralogs I stained cryosections of regenerating hearts at 3 dpa and 7 dpa using *sox9* antibody staining. The antibody does not distinguish between the Sox9a and Sox9b proteins, since it detects a common antigen shared by both proteins. While I could rarely detect *sox9* expression in uninjured control

hearts (**Fig 3.2.1A a'**) expression was upregulated at 3 dpa (**b'**) and also at 7 dpa (**c'**) in regenerating hearts (**Fig 3.2.1A**). Sox9 expression was localized to the wound area and was also detectable in the wound edges, both in the lateral wound edges consisting of the activated epicardium and the external myocardial layer and in central parts, represented by the trabeculated myocardium, near the wound border (ii).

As mentioned above, the sox9-antibody used for staining cannot discriminate between the two Sox9 variants. To identify the expressed Sox9 paralog, amputated hearts of multiple time points (2, 4, 7, 14, 21 dpa) as well as uninjured controls were stained for *sox9a* mRNA using RNA in situ hybridization. Hearts of sham amputated as well as untreated fish, were used as controls. I did not detect *sox9a* positive cells in both controls, hearts of untreated fish as well as sham amputated hearts, whereas I could verify the amputation specific upregulation of *sox9a* mRNA during heart regeneration (**Fig 3.2.1B**). *sox9a* mRNA was initially expressed in a few positive cells at the wound border at 2 dpa and became detectable in more cells at the wound edges and in the wound area from 4 dpa onwards while the number of *sox9a* positive cells decreased from 14 dpa until 21 dpa.

To test whether *sox9b* is expressed in regenerating zebrafish hearts I performed RNA in situ hybridization on regenerating hearts at 3 and 7 dpa and on uninjured controls. Since *sox9b* has been shown to be expressed in the ovary and brain of zebrafish, I included sections of both tissues to control for probe quality, tissue preparation and staining procedure (Chiang et al 2001, unpublished observations of J. Kaslin). I detected *sox9b* positive (*sox9b+*) cells in the previtellogenic oocytes of the ovary as well as in cells of the periventricular nucleus of the lateral recessus in the brain (Chiang et al 2001, unpublished observations of J. Kaslin) (**Fig 3.2.1C**). In contrast, *sox9b* expression was neither detectable during heart regeneration at 3 dpa and 7 dpa nor in uninjured control hearts.

Sox proteins within one subgroup share high amino acid similarity within their HMG domain. Similar transactivation properties and functional redundancy have been shown for subgroup E Sox proteins which are *sox8*, *sox9a*, *sox9b*, and *sox10* (Kiefer et al 2007; Chiang et al 2001). Thus I tested the expression levels of *sox* genes that belong to subgroup E during heart regeneration using quantitative PCR (qPCR). Importantly, I could detect only very low expression levels of *sox9b*, *sox8* and *sox10* mRNA relative to the *sox9a* mRNA level at 4 dpa (**Fig 3.2.1D**) indicating that Sox9a is the only subgroup E Sox transcription factor active during heart regeneration.

Thus in the following, although the Sox9 antibody does not discriminate between the two Sox9 paralogs, I assume that the staining shows Sox9a positive cells. Due to that, all Sox9

positive cells that were detected using antibody staining, are referred to as Sox9a positive cells

Figure next page

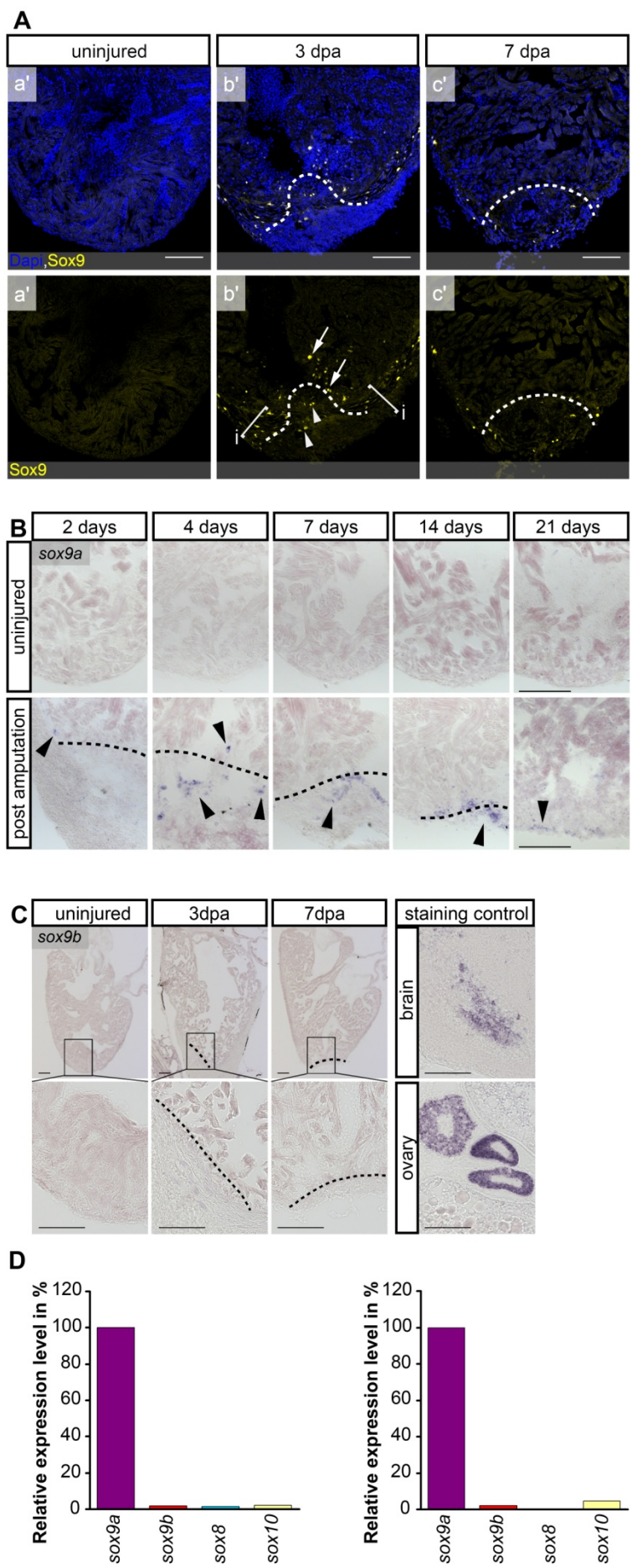
3.2.1 Sox9 expression pattern in zebrafish heart regeneration

A. Antibody staining for Sox9 on uninjured (a') and regenerating hearts at 3 dpa (b') and 7 dpa (c'). Upper panel shows merge of Dapi and Sox9 staining to indicate outlines of the ventricle. Lower panel shows only Sox9 staining to display localization of Sox9 staining at the lateral wound edges (brackets, i), central wound edges (ii) and in the wound area (grey arrows). Wound borders are indicated by white dashed lines. Scale bars are 100 μ m. Hearts 3 and 7 dpa n = 20 each, uninjured hearts n = 20 each time point.

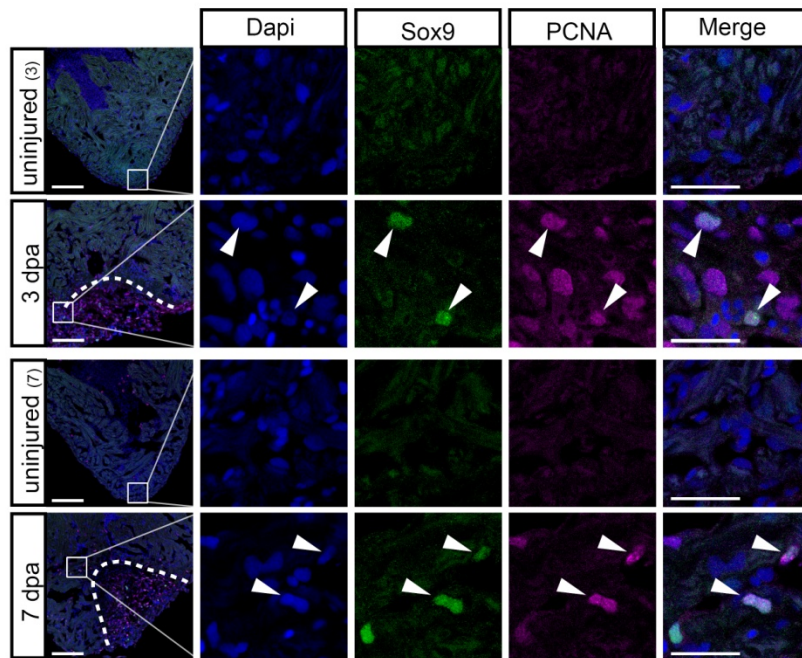
B. In situ hybridization for Sox9a mRNA on sections of regenerating hearts at 2, 4, 7, 14 and 21 dpa (lower panel) and corresponding uninjured control hearts (control hearts of 2,4,7,21 days are sham amputated, control heart of 14 days are derived from untreated fish) (upper panel). *sox9a* mRNA staining is localized to the wound edges and the wound area (black arrowheads). Wound borders are indicated by black dashed lines. Scale bars are 100 μ m. n = 3 for all time points.

C. *sox9b* mRNA is not detectable on sections of uninjured and regenerating hearts at 3 and 7 dpa using *in situ* hybridization. In contrast, staining for *sox9* mRNA is detectable in the periventricular nucleus of the lateral recessus in the brain and in the previtellogenic oocytes of the ovary (see staining control). Wound borders are indicated by black dashed lines. Scale bars are 100 μ m. Regenerating hearts n = 5, uninjured hearts n = 4.

D. Using qPCR, expression levels of *sox9b*, *sox8* and *sox10* mRNA were tested relative to *sox9a* mRNA in regenerating hearts at 4 dpa. Compared to *sox9a* mRNA, *sox9b*, *sox8* and *sox10* are expressed at very low levels at this time point. The results of 2 qPCRs are shown. n = 12 hearts.



During heart regeneration proliferation of various cell types is induced to replace lost cardiac tissue (Poss et al 2002). Thus I tested whether Sox9a+ cells display proliferative activity as well. Using antibody staining for Sox9a and PCNA, the proliferative nuclear antigen, I found that a subset, roughly a half, of all Sox9a+ cells at 3 and 7 dpa (**Fig 3.2.2**) expressed PCNA whereas no Sox9a+ cells and only few PCNA+ cells were detected in uninjured hearts.



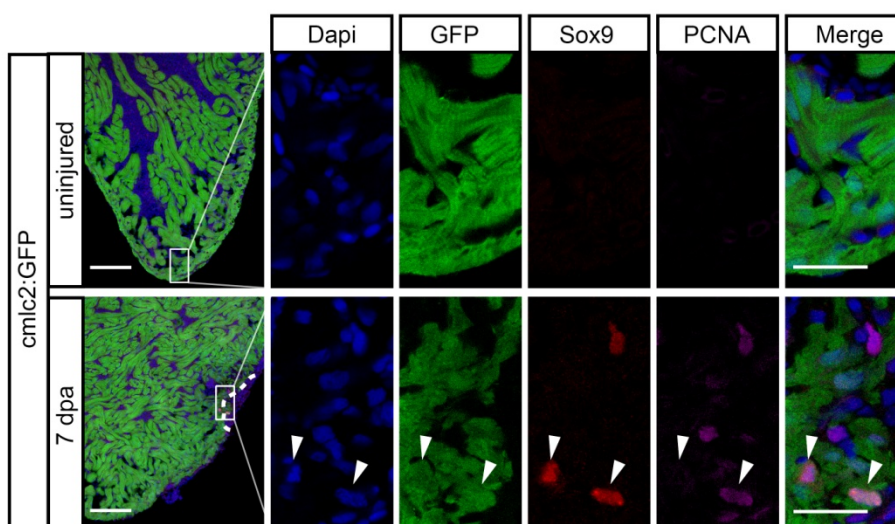
3.2.2 Sox9a+ cells are proliferating at 3 and 7 dpa while Sox9a+ and PCNA+ cells are not (PCNA rarely) detectable in uninjured hearts. Antibody staining for Sox9 and PCNA. White arrowheads indicate cells that are colabeled by PCNA and Sox9a. Nuclei are labeled by Dapi. Wound borders are indicated by white dashed lines. Scale bars in overviews are 100 μm , scale bars in magnifications are 25 μm . Hearts at 3 dpa $n = 9$, uninjured₍₃₎ $n = 12$; at 7 dpa $n = 13$, uninjured₍₇₎ $n = 13$. Uninjured hearts for each time point are shown, since they belong experimentally (3 and 7 day experiments with antibody staining at different days) to the respective regenerating heart.

In conclusion, *sox9a* is expressed specifically in regenerating zebrafish hearts starting within the first days post amputation. Sox9a+ cells are localized to the wound and the wound edges. Furthermore a subset of Sox9a+ cells shows proliferative activity.

3.2.1.2 Which cell types express Sox9a?

The zebrafish heart is primarily composed of three layers - the epicardium, myocardium and endocardium. All of these tissues are reconstituted in the process of regeneration (Lepilina et al 2006, Kikuchi et al 2010, Kikuchi et al 2011). To identify which of these layers express Sox9a⁺ cells I used reporter fish lines that express a fluorescent protein under control of a cell type specific promoter.

Cardiomyocytes are labeled in *cmlc2:GFP* (*Tg(myl7:GFP)*f1/+) (Huang et al 2003) transgenic fish expressing GFP under control of the *cardiac myosin light chain 2* promoter fragment. Activation of cardiomyocytes, indicated by activity of *gata4* promoter sequences in cardiomyocytes and proliferation of these myocardial cells, is detectable at 7 dpa as reported by Kikuchi and colleagues (Kikuchi et al 2010). To test whether Sox9a is expressed in proliferating myocardial cells at 7 dpa I used antibody staining against Sox9, GFP and PCNA. I detected Sox9a⁺ cells outside the myocardium (GFP negative) as well as Sox9a⁺ cardiomyocytes (GFP positive) at the wound border (Fig 3.2.3). A subfraction of Sox9a⁺ cardiomyocytes was proliferative as indicated by PCNA coexpression. In contrast, neither Sox9a nor PCNA induction was detectable in uninjured hearts (Fig 3.2.3). In summary, Sox9a is expressed in a subset of cardiomyocytes, part of which proliferate at 7 dpa.

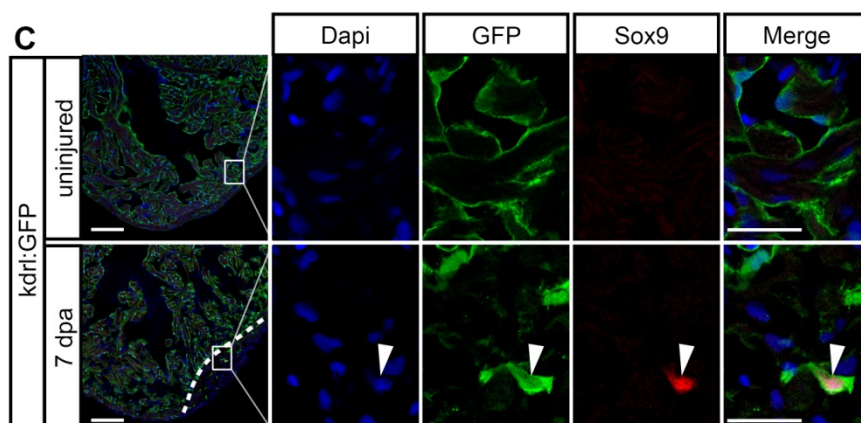
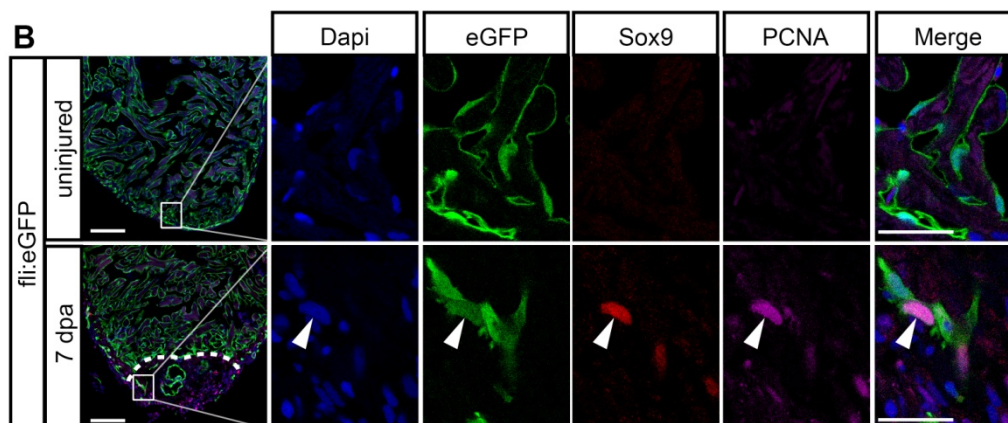
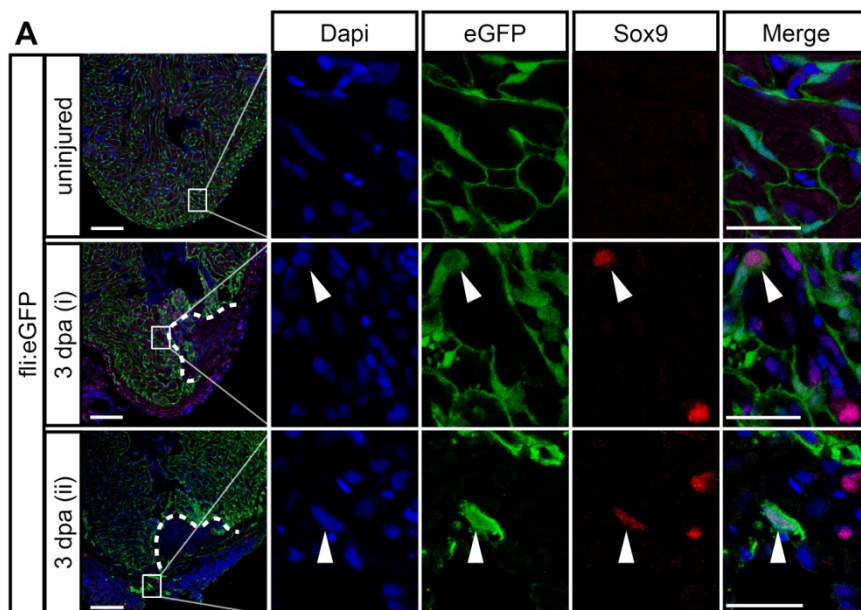


3.2.3 Sox9a+ is expressed in myocardial cells.

Hearts of TG(*cm1c2:GFP*) fish at 7 dpa and uninjured controls were stained for GFP, Sox9 and PCNA expression using respective antibodies. Sox9a is detectable in cardiomyocytes at the wound edges at 7 dpa (white arrowheads) and a few of these Sox9a+ myocardial cells proliferate (right white arrowhead). In contrast uninjured controls do not show Sox9a or PCNA positive cells. Nuclei are labeled by Dapi. Wound borders are indicated by a white dashed line. Scale bars in overviews are 100 μm , scale bars in magnifications are 25 μm . Hearts at 7 dpa and uninjured each n = 3.

The endothelial cells of vasculature and endocardium are labeled in the *fli1:eGFP* (*Tg(fli1:eGFP)y1*) and *kdrl:GFP* (*Tg(kdrl:GFP)la116*) fish lines (Lawson et al 2002, Jin et al 2005). The activity of the *fli1* promoter starts in early precursors of the endothelial lineage (Pham et al 2007, Ellertsdottir et al 2010). Expression of the early marker *fli1* precedes the expression of vascular markers such as *Flk1/Kdrl/Vegfr-2* (Pham et al 2007, Ellertsdottir et al 2010) and *VE-Cadherin1 (vecdn1)*, which label mature endothelial cells. Using antibody staining I analyzed uninjured and regenerating hearts of *fli1:eGFP* fish at 3 and 7 dpa for Sox9a expression. I detected Sox9a+ endothelial cells at 3 dpa and 7 dpa at the wound area and wound edges, while uninjured hearts showed GFP expression in endothelial cells but are devoid of Sox9a (**Fig 3.2.4A and B**). Furthermore, a subset of endothelial cells was PCNA+, and some endothelial cells both in the nonproliferative and proliferative population, were positive for Sox9a (**Fig. 3.2.4B**).

To confirm the endothelial character of a subpopulation of the Sox9a+ cells I performed antibody staining for Sox9a in regenerating hearts of TG(*kdrl:GFP*) transgenic fish showing GFP expression in the heart endothelium (Jin et al 2005). At 7 dpa, Sox9a was detected in endothelial cells localized at the wound border (**Fig 3.2.4C**).



3.2.4 A subset of endothelial cells, identified in *fli1:eGFP* or *kdr1:GFP* fish, express Sox9a at 3 and 7 dpa.

A. Hearts of TG(*fli1:eGFP*) fish at 3 dpa and uninjured controls were tested for Sox9a and GFP expression using antibody staining. Sox9a is detectable in GFP+ endothelial cells (white arrowheads) at the lateral wound edges (white box in overview of “ii”) and at the central wound border (white box in overview of “i”), representing presumably vascular endothelial (ii) and endocardial cells (i) cells. Sox9a staining is absent in uninjured hearts. Nuclei are labeled by Dapi. Wound borders are indicated by white dashed lines. Scale bars in overviews are 100 μ m, scale bars in magnifications are 25 μ m. Hearts at 3 dpa n = 6 and uninjured n = 8.

B. Sox9a and PCNA expression in endothelial cells were tested using TG(*fli1:eGFP*) hearts at 7 dpa and uninjured controls. Staining for GFP, Sox9a and PCNA verified proliferating Sox9a+ endothelial cells at the wound edges (white arrowheads). Nuclei are labeled by Dapi. Wound border is indicated by a white dashed line. Scale bars in overviews are 100 μ m, scale bars in magnifications are 25 μ m. Hearts at 7 dpa n = 5 and uninjured n = 6.

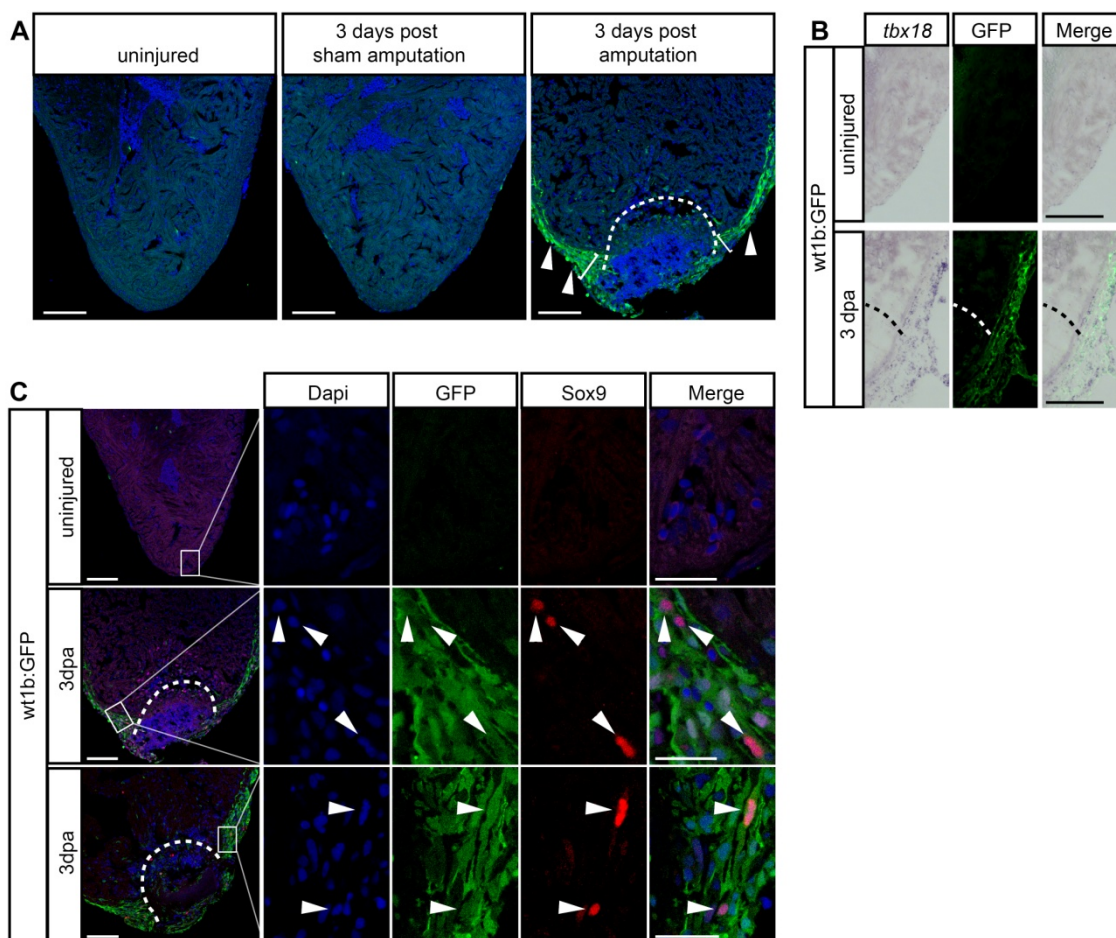
C. Sox9a is expressed in mature endothelial cells of the TG(*KDRL:GFP*) fish line at 7 dpa as indicated by anti-Sox9 and anti-GFP antibody staining. Sox9a expressing endothelial cells are detectable in the wound (white arrowhead). Uninjured hearts show endothelial GFP expression but are devoid of Sox9a signal. Nuclei are labeled by Dapi. Wound border is indicated by a white dashed line. Scale bars in overviews are 100 μ m, scale bars in magnifications are 25 μ m. Hearts at 7 dpa n = 3 and uninjured n = 3.

Next, I tested whether Sox9a is expressed in epicardial cells as well. The activation of the epicardium in the entire heart is an early response to ventricular amputation in zebrafish. The activated epicardium upregulates the expression of genes like the transcription factor *tbx18*, which are expressed in the developing epicardium but not in the adult uninjured heart (Lepilina et al 2006). Wilms tumor 1 (*wt1*) is a marker for the developing vertebrate epicardium (Männer et al 2001, Martinez Estrada 2010, Serluca 2008); the expression of both *wt1a* as well as *wt1b* have been reported in the adult zebrafish heart (Bollig et al 2006). However, whether *wt1* is expressed in the regenerating heart has not been tested. Since a transgenic fish line expressing eGFP under the control of *wt1b* regulatory sequences is available (Tg(*wt1b:eGFP*)^{li1}, Perner et al 2007), I asked whether there is reporter activity in the epicardium this fish line. I stained cryosections of regenerating hearts at 3 dpa and uninjured controls extracted from sham amputated and untreated fish

for GFP expression. While GFP activity was absent in the epicardium of both sham amputated and untreated controls, strong GFP expression was evident in the outermost layer of the heart at 3 dpa (**Fig 3.2.5A**). To confirm that GFP expression in this transgenic line is confined to epicardial cells, I costained sections of amputated hearts (3 dpa) and uninjured hearts for *tbx18* mRNA and GFP protein. While neither GFP nor *tbx18* expression is detectable in uninjured hearts, I found that expression of *tbx18* and GFP overlapped in injured hearts indicating that the *wt1b:GFP* (*Tg(wt1b:eGFP)li1*) transgenic fish line is a useful tool to label injury-activated epicardial cells in adult zebrafish hearts (**Fig 3.2.5B**). Furthermore, a thickening of the GFP+ cell layer, also indicating an activation of the epicardial cell layer (Lepilina et al 2006), was evident at the wound edges. Since the epicardial cell layer is activated early during regeneration I asked whether Sox9a is expressed in these cells. Using antibody staining on uninjured and regenerating TG(*wt1b:GFP*) hearts at 3 dpa for GFP and Sox9a expression I found that Sox9a is expressed in a subfraction of GFP+ epicardial cells (**Fig 3.2.5C**).

In conclusion, activation of the *wt1b:GFP* transgene in the epicardium of the injured heart confirms the reactivation of a developmental gene program in this heart layer in response to injury.

In addition, the activation of the myocardial and endothelial cell layer in response to amputation is indicated by an increase in proliferation of cardiomyocytes and endothelial cells. Interestingly, Sox9a expression is detectable in a subset of cells of all three examined layers of the heart in the early phase of the regeneration process. Both proliferative and non-proliferative cells express Sox9a. Careful quantification will be required to ask whether Sox9a is overrepresented in one cell type and whether it is preferentially expressed in proliferative cells.



3.2.5 Episcardial cells labeled in *wt1b:GFP* fish display *Sox9a* expression.

A. Uninjured control hearts derived from untreated and sham amputated *wt1b:GFP* fish as well as regenerating transgenic hearts at 3 dpa were stained for GFP expression using antibody staining. GFP expression in the outermost layer of the ventricle is activated after amputation presumably indicating *wt1b* expression (white arrowheads). Thickening of the episcardial layer is evident at the wound edges (brackets). Neither sham amputated nor untreated samples display GFP upregulation. Nuclear staining by Dapi indicates the outlines of the ventricle. Wound border is indicated by a white dashed line. Scale bars are 100 μ m. Hearts are $n = 11$ at 3 dpa, $n = 6$ at 3 days post sham amputation, $n = 5$ for untreated.

B. GFP expression in amputated *wt1b:GFP* transgenic hearts is confined to the episcardium. Coexpression of the episcardial marker *tbx18* and GFP is detected via in situ hybridization and anti-GFP antibody staining at 3 dpa. Uninjured hearts do neither show GFP nor *tbx18* expression. Wound border is indicated by a black dashed line. Scale bars are 100 μ m. Hearts for each treatment are $n = 3$.

C. Sox9a is expressed in epicardial cells at 3 dpa. Uninjured and regenerating wt1b:GFP hearts at 3 dpa were stained for GFP and Sox9 expression. Magnifications of wound edges at 3 dpa show Sox9a expression in epicardial cells (white arrowheads). Uninjured samples are devoid of GFP and Sox9a staining. Nuclei are labeled by Dapi. Wound borders are indicated by white dashed lines. Scale bars in overviews are 100 μm , scale bars in magnifications are 25 μm . Hearts at 3 dpa and uninjured each $n = 8$.

3.2.2 Is Sox9a necessary for zebrafish heart regeneration?

Sox9 is required for maintenance of progenitor cell in liver, which are also involved in adult liver regeneration (Furuyama et al 2010). Thus, I was wondering whether Sox9a function is required for regeneration of cardiac cell lines during zebrafish heart regeneration.

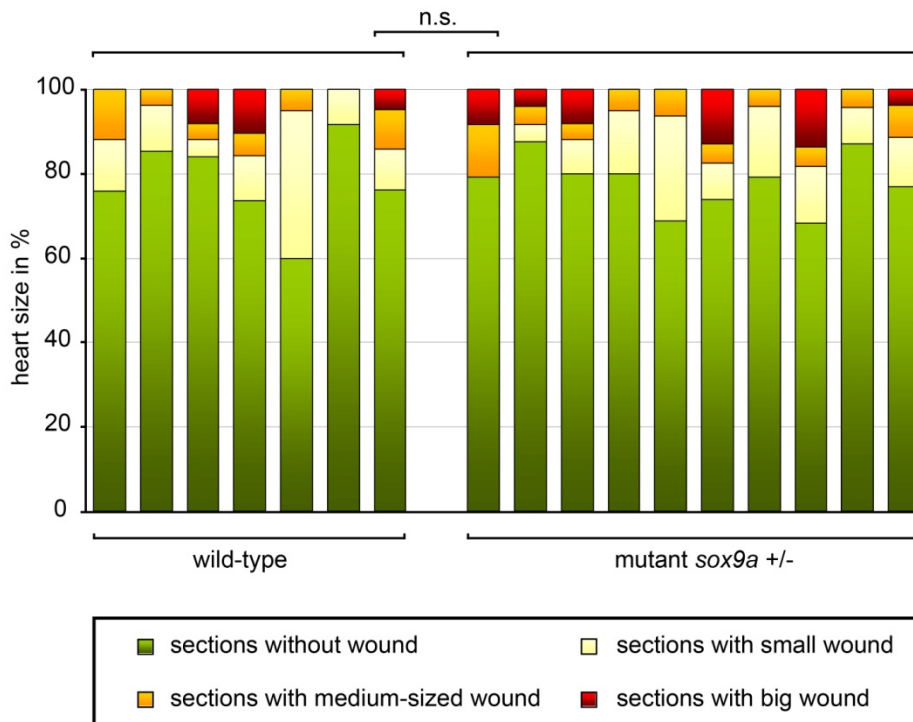
After studying the *sox9a* expression pattern during early regeneration, I aimed to analyze Sox9a function by using mutant fish lines. In contrast to heterozygous *sox9* mouse mutants, which die presumably due to haploinsufficiency; heterozygous *sox9a* and *sox9b* zebrafish mutants are viable and fertile (Akiyama et al 2004, Yan et al 2002, Yan et al 2005). Since homozygous mutants of either paralog die at around 5 dpf, I asked whether adult heterozygous *sox9a* mutants display heart regeneration defects (Yan et al 2002); yet heterozygous mutants are likely to have hypomorphic *sox9a* mutant phenotypes.

3.2.2.1 Is Sox9a required for morphological regeneration and/or wound resolution?

To test the functional role of *sox9a* in heart regeneration I used heterozygous *sox9a* mutant adult fish (*jellyfish*^{tw37}).

In a first experiment, I amputated heterozygous *sox9a* mutant adult fish and their wild-type siblings while uninjured fish of either genotype served as controls. After a regeneration time of 35 days, hearts were extracted, cryosectioned and examined histologically to assay for the progress of regeneration. Uninjured controls of *sox9a*^{+/-} fish did not show differences in morphology of the heart compared to uninjured wild-type hearts (data not shown). I classified the hearts sections according to the severity of the wound into different

groups: “sections without a wound”, ”sections with a small wound”, “sections with medium sized wound” and “sections with a big wound”. Analysis of amputated *sox9a* +/- hearts and wild-type siblings did not reveal a significant difference regarding the regeneration process in the heart (Fig 3.2.6).



3.2.6 No difference in regenerative capability between Sox9a heterozygous mutants (*sox9a* +/-) and wild-type siblings. *Sox9a* +/- and wild-type fish were allowed to regenerate until 35 dpa. Hearts were extracted and histology (AFOG staining) was used to assess the progress of regeneration by sorting the sections into different groups: “sections without a wound”, ”sections with a small wound”, “sections with medium sized wound” and “sections with a big wound”. There is no significant wound size difference in *Sox9a* +/- versus wild-type regenerating hearts. Wild-type hearts n = 7, *sox9a* +/- hearts n = 10. Qui square test.

In summary, I could not verify a role of Sox9a in heart regeneration using adult heterozygous *sox9a* mutant fish. It is, however, not unexpected to see weak or no phenotypic effects in *sox9a* heterozygous mutants. Due to the lack of adult homozygous *sox9a* mutants, I aimed to develop an alternative way to interfere with Sox9a during heart regeneration.

Thus, a dominant negative inhibitor construct was developed by combining the *sox9a* DNA binding HMG domain with the Engrailed transcriptional repressor domain to produce a repressor that competes with Sox9a binding to target genes and represses Sox9a target gene transcription. Sakai et al (2006) successfully used a similar strategy; a repressor form of Sox9, which contains the N-terminal HMG domain combined with an Engrailed 2 repression domain, caused the downregulation of Sox9 target genes in quail embryos and cell culture.

In my study, a C-terminal deletion construct of *sox9a* (*sox9a* Δ C), which still contained the HMG domain and additional protein interaction domains keeping most of the *sox9a* DNA binding specificity, was fused to the Engrailed domain (Kamachi et al 1999, Hsiao et al 2003, Chiang et al 2001). This construct was named *sox9a* Δ CEngrailed (abbr.: *sox9aEng*) (**Fig. 3.2.7A**).

I tested the functionality and specificity of the *sox9aEng* repressor construct using RNA injections into zebrafish embryos. Injection of *sox9aEng* induced a range of phenotypes at 1 dpf, which were sorted according to severity into three classes (class0/wt, class I, class II **Fig. 3.2.7B**). Class II embryos displayed the strongest phenotype with reduced anterior and posterior structures and an open neural tube. Class I embryos displayed reduced head structures whereas Class 0 showed the wild-type phenotype.

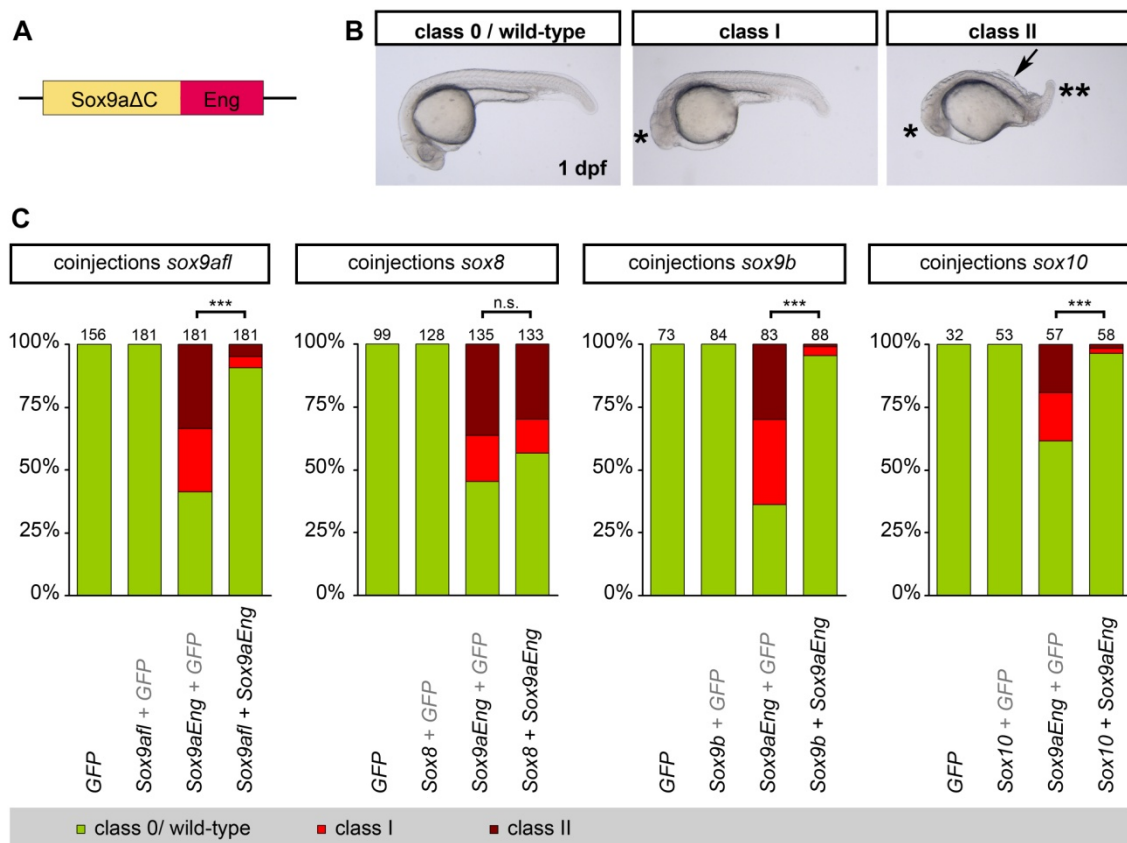
Notably, *sox9aEng* injected embryos did not resemble *sox9a* homozygous mutant (-/-) phenotypes, since these show defects in cartilage development. Thus, *sox9a*^{-/-} embryos are characterized by reduced or missing cartilage replacement bones (Yan et al 2002), while homozygous mutants for both paralogs (*sox9a*^{-/-}, *sox9b*^{-/-}) show more severe defects in craniofacial skeleton (Yan et al 2005). Early developmental defects as caused by Sox9aEng are not detectable in *sox9a*^{-/-} or *sox9a*^{-/-},*sox9*^{-/-} embryos (Yan et al 2002, Yan et al 2005). Sox9a-morpholino injection reproduced very similar phenotypes, suggesting that mutant phenotypes represent a complete loss of Sox9a function (Yan et al 2002). Thus Sox9aEng causes phenotypes during embryogenesis that are not consistent with *sox9a*^{-/-} phenotypes, indicating that Sox9aEng might (also) influence transcriptional activity of other Sox transcription factors.

To test to which extent the *sox9aEng* repressor construct showed specificity for interfering with Sox9a target genes or whether it likely also suppressed expression of genes regulated by other Sox E family members, I asked whether the effects of the construct on embryogenesis could be overcome by coexpression of full-length versions of *sox9a* (*sox9a full length*; abbr.: *sox9afl*), *sox9b*, *sox8* or *sox10*. First, I coinjected *sox9aEng* with *sox9afl*

and compared it to *sox9aEng* only. The injection of *sox9afl* RNA alone did not show any phenotypic effects at tested concentrations (**Fig 3.2.7C**, graph 1) while it significantly reduced the percentage of affected embryos when co-injected with *sox9aEng*, suggesting that Sox9aEng and Sox9a compete for binding to the same promoters.

I also asked whether the *sox9aEng* repressor can compete with other members of the subgroup E. I performed coinjection experiments of *sox9aEng* with *sox9b*, *sox8* or *sox10* RNA using the same experimental setup. Phenotypic effects are not detectable after injection of *sox9b*, *sox8* or *sox10* RNA alone at tested RNA concentrations (**Fig 3.2.7C**). However, I observed a significant rescue of *sox9aEng* phenotypes when coinjected with *sox9b* or *sox10* RNA, but not with *sox8* RNA.

In summary, I found that the repressor Sox9aEng presumably repressed transcription of genes, which are regulated by Sox9a but also Sox9b and Sox10. Interestingly, Sox8 regulated genes were not affected by Sox9aEng. However, an influence on Sox9b and Sox10 regulated genes should be of minor relevance for my studies, since *sox9a* appears to be the only factor of subgroup E being expressed during heart regeneration (see **Fig 3.2.1D**).



3.2.7 Inhibitory construct Sox9aΔCEngrailed (Sox9aEng) presumably interferes with Sox9a but also Sox9b and Sox10 target genes; Sox8 target genes were not influenced by the repressor.

A. The C-terminal deletion construct of Sox9a (Sox9aΔC), which still contains the DNA binding motif (HMG domain) and additional protein interaction domains was fused to the Engrailed domain (Eng).

B. Injection of *sox9aEng* RNA into zebrafish embryos induces different phenotypes at 1 dpf, which are distinguished into three classes according to severity. Class 0 embryos have the wild-type phenotype. Reduced head structures (*) are shown by embryos of class I. The strongest phenotype with reduced anterior (*) and posterior structures (***) and an open neural tube (black arrow) is displayed by class II embryos.

C. *sox9aEng* induced phenotypes are rescued by *sox9a* full length (Sox9a*fl*), *sox9b* and *sox10* mRNA coinjection. Injections were performed with zebrafish embryos up to the 2 cell stage. *sox9aEng* RNA was injected with a concentration of 15 ng/μl, and other used RNAs were injected in equimolar concentrations. RNAs of *sox9afl*, *sox8*, *sox9b* or *sox10* were coinjected with *sox9aEng* RNA. Injection of *gfp* RNA served as injection control and to adjust molarities in coinjections of *sox9aEng*, *sox9afl*, *sox8*, *sox9b* or *sox10* RNA alone. Coinjection of *sox9afl* (first graph), *sox9b* (third graph), and *sox10* (fourth graph) RNA significantly rescues the phenotypes caused by *sox9aEng*, whereas *sox8* (second graph) coinjection does not. Number of injected embryos is indicated above each graph. Chi square test was used for statistics. n.s. = not significant. $p < 0.001$ (***).

To interfere with Sox9a-mediated gene expression in adult heart regeneration I generated transgenic zebrafish lines expressing the *sox9aEng* construct. *sox9aEng* was tagged with a nuclear dTomato via the viral p2a peptide, which results in translation of separate proteins from a single open reading frame (Provost et al 2007) (**Fig 3.2.8A**). The heat-shock protein 70l promoter was used for inducible expression of the construct in all cells types (Halloran et al 2000).

To test the transgenic fish line Tg(hsp70l: dTomato p2A Sox9aΔCEngrailed) (in short: hsSox9aEng) for expression of the construct I used the dTomato fluorescence and the phenotype assay in embryos. First, I heat-shocked embryos from outcrosses of heterozygous hsSox9aEng fish to wild-type at 24 hours post fertilization (hpf) and detected wild-type and transgenic dTomato⁺ embryos at 30 hpf, showing no phenotypic abnormalities that early after transgene induction (**Fig 3.2.8B**). Second, I heat-shocked embryos of a hsSox9aEng outcross at shield (6hpf) and obtained phenotypes at 1 dpf that

recapitulated the classes observed in *sox9aEng* RNA injection experiments as described (compare **Fig 3.2.7B** and **Fig 3.2.8C**).

To assess functionality of the repressor construct I analyzed the expression levels of Sox9a target genes after Sox9aEng induction. Since we do not know of Sox9a targets in adult heart regeneration, I tested the influence of the repressor on expression of *collagen type II alpha-1a (col2a1a)* and *collagen type XI alpha 2 (col11a2)*, which have been described to be directly regulated by Sox9a in mammalian chondrocytes and zebrafish cartilage development (Oh et al 2010, Yokoi et al 2009), in transgenic TG(hsSox9aEng) embryos and in wild-type siblings. I gave a single heat-shock to the embryos at 24 hpf or two heat-shocks at 24 and 30 hpf and isolated RNA at 29 hpf or 48 hpf, respectively. Using qPCR, I detected that *col11a2* expression was downregulated in transgenic embryos compared to their wild-type siblings, with a stronger decrease of *col11a2* mRNA levels after two inductions of *sox9aEng* transgene (**Fig 3.2.8D**). Induction of *sox9aEng* with a single heat-shock had no effect on *col2a1a* expression whereas a stronger induction with two heat-shocks resulted in a downregulation of this gene (**Fig 3.2.8E**). Thus, Sox9aEng can interfere with Sox9a target gene expression in a concentration dependent manner.

Figure next page

3.2.8 Inhibitory function of Sox9aEng construct in TG(hsp70l: dTomato p2A Sox9aΔCEng) transgenic fish (short: hsSox9aEng) on Sox9a target gene expression.

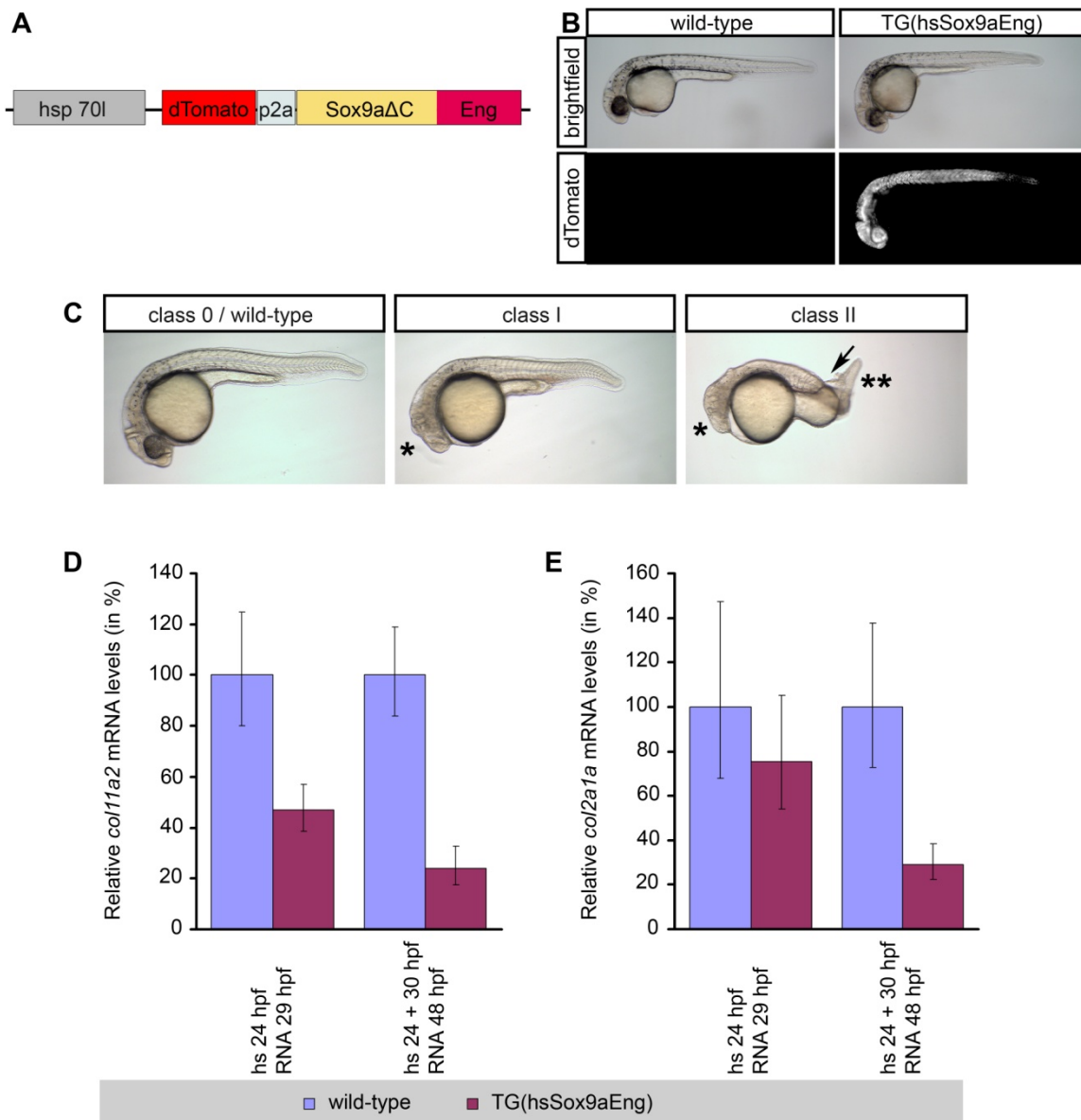
A. Construct to generate transgenic fish using the heat-shock promoter (hsp70l), which drives the expression of nuclear dTomato and Sox9aEng as separate proteins due to the viral p2A sequence.

B. Transgenic and wild-type embryos were heat-shocked at 24 hpf and assayed for expression of the transgene, as visualized by dTomato fluorescence in the whole embryo, at 30 hpf.

C. Induction of the transgene in hsSox9aEng embryos at shield stage caused different classes of phenotypes at 1 dpf that reproduce *sox9aEng* injection phenotypes.

Class 0 embryos show the wild-type phenotype. Class I embryos have reduced anterior structures (*). Further reduced anterior (*) and posterior structures (**) and an open neural tube (black arrow) are apparent in class II embryos.

D. and E. Sox9aEng induction decreases expression of *col11a2* and *col2a1a* mRNA in embryos in a concentration dependent manner. Transgenic hsSox9aEng and wild-type embryos were heat-shocked once at 24 hpf or twice at 24 and 30 hpf and assayed for *col11a2* (**D.**) and *col2a1a* (**E.**) mRNA expression at 30 and 48 hpf. Embryos for each time point and each genotype are n = 25. Error bars show standard deviations.



In conclusion, injections of *sox9aEng* RNA or early induction of *sox9aEng* transgene produced very severe phenotypes that did not resemble mutant phenotypes. As mentioned above, *sox9a*^{-/-} homozygous mutant fish are characterized mainly by cartilage defects and *sox9a*^{-/-}/*sox9b*^{-/-} mutants by more severe cartilage and bone defects as well as the absence of the otic vesicle (Yan et al 2002, Yan et al 2005). Besides repressing Sox9a target genes, Sox9aEng thus presumably also influences target genes of other Sox factors during development. However, *sox9a* appears to be the only factor of subgroup E that is expressed during zebrafish heart regeneration

To control for *sox9aEng* expression in adult heterozygous transgenic TG(*hsSox9aEng*) fish I tested heart tissue for expression of nuclear dTomato using antibody staining (**Fig**

3.2.9A). I detected nuclear dTomato in transgenic but not in control hearts; yet it was not detectable in all cells and therefore present in a mosaic expression pattern as explained below (**Fig 3.2.9A**).

3.2.2.2 Interfering with Sox9a-dependent gene expression – consequences on adult heart regeneration zebrafish

Since Sox9a is expressed in endothelial and myocardial cells during regeneration, I examined the influence of *sox9aEng* expression on regeneration of endothelial cells, labeled by *fli1:eGFP* reporter, and myocardial cells, identified by anti-myosin staining. I amputated double heterozygous *hsSox9aEng* x *fli1:eGFP* and their *fli1:eGFP* siblings; uninjured fish of either genotype served as controls. All fish were heat-shocked 6 hours before amputation and a series of heat-shocks was applied with one heat-shock per day starting 24 hours after amputation until 28 dpa.

At first, I tested double transgenics and control hearts for expression of the *sox9aEng* construct (dTomato+) in endothelial cells (eGFP+) and myocardial cells (myosin+) using antibody staining and detected Sox9aEng induction in endothelial and myocardial cells; yet Sox9aEng expression is not detectable in all cells, which indicates a mosaic expression pattern in TG(*hsSox9aEng*) transgenic hearts (**Fig 3.2.9A**).

Next, I examined the extent of regeneration of the myocardial and endothelial lineage at 28 dpa using antibody staining for myosin and GFP. I defined that the wound area as the area devoid of myosin staining and measured its size (**Fig 3.2.9B**). I found that Sox9aEng+ hearts displayed significantly enlarged wounds compared to regeneration controls suggesting that myocardial regeneration is reduced after interfering with Sox9a-dependent gene expression (**Fig 3.2.9B** and **C**). Furthermore, I determined endothelial regeneration by measuring the strength of *fli1:eGFP* expression (i.e. the GFP intensity per area) in the wound area (**Fig 3.2.9D**). While a difference in GFP intensities (GFP intensity normalized to a measured area) is not detectable in uninjured Sox9aEng+ hearts compared to control hearts (**Fig 3.2.9F**), the intensity of GFP signal, which corresponds to the amount of endothelial cells, in the wound is significantly reduced in Sox9aEng+ hearts compared to the regeneration control (**Fig 3.2.9D** and **E**), indicating a negative influence of *sox9aEng* expression on endothelial regeneration.

In conclusion, interfering with Sox9a-dependent gene expression causes a significant inhibition of myocardial and endothelial/endocardial tissue regeneration suggesting that

Sox9a function is important for reconstruction of essential tissues in adult heart regeneration.

Figure next page

3.2.9 Induction of *sox9aEng* transgene impairs endothelial and myocardial regeneration.

Double transgenic *hsSox9aEng* x *fli1:eGFP* hearts and single transgenic *fli1:eGFP* hearts as regeneration control were amputated 6 h after a heat-shock. A series of heat-shocks (hs) with 1 hs/day started at 24 h post amputation. Uninjured and regenerating hearts were extracted after 28 dpa and stained for dTomato (labeling cells expressing the Sox9aEng protein), GFP and myosin using antibody staining. Nuclei were labeled via Dapi staining.

A. Uninjured hearts of both genotypes show *fli1:eGFP* expression in endothelial cells (GFP+) and myosin staining in cardiomyocytes. Double transgenic *hsSox9aEng* x *fli1:eGFP* display heat-shock driven transgene induction (dTomato+) in endothelial cells (white arrowheads) and myocardial cells (yellow arrowheads). Yet the transgene is not expressed in all cells as few cells are devoid of dTomato staining (*). These cells represent presumably red blood cells.

Scale bars in overviews are 100 μ m, scale bars in magnifications are 25 μ m. Uninjured hearts each genotype n = 5. 28 dpa *fli1:eGFP* hearts n = 10 and *Sox9aEng* x *fli1:eGFP* hearts n = 9.

B. Wound size is increased after *Sox9aEng* induction for 28 days of regeneration. Myosin staining indicates increased wound area in *Sox9aEng* induced hearts compared to regeneration control. Wound border is marked by a red dashed line. Scale bar is 100 μ m.

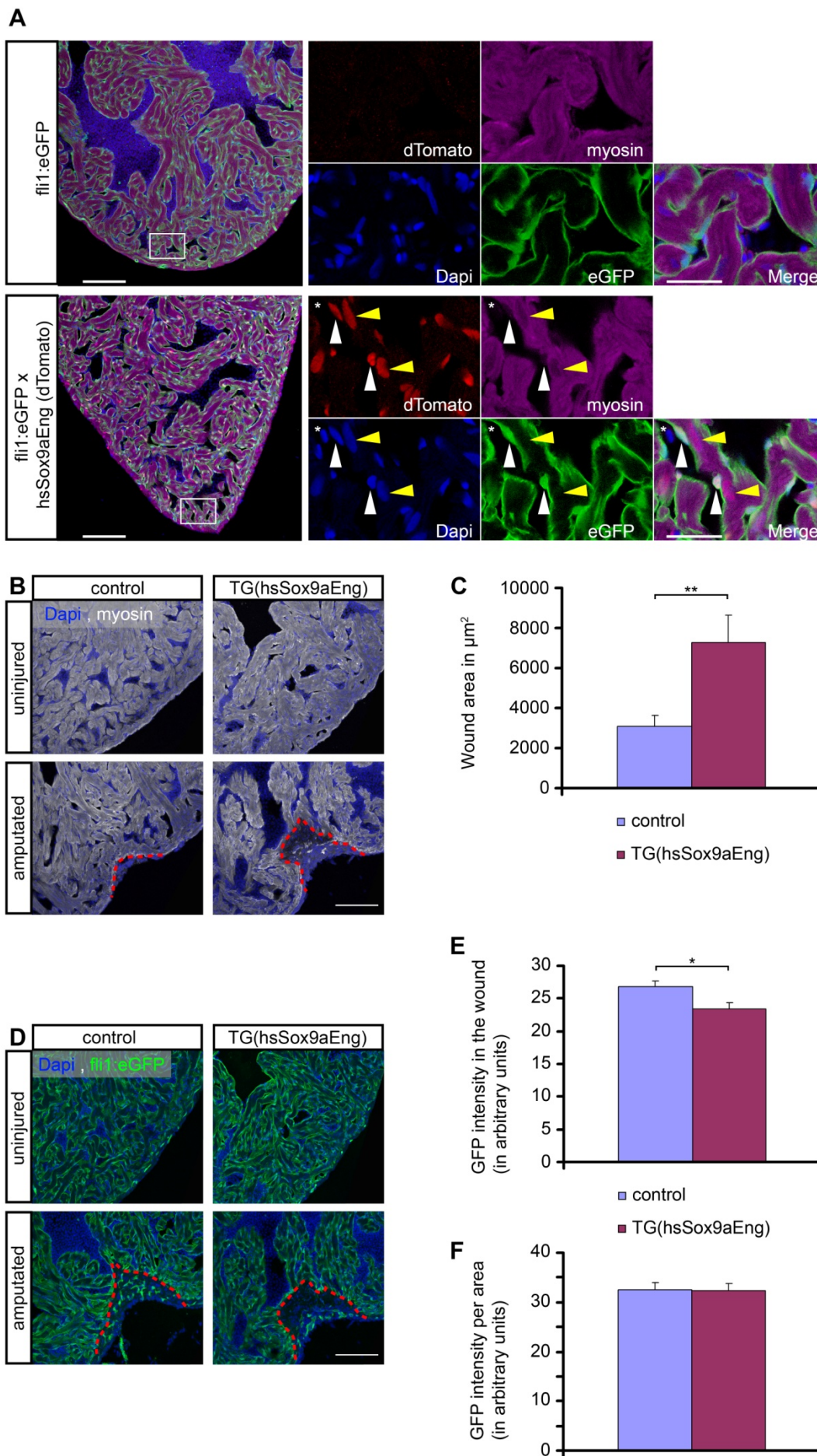
C. Quantification of the wound area (example in B.) in wild-type and *Sox9aEng* induced hearts at 28 dpa. The wound area is significantly smaller in wild-type versus transgenic hearts ($p = 0.005$). Mann-Whitney Rank Sum Test.

D. Impaired regeneration of endothelial cells after induction of *Sox9aEng*. Staining for GFP+ endothelial cells shows less regenerated endothelial (GFP+) cells in the wound area in *Sox9aEng* induced hearts versus regenerating wildtype controls. Pattern or amount of endothelial cells is unchanged in uninjured hearts of both genotypes. Wound border is indicated by a red dashed line. Scale bar is 100 μ m.

E. Quantification of GFP+ endothelial cells in the wound of regenerating hearts; *Sox9aEng* expressing versus control hearts. GFP intensity in the wound area was measured and is significantly reduced in *Sox9aEng* expressing hearts compared to control hearts ($p = 0.013$). Student's t-test.

F. Quantification of GFP expression in uninjured *Sox9aEng* induced versus control hearts. GFP intensity per area was measured and does not differ in uninjured *hsSox9aEng* x *fli1:eGFP* compared to *fli1:eGFP* hearts.

A-F. Uninjured hearts each genotype n = 5; each n = 15 sections. 28 dpa *fli1:eGFP* hearts n = 10 ; sections = 25 and *Sox9aEng* x *fli1:eGFP* hearts n = 9; sections = 23.



3.3.1 Alternative heart infarct model in zebrafish

3.3.1.1 The zebrafish heart regenerates after cryoinjury

Currently, surgical resection of the ventricular apex, about 20% of the ventricle, is used to cause injury in the zebrafish heart (Poss et al 2002). Yet, this injury type differs from mammalian heart infarctions, which are caused by tissue death, typically due to ischemia (Cleutjens et al 1999, Abarbanell 2010). Hence, I aimed to develop an injury method that is associated with cell death and thus is more comparable to heart infarction.

Therefore I established a cryoinjury procedure, during which, after opening of the body wall and pericardial sac, I exposed the ventricular apex to dry ice to cause tissue death. I analyzed the regenerative capacity of the injured heart at 4, 14 and 60 days post cryoinjury (days post injury = dpi) by histological Acid Fuchsin Orange G (AFOG) staining, which stains collagen in blue, fibrin in red and myocardium in orange (**Fig 3.3.1A - D**). I detected reduced tissue organization, loss of myocardium and massive accumulation of fibrin in the wound area at 4 dpi (**Fig 3.3.1B**). Thus morphological analysis revealed the presence of fibrin rich wound tissue at 4 and 14 dpi, which is typical for ventricular resection as well (**Fig 3.3.1B** and **C**). However, remaining wound tissue at 60 dpi stained for collagen indicating that some scar tissue had formed (**Fig 3.3.1D**). Nevertheless, I detected interspersed myocardial cells in the lesioned tissue at 60 dpi which indicates that newly formed cardiomyocytes had penetrated/invaded the lesion (**Fig 3.3.1D**).

To estimate the extent of tissue recovery, I measured the size of the lesioned area relative to the total ventricle area in the histological section showing the biggest wound (thus the largest wound diameter) in the cryo-lesioned heart (**Fig 3.3.1E** and **F**). Using this estimation at 4 dpi, I found that the procedure reproducibly damaged 25% of the ventricle (**Fig 3.3.1E**). Thus, similar to ventricular resection, which is the loss of ~20% after ventricular resection (Poss et al 2002), zebrafish also tolerate large necrotic heart lesions (25% of the ventricle) caused by cryoinjury. More importantly, I detected a significant reduction of the wound size over time, indicating regeneration of the damaged heart tissue. Histological analysis and estimation of heart regeneration showed a decrease in wound size from 25% at 4 dpi down to 2% at 60 dpi (**Fig 3.3.1E**).

To quantify the recovery of lesions and regenerative progress more precisely, the time course experiment was repeated and the hearts at 3, 41 and 60 dpi were sectioned to

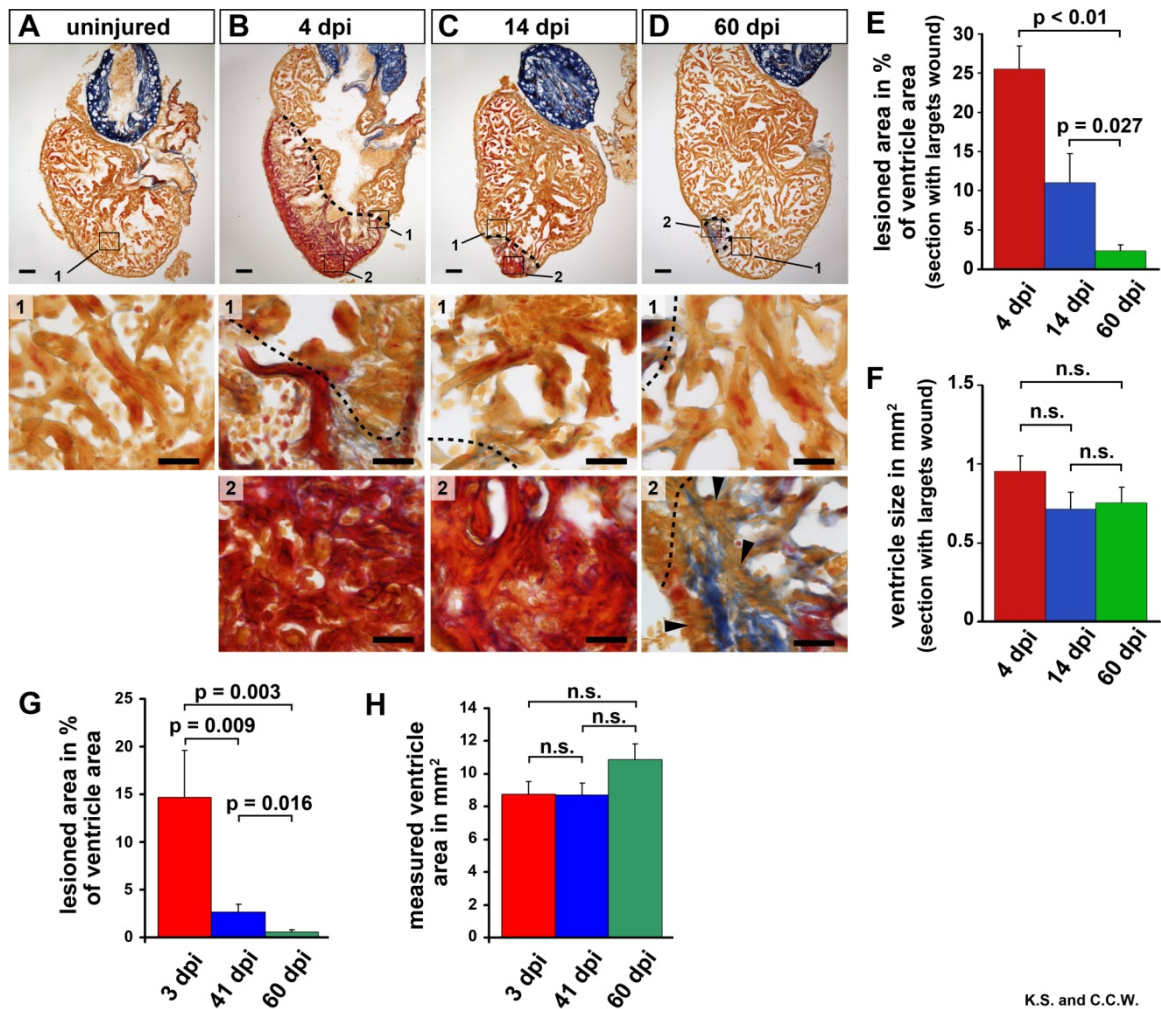
measure representatively the ventricle and wound size (**Fig 3.3.1G** and **H**). More precise quantifications are explained below.

But at first, to compare the second time course with the first one, I measured the ventricle and wound of every heart at 3 dpi on one histological section showing the biggest lesion. I found that the largest wound diameter affected on average 26% of ventricle (data not shown), which is very similar to the lesion in the first time course and indicates that this method causes reproducible lesions.

For more precise quantifications, measurements of ventricle and wound size were carried out on every fifth heart section in serial tissue cryosections, which was thus representative for the entire ventricle. Hence, I quantified the ventricles and lesioned areas, by measuring every fifth section, and found a lesioned area of 15% compared to the ventricular size at 3 dpi (**Fig 3.3.1G**). A strong reduction of the lesioned area to 3% at 41 dpi and further to 0.5% at 60 dpi was detectable displaying a dramatic reduction of the wound size within 60 days (**Fig 3.3.1G**). Additionally, the ventricle area is in average unchanged comparing all time points in both sets of experiments, indicating that compensatory growth of new myocardium had occurred (**Fig 3.3.1F** and **H**).

Comparison of the regenerative progress after cryoinjury or ventricular resection showed that regeneration proceeded in similar time windows in the two models. The largest wound diameter after cryoinjury is ~26% of the ventricle and was reduced to 12% at 41 dpi, which is comparable with resection showing that after amputating 20% of the heart, 14% of the ventricle was still missing at 30 dpa as reported by Poss and colleagues (Poss et al 2002). Using the combined data of both time course experiments with respect to regenerative outcome, 3 out of 12 fish with cardiac cryoinjury showed no sign of collagen deposition whereas others displayed some scar tissue at 60 dpi. However, ventricular resection can also result in some scar formation as indicated by small collagen deposits at 60 dpa (Poss et al 2002). Hence, result of regeneration after cryoinjury and ventricular resection were comparable in speed and completeness.

Thus zebrafish were able to regenerate lesions associated with widespread tissue damage caused by cryoinjury with little scar formation.



K.S. and C.C.W.

3.3.1 The zebrafish heart regenerates tissue damage after cryoinjury.

Sections of uninjured control hearts (A) and hearts at 4 (B), 14 (C) and 60 (D) days after cryoinjury (dpi = days post injury) were stained with Acid Fuchsin Orange G (AFOG), which labels cardiomyocytes in orange, fibrin in red and collagen in blue (experimental set 1). Healthy myocardium is shown in magnification #1 of the uninjured heart. Magnifications #1 of lesioned hearts show cardiomyocytes at the wound edges and parts of the wound tissue. Magnifications #2 show close ups of the lesioned area. Note that the lesioned area, showing fibrin accumulation at 4 dpi and 14 dpi and minor deposits of collagen at 60 dpi is decreasing in size. Myocardial cells are missing at 4 and 14 dpi whereas at 60 dpi collagen rich lesion tissue is interspersed with cardiomyocytes (black arrowheads). Wound edges are indicated by black dashed lines. Scale bars are 100 μ m in overviews and 25 μ m in magnifications.

E. Quantification of the size of cryolesions. The largest extent of the lesioned area was quantified and normalized to the size of the ventricle in experimental set 1. Measurements were performed on the section displaying the biggest wound for each heart. Error bars = s.e.m., significance tested by Student's t-test. n = 5 hearts 4 dpi, 5 hearts 14 dpi, 4 hearts 60 dpi. **F.** Quantification of the ventricular area at 4, 14 and 60 dpi. The ventricular area was quantified on sections analyzed in E. One - way Anova test was used to show that ventricular areas are not significantly different. **G.** Quantification of the lesioned area normalized to the ventricular size in the experimental set 2. Measurements of the lesion size and ventricular size were performed on all serial sections of each heart. Error bars = s.e.m., significance tested by Student's t-test (41 dpi and 60 dpi) and Mann-Whitney rank sum test (others). n = 5 hearts 3 dpi (73 sections), 6 hearts 41dpi (89 sections), 7 hearts 60 dpi (118 sections). **H.** Quantification of the ventricular area of the hearts analysed in G.

Measurements of ventricular size were done on all sections for each heart. Significance tested by Student's t-test (41 dpi and 60 dpi) and Mann-Whitney rank sum test (others).

(Experiments performed by K.S. and C.C.W.)

3.3.1.2 Characterization of the cellular damage caused by cryoinjury

To characterize/examine the cellular damage caused by cryoinjury, I analyzed hearts at 1 dpi and 3 dpi as well as uninjured hearts using semi thin plastic sections stained by toluidine blue (**Fig 3.3.2**). The internal cardiomyocytes organized into trabeculae are demarcated from the external layer of compact cardiomyocytes as visible in uninjured hearts (**Fig 3.3.2B** and **E**). Erythrocytes are detectable in the intra-trabecular space (**Fig 3.3.2C**). The epicardial epithelium lining the external myocardial layer is evident as single cell layer (**Fig 3.3.2E**). Myocardial cells show the typical striated pattern or a granular structure depending on their orientation relative to the sectioned plane and nuclei with a prominent nucleolus (**Fig 3.3.2D** and **G**).

At 1 dpi, I detected a reduced width of the external myocardial layer, which is in addition devoid of cells with a myocardial morphology (**Fig 3.3.2I**). Most cells in the trabecular area lost the typical striated pattern and nuclei; yet they display vacuolar structures (**Fig 3.3.2J - K**). Moreover, erythrocytes are clearly enriched in the lesioned area (**Fig 3.3.2J - K**). Leukocytes, mostly granulocytes, are aligned at the wound borders and infiltrated the wound area, which indicates an inflammatory response to clear cellular debris from the affected area (**Fig 3.3.2L - N**).

Further remodeling of the wound area is obvious at 3 dpi (**Fig 3.3.2O**). I detected a loose morphology of the external ventricular layer which displays intracellular spaces and lacks tightly packed cardiomyocytes (**Fig 3.3.2P**). The inner part of the affected area is completely filled with erythrocytes and lacks trabecular structures (**Fig 3.3.2Q - R**); instead it shows remaining cell debris that is often closely associated with leukocytes (**Fig 3.3.2S**).

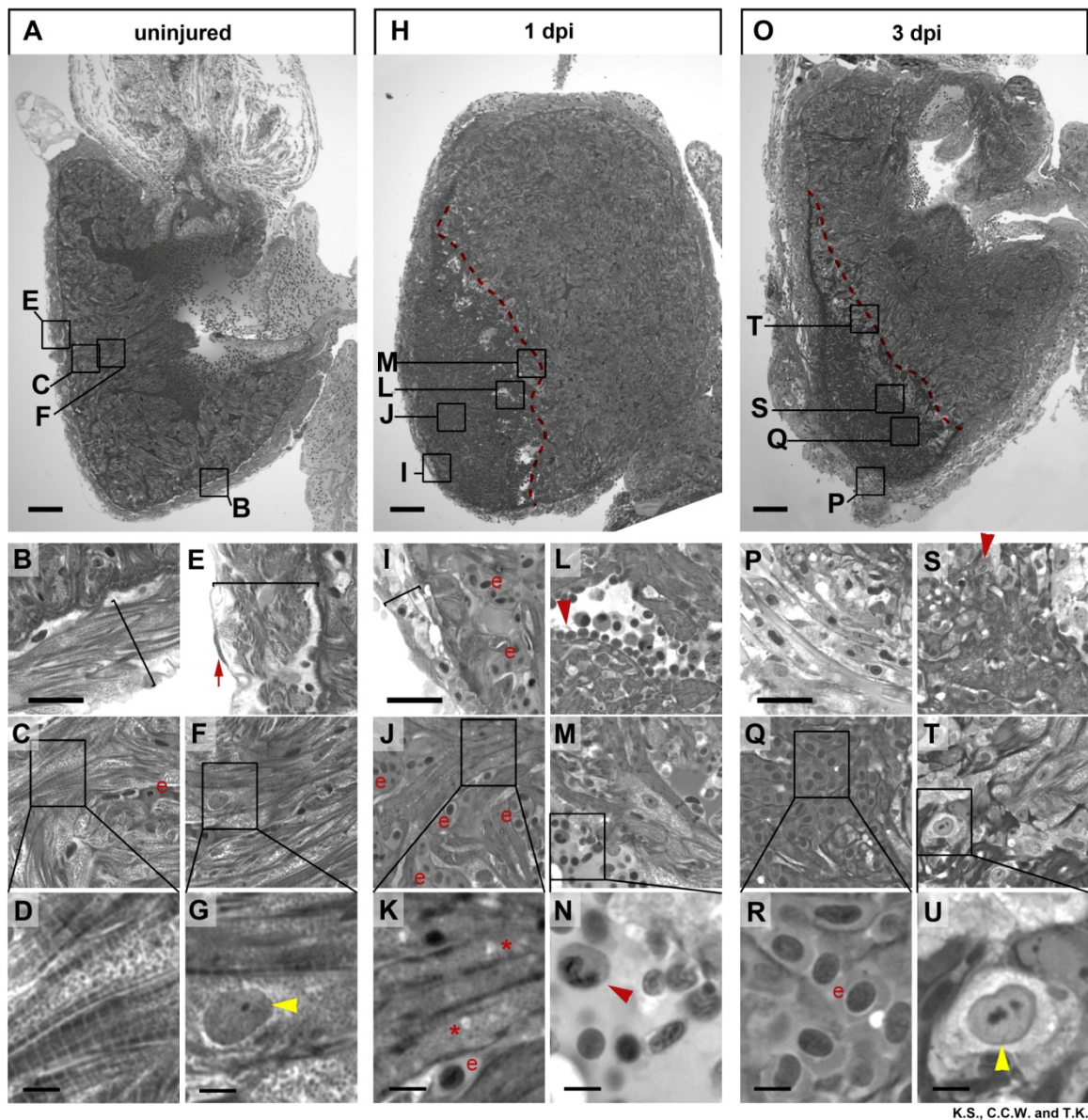
Recent studies have suggested that mature cardiomyocytes lose their sarcomeric myofilament structure and thus that cardiomyocytes dedifferentiate, which is presumably preceding myocardial proliferation during heart regeneration (Kikuchi et al 2010, Jopling et al 2010). Interestingly, I found the wound edges at 3 dpi were lined by cells of unknown origin displaying the nuclear morphology of cardiomyocytes with the prominent nucleolus; but the typical striated or granular structure of the cytoplasm is absent (compare **Fig 3.3.2D** and **G** with **Fig 3.3.2T - U**). Thus due to these findings, I speculate that these cells might be activated cardiomyocytes possibly with reduced myofilaments.

Figure next page

3.3.2 Cryoinjury causes myocardial cell death, inflammatory response, massive changes in tissue morphology and appearance of activated cardiomyocytes at the wound edges.

Semi-thin histological sections of an uninjured heart (**A - G**) and cryolesioned hearts at 1 dpi (**H - N**) and at 3 dpi (**O - U**) were stained with Toluidin blue. Wound edges are indicated by red dashed lines (**H, O**). Striated cardiomyocytes in the compact external (**B**) and in the trabeculated internal (**C, D**) myocardium as well as a nucleus of a myocardial cell with a prominent nucleolus (**F, G**, yellow arrowhead) are shown in the uninjured heart. The single layer of epicardial epithelium covers the underlying myocardium (red arrow in **E**).

At 1 dpi the thickness of the external myocardial layer is reduced (compare brackets in **B** and **I**) in the lesioned area. Most cardiomyocytes have lost striations suggesting myofibril disassembly (**L, J, M**) and vacuolar structures further suggest destroyed cardiomyocyte structure (**J**, red stars in **K**). Leucocytes, largely heterophil/neutrophil granulocytes, delineate the wound edges (red arrowheads in **L, M, N**).

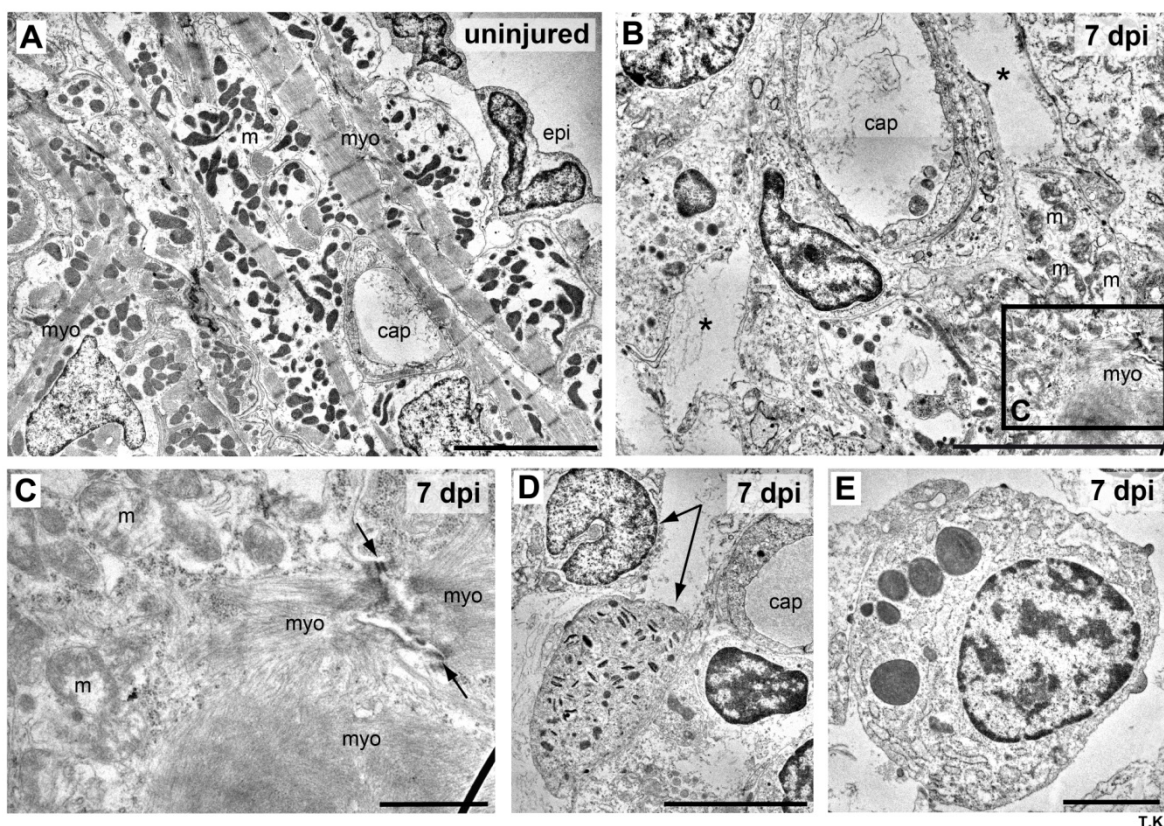


K.S., C.C.W. and T.K.

At 3 dpi a loosened morphology devoid of cardiomyocytes is apparent in the external myocardial layer (**P**). The wound area is largely filled with erythrocytes (*e* in **Q**, **R**). Cellular debris is often associated with granulocytes (red arrowhead in **S**). Cells at the wound edges display nuclei with a prominent nucleolus (yellow arrowhead in **U**, **T**), which are similar to myocardial nuclei (compare **G** and **U**), and are devoid of the striated cellular structure (**U**). For each time point $n = 3$ hearts. Scale bars in **A**, **H** and **O** are 100 μm . Scale bars in **B**, **I** and **P** are 25 μm . Scale bars in **D**, **G**, **K**, **N**, **R** and **U** are 5 μm . *e* = erythrocytes.

(Experiments performed by K.S., T.K. (staining) and C.C.W.)

Scanning electron microscopy revealed that subepicardial cardiomyocytes have characteristic myofilaments and electron dense mitochondria in uninjured hearts (**Fig 3.3.3A**). The epicardial epithelium was evident as single cell layer as well (**Fig 3.3.3A**). In contrast, cellular debris and large tissue gaps were detected in the lesioned area at 7 dpi (**Fig 3.3.3B**). Myocardial cells within the affected area showed highly disorganized myofilaments and destroyed mitochondria (**Fig 3.3.3B - C**). Additionally heterophil/neutrophil and eosinophil granulocytes were detectable in the lesioned area (**Fig 3.3.3D - E**).



3.3.3 Ultrastructural analysis of cryolesioned myocardium reveals cardiomyocyte cell death and an inflammatory response.

Electron micrographs of uninjured (A) and cryolesioned (7 dpi, B - E) zebrafish heart tissue. A. A normal organization of ventricular periphery with epicardial epithelium (epi) and subepicardial cardiomyocytes that display organized striated myofilaments (myo) with Z lines and electron dense mitochondria (m). A capillary (cap) is visible as well.

B. The lesioned area at 7 dpi displays cellular debris and large tissue gaps (*) around a small capillary (cap). Cardiomyocytes show damaged mitochondria (m) and disorganised myofilaments (myo) (box in B).

C. A cryoinjured cardiomyocyte with disorganized mitochondria (m), disorganized myofilaments (myo), and a destroyed intercalated disc (arrows) is shown.

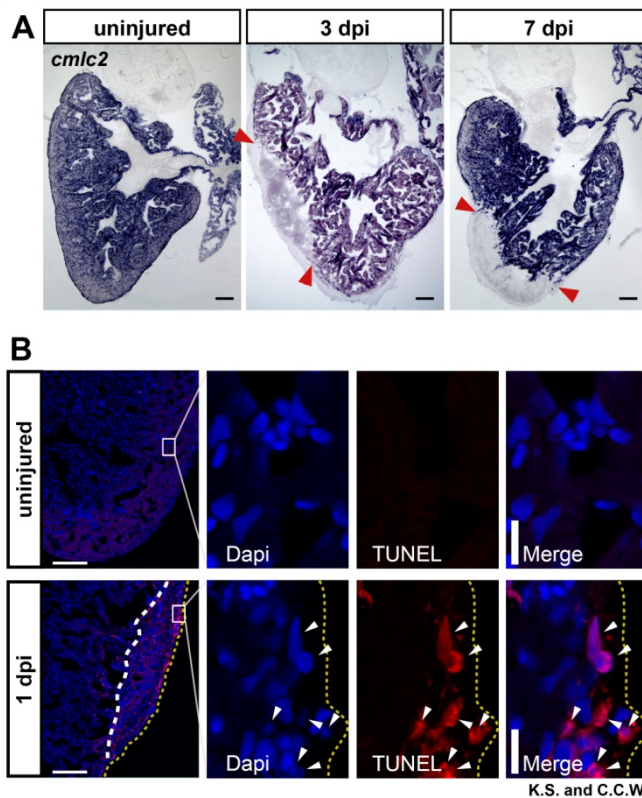
(D, E) Granulocytes in the wound area. **(D)** Heterophil/neutrophil granulocytes (arrows), the upper one with a peripheral, nonsegmented nucleus, the lower one with characteristic, cigar-shaped cytoplasmic granules. **(E)** Eosinophil granulocyte. Scale bars are 5 μm in A, B, and D, 1 μm in C, and 2 μm in E.

(Experiments performed by T.K. (imaging and analysis))

In summary, cell death and the loss of cardiomyocytes in the affected area were detectable after cryoinjury using histological as well as ultrastructural analysis. Moreover, infiltration of leukocytes and erythrocytes were initial responses to a cryoinjury event. Histological stainings, however, revealed the presence of cells at 3 dpi at the wound borders, which might be myocardial cells showing reduced myofilaments.

To further verify the loss of cardiomyocytes after cryoinjury, I examined the expression of the myocardial marker *cardiac myosin light chain 2 (cmlc2)* using in situ hybridization (**Fig 3.3.4A**). Lesioned hearts at 3 and 7 dpi showed a wound specific loss of *cmlc2* expression (**Fig 3.3.4A**). The absence of *cmlc2* transcript in the lesioned area within the next days after cryoinjury further supported the loss of cardiomyocytes due to cell death, which was indicated before by morphology (see **Fig 3.3.2** and **3.3.3**).

To test whether apoptosis is induced and thus contributing to cell death in the injured area I stained uninjured and lesioned hearts at 1 dpi for apoptotic cells using TUNEL (TdT-mediated dUTP-biotin nick end labeling) method. (**Fig 3.3.4B**). I could rarely detect TUNEL positive cells in uninjured hearts, while lesioned hearts displayed a strong enrichment of apoptotic cells in the affected area (**Fig 3.3.4B**). Thus, cell death within the lesion was partly caused by apoptosis.



3.3.4 Cryoinjury causes loss of cardiomyocyte specific marker gene expression and upregulation of apoptosis

A. In situ hybridization shows loss of *cmlc2* expression in the lesioned area at 3 and 7 dpi. The lesioned area is indicated by red arrowheads. Scale bars are 100 μm . $n = 3$ hearts for each uninjured, 3 dpi and 7 dpi.

B. TUNEL assay on hearts at 1 dpi verifies increased number of apoptotic cells (white arrowheads) compared to uninjured hearts. The wound area is indicated by a white dashed line and the periphery of the

heart is marked by a yellow dashed line. The nuclei are stained with Dapi. Scale bar in overview is 100 μm and in close ups 10 μm . $n = 3$ hearts each uninjured and 1 dpi.

(Experiments performed by K.S. and C.C.W.)

3.3.1.3 Organ-wide response of the epicardium to cryoinjury

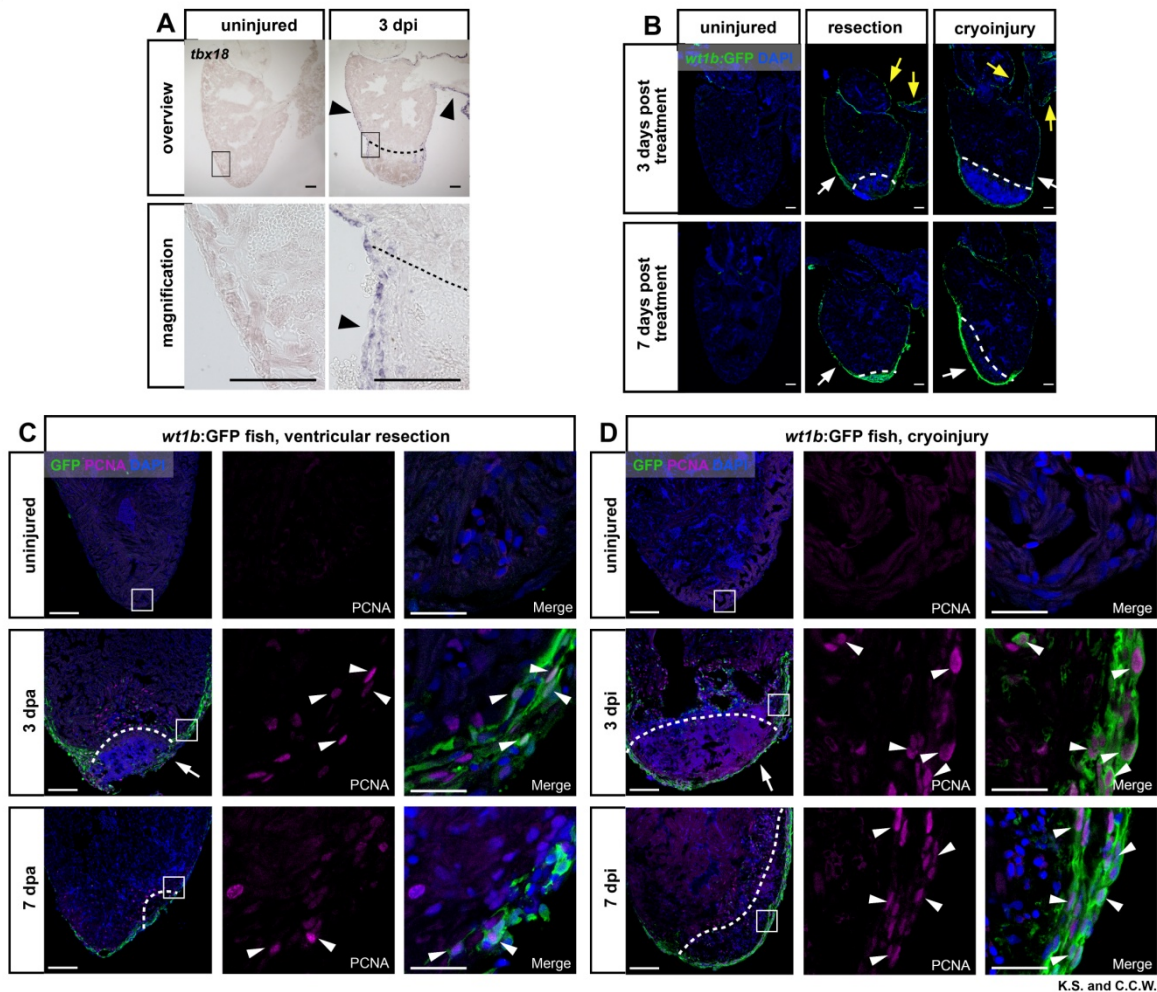
Ventricular resection causes an activation of the epicardium in the entire heart as a very early response to the injury. This activation is characterized by the increased proliferation of epicardial cells and the activation of a developmental gene expression program (Lepilina et al 2006). Thus genes like *tbx18* and *wt1b*, which are expressed during epicardial development in vertebrates (Kraus et al 2001, Männer et al 2001), are upregulated in epicardial cells early after injury/amputation (Lepilina et al 2006 and see part 3.2.1.2). Hence, I tested whether a similar activation of the epicardium occurs after ventricular cryoinjury.

Therefore, lesioned hearts at 3 dpi and uninjured controls were stained via in situ hybridization for *tbx18* expression (**Fig 3.3.5A**). Whereas *tbx18* expression was absent in uninjured hearts, I detected cryoinjury activated *tbx18* transcription at 3 dpi (**Fig 3.3.5A**). Next, I used the transgenic fish line *wt1b:GFP* ($\text{Tg}(wt1b:e\text{GFP}^{\text{li1}})$), which labels epicardial

cells after ventricular resection (see part 3.2.1.2), and compared GFP expression in cryoinjured and amputated hearts at 3 and 7 dpi. While GFP expression was not upregulated in uninjured hearts I detected strong GFP activity in the outermost cell layers, which likely represents the epicardium, at 3 and 7 days after ventricular resection as well as after cryoinjury (**Fig 3.3.5B**). After both types of injury activation of the epicardium was detectable in the entire surface of the heart including ventricle, atrium and bulbus.

Furthermore, I tested the activation of the epicardium after ventricular resection and cryoinjury in *wt1b:GFP* hearts using costaining for GFP and the proliferation marker PCNA. In contrast to uninjured hearts, I detected proliferating GFP⁺ cells in the epicardium of amputated hearts at 3 and 7 dpa (**Fig 3.3.5C**). Morphological changes caused by ventricular resection were evident by the thickening of the epicardial layer at the wound edges at 3 dpa (**Fig 3.3.5C**). Furthermore, GFP⁺ cells were partially covering the wound area suggesting that epicardial cells moved along the wound edges and around the outer surface of the wound area. At 7 dpa, the wound was covered by an epicardial layer (**Fig 3.3.5C**). Likewise, I detected proliferating epicardial cells after cryoinjury at 3 and 7 dpi (**Fig 3.3.5D**). The thickening of the epicardial layer was evident at 3 dpi. A complete covering of the lesioned tissue by epicardial cells was already detectable at 3 dpi and still present at 7 dpi, suggesting that migration of epicardial cells occurred more quickly after cryolesion (compare **Fig 3.3.5C** and **D**).

In conclusion, the epicardium was activated after cryolesion as shown by the upregulation of a developmental gene expression program in the entire organ. Furthermore, proliferating epicardial cells were detectable after both types of injury. The epicardial response after resection and cryoinjury was similar with respect to the temporal pattern, level of gene expression activation and proliferation rate. In contrast to resected hearts at 3 dpa, I detected complete coverage of the wound area in cryolesions at 3 dpi suggesting that epicardial cells migrated faster after cryoinjury than after ventricular resection.



3.3.5 Organ-wide activation of embryonic gene expression and cell proliferation in the epicardium in response to cryoinjury and ventricular resection.

A. In situ hybridization for *tbx18* shows expression in the entire epicardium (black arrowheads). Wound edges are indicated by black dashed lines. Scale bars are 100 μ m. n = 3 hearts each uninjured control and 3 dpi.

B. The entire epicardium is activated after cryoinjury and ventricular resection as indicated by GFP expression in TG(*wt1b:GFP*) transgenic hearts at 3 and 7 days after cryoinjury and ventricular resection. Uninjured hearts show no GFP induction in the epicardium. Transgene induction is visible in the thickened epicardium near the wound (white arrows) but as well in the epicardium lining the bulbus arteriosus (yellow arrows). Nuclei were stained with Dapi. White dashed lines indicate wound edges. Scale bars are 100 μ m. n = 5 hearts at all time points.

C. and **D.** Activation of epicardial proliferation in response to ventricular resection (**C**) and cryoinjury (**D**). Uninjured and amputated hearts at 3 and 7 dpa (**C**) or cryoinjured hearts at 3 and 7 dpi (**D**) of *wt1b:GFP* transgenic fish were stained for GFP and PCNA expression. Proliferating epicardial cells are indicated by white arrowheads.

Nuclei were stained with Dapi. Note partial coverage of the wound with GFP positive epicardial cells in C (overview 3 dpa) and full coverage in D (overview 3 dpi) (white arrow). “Merge” in close ups shows Dapi, PCNA and GFP expression. Scale bars are 100 μm in the overview and 25 μm in the close ups. The wound planes are indicated by white dashed lines. $n = 3$ hearts (9 sections) for all conditions.

(Experiments performed by K.S. and C.C.W.)

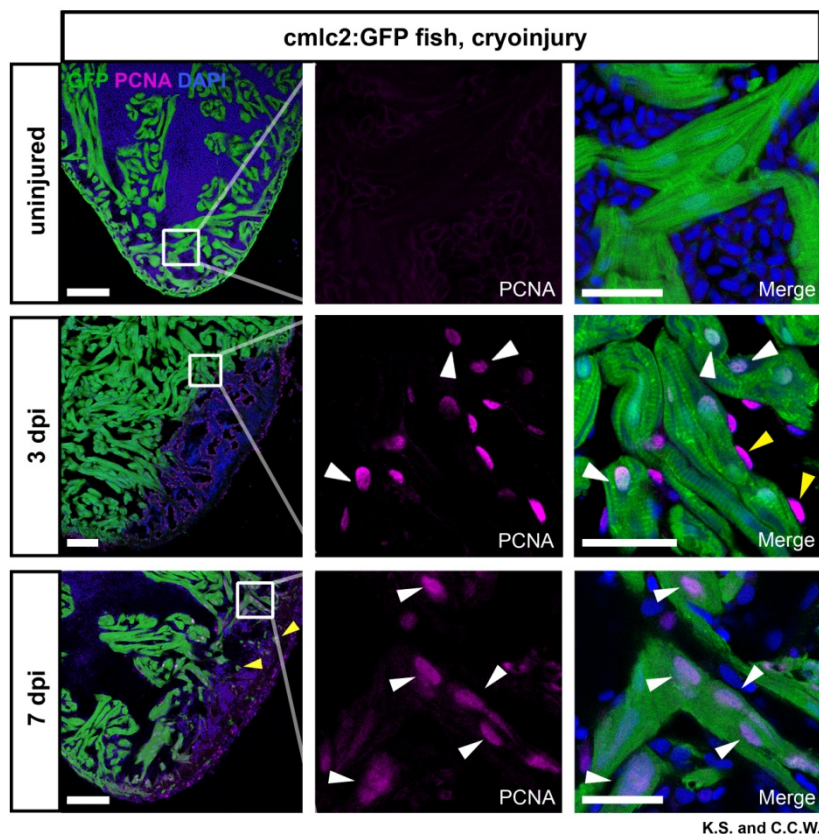
3.3.1.4 Induction of cardiomyocyte proliferation after cryoinjury

The proliferation of cardiomyocytes and thus the generation of new myocardial cells were shown for the regeneration process after ventricular resection (Lepilina et al 2006, Poss et al 2002). Recent studies using lineage tracing approaches showed that regenerated new cardiomyocytes are derived from mature myocardial cells (Kikuchi et al 2010, Jopling et al 2010).

Thus I intended to test whether proliferation of cardiomyocytes occurs in response to cryoinjury as well. Therefore I used *cmlc2:GFP* (*Tg(myl7:GFP)^{f1/+}*) fish, which express GFP in differentiated cardiomyocytes and tested these for coexpression of PCNA in uninjured and lesioned hearts at 3 and 7 dpi. Only few PCNA positive cells could be detected in uninjured hearts. In contrast, lesioned hearts displayed more PCNA⁺ cells, including proliferating cardiomyocytes close to the wound edges already at 3 dpi (**Fig 3.3.6**). The detection of proliferating cardiomyocytes at 3 dpi at the wound edges is consistent with detection of cells, which might be myocardial cells with reduced myofilament content at 3 dpi at the wound edges as described before (**Fig 3.3.2U**). Thus I speculate that possibly myocardial cells with reduced myofilaments were proliferating at 3 dpi at the wound edges.

Proliferating cardiomyocytes (GFP⁺/PCNA⁺) were detectable at 7 dpi as well and many of GFP⁺ PCNA⁺ cells were located close to the wound borders. Whereas the wound area at 3 dpi was devoid of GFP⁺ cells, individual cardiomyocytes were found in the wound area indicating that cardiomyocytes had started to invade into the lesion (**Fig 3.3.6**).

Conclusively, myocardial proliferation was initiated after cryolesion at 3dpi and invasion of cardiomyocytes into the wound area was detectable.



3.3.6 Activation of myocardial proliferation in response to cryoinjury.

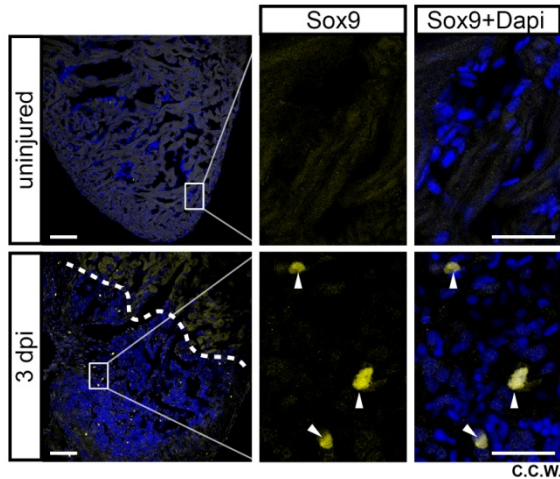
Uninjured and cryolesioned hearts (3 and 7 dpi) of TG(*cmlc2:GFP*) transgenic fish were stained for GFP and PCNA. Proliferating mature cardiomyocytes are located close to the lesion in the uninjured myocardium (white arrowheads). Individual GFP⁺ cardiomyocytes are located inside the lesioned area at 7 dpi (yellow arrowheads). “Merge” in close ups shows Dapi, PCNA and GFP expression. Scale bars are 100 μ m in the overview and 25 μ m in the magnifications. n = 3 hearts (9 sections) at all conditions.

(Experiments performed by K.S. and C.C.W.)

3.3.1.5 Sox9 induction after cryoinjury

Cellular mechanisms like proliferation of different lineages and molecular signals like *tbx18* and *wt1b* upregulation are detectable after both types of injury, i.e. ventricular resection and cryoinjury. Since Sox9a is induced early after resection and Sox9a function is important for myocardial and endothelial regeneration, it was tested whether this transcription factor is also expressed after cryoinjury. Injury specific Sox9 staining was

detected at 3 dpi (**Fig 3.3.7**) indicating that both injury types induced several common molecular responses. Whether the paralog Sox9a, whose expression is present after ventricular resection, is also upregulated after cryoinjury needs to be further examined.



3.3.7 Activation of Sox9 expression after cryoinjury

Uninjured and cryolesioned hearts (3 dpi) were stained for Sox9 expression. Sox9 positive cells are located in and near the wound area (white arrowheads). Nuclei are stained by Dapi. Wound edges are indicated by a white dashed line. Scale bars are 100 μm in the overview and 25 μm in the close ups. $n = 3$ hearts for each uninjured and 3 dpi. (Experiment performed by C.C.W.)

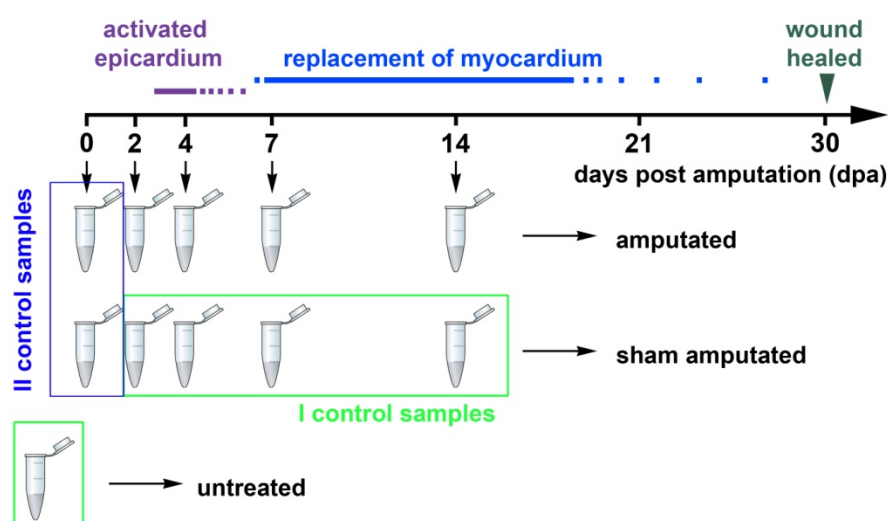
Parts of these results were published in Schnabel et al (2011). At the same time, others also showed regeneration of the zebrafish heart after cryoinjury/cryocauterization (González-Rosa et al 2011, Chablais et al 2011).

Experiments were performed by Kristin Schnabel (K.S.), Chi Chung Wu (C.C.W.) and Thomas Kurth (T.K.; histology facility), as indicated in the figures and figure legends.

3.4 Gene expression profiling during zebrafish heart regeneration

The knowledge about molecular signals initiating cardiac regeneration or regulating cell proliferation during the regeneration process remains incomplete. Thus I focused my gene expression profiling analysis on early stages of heart regeneration and collected hearts at 2, 4, 7 and 14 days after amputation (dpa). To enrich for amputation specific genes, I included hearts of sham amputated (for each time point) and untreated fish as control. Since blood accumulates after amputation and during heart extraction, I used amputated and sham amputated hearts at 0 hours post amputation / hours post sham amputation (hpa and hpsa) as controls to exclude blood specific genes. To enrich for regeneration specific transcripts that are accumulating at the amputation plane I dissected one third of the ventricle containing the amputation plane and the apex, respectively.

I used customized zebrafish 4x44K expression oligomicroarrays for gene expression profiling and performed statistical evaluation (see Methods 2.2.23.3) and the filtering according to the criteria p-value cutoff $p \leq 0.05$ and with Fold changes $\leq -1,5$ and $\geq 1,5$ (if not indicated otherwise) to compare amputated versus control hearts of sham amputated and untreated fish (**Fig 3.4.1**). I excluded transcripts that are regulated in the 0 hpa and hpsa time points (**Fig 3.4.1**) to achieve an amputation specific pool of upregulated genes for each time point. In these lists I analyzed overall cellular processes and identified regulated genes at each time point.



3.4.1 Scheme of sample collection.

Wild-type hearts were collected at 2, 4, 7 and 14 dpa and sham amputated hearts of each time point as well as hearts of untreated fish served as controls. Hearts at 0 hpa, 0 hpsa served also as controls to exclude blood specific transcripts. One third of the ventricle containing the amputation plane or the apex was used for analysis, respectively. To enrich for amputation specific genes, amputated samples were compared to the “I control sample” group (sham amputated and untreated; green boxes). Blood specific transcripts, which were regulated in the “II control sample” group (0 hpa and 0 hpsa; blue box), were excluded from lists of differentially expressed genes in each time point.

Using biological gene annotation of the Panther database, I found that genes controlling certain biological processes such as cell cycle and cellular adhesion are overrepresented during zebrafish heart regeneration. For example, I detected the group of cell cycle genes to be more than 2 fold upregulated from 2 to 14 dpa (**Table 3.4.1**) suggesting that cell proliferation is activated during the entire regeneration. The detectable early increase in proliferation and the cell proliferation later during regeneration was further supported by immunohistochemistry at 3, 7 and 14 dpa (see Fig 3.3.5.C and 3.3.6 this study; Poss et al 2002) and expression profiling analysis (Lien et al 2006). Upregulation of carbohydrate metabolism genes at 2dpa indicated increased energy requirement very early during regeneration (**Table 3.4.1**). The increase in cell motility class transcripts during the entire examined time course might indicate the presence of migrating cells such as epicardial cells, inflammatory cells and others (**Table 3.4.1**). On the other hand the abundance of cell adhesion genes possibly reflected the fact that tissue structures were reestablished to rebuilt the mechanical properties of the heart muscle (**Table 3.4.1**). The incidence of developmental genes possibly indicated that transcripts important during heart development are also expressed during heart regeneration and that these are responsible for re-establishment of cardiac structures (**Table 3.4.1**).

Thus the first 14 days of regeneration are characterized by an increased expression of genes that regulate metabolic processes, cell proliferation and morphological tissue remodeling.

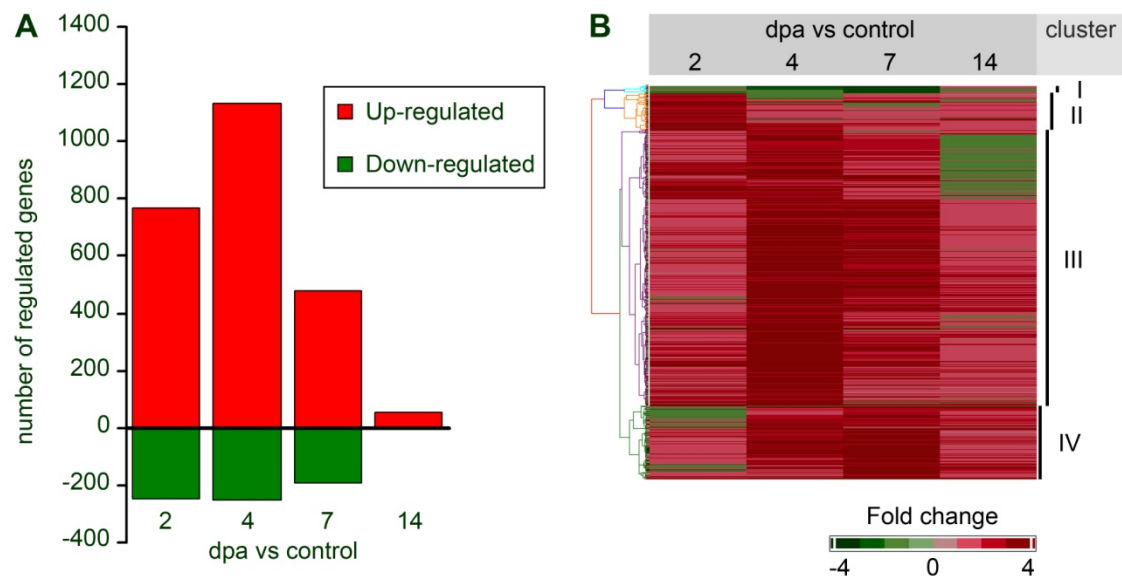
		p-value	fold enrichment
2dpa vs control	blood circulation and gas exchange	**	3.04
	cell cycle	***	2.0
	carbohydrate metabolism	**	1.7
	transport	***	1.61
	cell structure and motility	*	1.41
4dpa vs control	cell cycle	***	2.02
	cell adhesion	***	1.7
	protein targeting and localization	*	1.68
	cell structure and motility	***	1.52
7dpa vs control	cell cycle	***	2.57
	cell adhesion	***	2.36
	muscle contraction	*	2.29
	cell structure and motility	***	1.76
14dpa vs control	cell cycle	***	6.97
	cell structure and motility	***	3.33
	developmental process	*	2.0

Table 3.4.1 Biological gene annotation from the Panther database according to biological process level I.

Statistical analysis performed on gene lists 2 dpa vs control, 4 dpa vs control, 7 dpa vs control and 14 dpa vs control. The following filtering criteria were applied: $p \leq 0.05$, Fold change $\leq -1,5$ and $\geq 1,5$. Statistics are described in Methods part 2.2.23.4. * = $p \leq 0.05$, ** = $p \leq 0.005$, *** $p \leq 0.0005$

Overall expression analysis revealed that most of the amputation specific genes are upregulated rather than downregulated and that the peak of upregulated transcripts was detectable at 4 dpa (**Fig 3.4.2A**). The number of regulated genes decreased substantially up to 14 dpa, whereas the number of downregulated transcripts was not altered considerably among the time points 2, 4 and 7 dpa (**Fig 3.4.2A**).

To perform a hierarchical clustering of the differentially expressed genes based on the similarity of their expression pattern, I used transcripts that were differentially expressed in at least one of the four time points according to the filtering criteria $p \leq 0.05$ and Fold change ≤ -2.5 and ≥ 2.5 . Using these criteria about 3 % of the genes were downregulated; roughly 11 % of the transcripts were preferentially expressed during early regeneration (at 2 dpa); with about 70 % the majority of genes was notably upregulated at 4 and 7 dpa; and roughly 17 % were most highly expressed at 7 dpa (**Fig 3.4.2B**). Some of the regulated genes and their clusters are illustrated in **Table 3.4.2 and 3.4.3**.



3.4.2 Most genes are differentially regulated early after amputation

A. The majority of transcripts were upregulated during the examined regeneration time frame and the maximum number of genes is differentially expressed at 4 dpa. Used gene lists were 2 dpa vs control, 4 dpa vs control, 7 dpa vs control and 14 dpa vs control. The following filtering criteria were applied: $p \leq 0.05$, Fold change ≤ -1.5 and ≥ 1.5 .

B. Hierarchical clustering of the differentially expressed genes based on the similarity of their expression pattern.

Clustering analysis was performed on gene lists 2 dpa vs control, 4 dpa vs control, 7 dpa vs control and 14 dpa vs control that were generated according to the following filtering criteria: $p \leq 0.05$, Fold change ≤ -2.5 and ≥ 2.5 . Hierarchical clustering was carried out according to Pearson's dissimilarity and average linkage to cluster genes based on their similarity of their expression pattern. 4 different clusters were derived and some genes in cluster III and IV are shown in Table 3.4.2 and 3.4.3.

Comparative analysis of my data with previously published array results (Lien et al 2006) confirmed that several transcripts such as *apoeb*, *mdka*, *tbx18*, several matrix metalloproteinases (*mmps*) appear as differentially expressed during heart regeneration in both arrays (**Table 3.4.2**). Besides, I found additional genes like *tbx1*, *sox4b*, *tbx2.3*, *gli2a*, *snai2*, *snai1a* and *pea3* to be differentially regulated during zebrafish heart regeneration (**Table 3.4.3**).

Table 3.4.2

Probeset ID	Gene Name	Fold change	Cluster
A_15_P107195	apoeb		III
LOLS08450	cd9l		III
A_15_P112924	mdka		III
A_15_P120314	cathepsin S		III
A_15_P111146	vegfc		n.a.
A_15_P106744	cathepsin B		III
A_15_P114464	mmp14b		III
LOLO1785	cxcl12a		IV
A_15_P121217	mmp2		IV
LOLS09370	anxa1a		n.a.
A_15_P116364	tbx18		n.a.
LOLS00149	pdgfaa		n.a.
A_15_P112832	ctgf		IV
A_15_P104163	mmp14a		IV
LOLG127	frzb		IV

Table 3.4.3

Probeset ID	Gene Name	Fold change	Cluster
A_15_P111798	sox4b		III
A_15_P112704	tbx1		III
A_15_P114867	gli2a		III
A_15_P108411	snai2		IV
LOLS00475	snai1a		n.a.
A_15_P112093	tbx2a		IV
LOL03913	pea3		n.a.

Table 3.4.3 Novel identified differentially expressed genes during early heart regeneration.

Transcripts are differentially expressed according to filtering criteria: $p \leq 0.05$, Fold change $\leq -1,5$ and $\geq 1,5$ at the time points 2, 4, 7 and 14 dpa as indicated by the color code. Grey color for a time point shows no significant regulation (due to a Fold change of $\geq -1,5$ and $\leq 1,5$ and/or $p \geq 0.05$). Indicated cluster numbers are generated according to 3.4.2.B. Genes that show n.a. were not analyzed in hierarchical clustering.

To summarize, the majority of transcripts is differentially regulated in the initial phase and fewer genes control processes during later regeneration stages. This analysis confirmed expression of several known transcripts and identified additional novel upregulated genes during heart regeneration. (The complete list of regulated genes is available from Dr. Gilbert Weidinger (e-mail: gilbert.weidinger@biotec.tu-dresden.de) upon request.)

Table 3.4.2 Genes known to be upregulated within the first 14 days of heart regeneration.

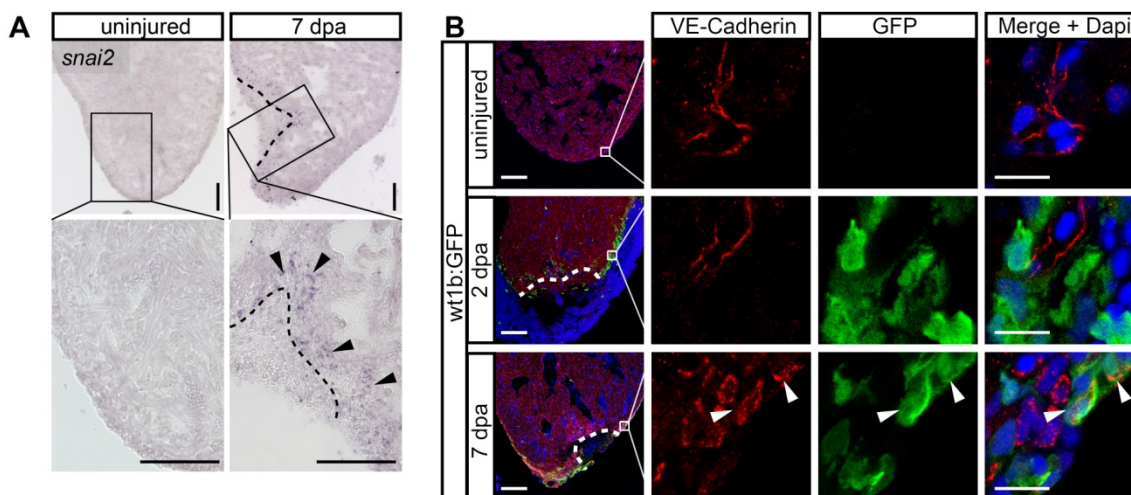
Differentially expressed transcripts according to filtering criteria: $p \leq 0.05$, Fold change $\leq -1,5$ and $\geq 1,5$ are shown at the time points 2, 4, 7 and 14 dpa as indicated by the color code. These genes are known to be expressed during heart regeneration. Grey color for a time point shows no significant regulation (due to a Fold change of $\geq -1,5$ and $\leq 1,5$ and/or $p \geq 0.05$). Indicated cluster numbers are generated according to 3.4.2.B. Genes with “n.a.” were not analyzed in

3.4.1 FGF signaling targets and Epithelial - to - mesenchymal transition are presumably activated early during heart regeneration as indicated by the microarray results

I found that *snai2*, which is described to be involved in cellular processes like epithelial to mesenchymal transition (EMT) during embryonic development (Sakai et al 2006) and upregulated during cardiac regeneration (Kim et al 2010), also appears to be upregulated in my array. Using in situ hybridization on heart sections, I detected amputation specific *snai2* upregulation at the wound border at 7 dpa (**Fig 3.4.3A**).

Furthermore, it has been suggested that epicardial cells contribute to the newly formed coronary blood vessels by activating cellular EMT programs during heart regeneration (Lepilina et al 2006, Kim et al 2010). To address this topic, I tested whether cells of epicardial origin can adopt an endothelial fate and stained uninjured and regenerating *wt1b*:GFP+ hearts at 2 and 7 dpa for expression of GFP, presumably indicating epicardial cells during regeneration, and VE-cadherin, a marker for mature endothelial cells (Montero-Balaguer M. et al 2009). *wt1b*:GFP expression was detectable in amputated hearts at 2 and 7 dpa while uninjured heart did not show any GFP expression in epicardial cells (**Fig 3.4.3B**). VE-cadherin was normally expressed in endocardium and vessels in uninjured and injured hearts (**Fig 3.4.3B**). In addition to single GFP+ and single VE-cadherin+ cells there were double positive GFP+/VE-cadherin+ cells detectable at 7 dpa (**Fig 3.4.3B**), which might suggest that some cells of epicardial origin could express endothelial markers. The absence of GFP+/VE-cadherin+ positive cells at 2 dpi might indicate that cells of epicardial origin did not activate endothelial transcripts at that early time point (**Fig 3.4.3B**).

In summary, EMT processes are indicated through expression of *snai* genes. Due to double positive *wt1*:GFP (epicardial) /VE-cadherin cells, I speculate that cells of epicardial origin can possibly acquire endothelial characteristics after surgery.



3.4.3 Epithelial - to - mesenchymal transition might be activated during heart regeneration.

A. *snai2* mRNA is upregulated in regenerating hearts at 7 dpa.

In situ hybridization shows *snai2* mRNA expression at the wound edges of the regenerating heart at 7 dpa (black arrowheads). Hearts of sham amputated fish served as uninjured control hearts. Uninjured hearts and regenerating hearts: n = 3 each. Scale bars in overviews and magnifications are 100 μ m.

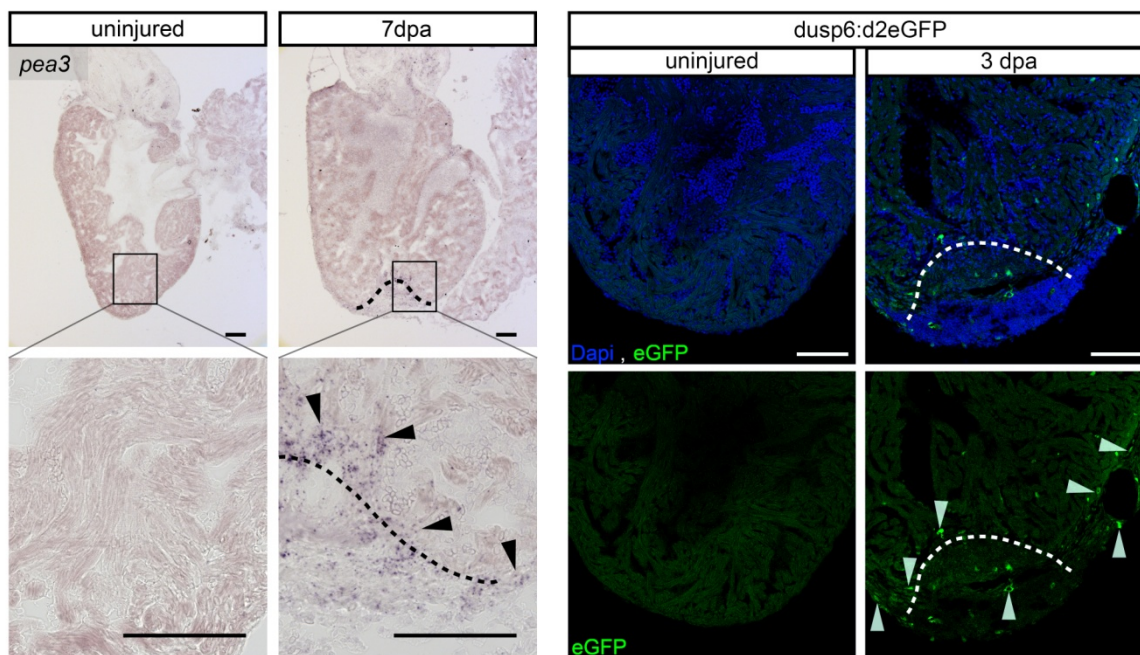
B. Cells of epicardial origin possibly display endothelial characteristics at 7 dpa.

Uninjured wt1b:GFP hearts and transgenic hearts at 2 and 7 dpa were stained for GFP and VE-cadherin via immunohistochemistry. At 7 dpa GFP+ cells that also express VE-Cadherin were detectable (white arrowheads). Dapi shows nuclear staining. Scale bars in overviews are 100 μ m and scale bars in magnification are 10 μ m. Uninjured hearts and regenerating hearts at 2 and 7 dpa: n = 3 each.

Few molecular signaling pathways have been shown to play a role in heart regeneration. For instance, Fgf signaling has been implicated in regulating revascularization of the new myocardial wall (Lepilina et al 2006). Hence, I validated the amputation specific expression of *pea3*, a target of the Fgf pathway (Roel and Nüsslein-Volhard 2001, Raible and Brand 2001), at the wound edges and in the wound area at 7 dpa using in situ hybridization (**Fig 3.4.4A**). Another target gene of the Fgf pathway is *dusp6* (dual-specificity phosphatase 6)/MKP3 (MAPK phosphatase 3) (Ekerot et al 2008); its expression pattern is reported in the fish line *dusp6:d2eGFP* (Tg(*dusp6*:EGFP)pt6) driving eGFP downstream of the *dusp6* promoter elements (Molina et al 2007). Using this fish line

I detected eGFP⁺ cells in amputated hearts at 3 dpa but not in uninjured hearts (**Fig 3.4.4A**).

In conclusion, FGF signaling appears to be upregulated during early heart regeneration as shown by two pathway target genes, *pea3* and a reporter for *dusp6*.



3.4.4 Fgf target genes are activated at 3 and 7 dpa

A. *pea3* mRNA is upregulated in regenerating hearts at 7 dpa.

pea3 mRNA is expressed at the wound edges of the regenerating heart at 7 dpa as shown by in situ hybridization. Hearts of sham amputated fish served as uninjured control hearts. Uninjured hearts and regenerating hearts: n = 3 each. Scale bars in overviews and magnifications are 100 μ m.

B. GFP expression is activated in *dusp6:d2eGFP* in response to amputation at 3 dpa.

Antibody staining for eGFP in *dusp6:d2eGFP* hearts indicates *dusp6* promoter activity in response to amputation. Uninjured hearts and 3 dpa hearts: n = 6 each. Scale bars are 100 μ m.

4.1 No evidence for a role of Wnt/ β -catenin signaling in zebrafish heart regeneration

4.1.1 Target genes of the Wnt/ β -catenin pathway are not detectable in the first days after ventricular resection

The knowledge about molecular signals regulating the process of heart regeneration in zebrafish is limited; yet the reactivation of a developmental gene program was shown for instance for the epicardial layer after injury (Lepilina et al 2006, Kim et al 2010). Considering the crucial role of Wnt/ β -catenin signaling in embryonic development, its stringent regulation during heart development and the necessity of the pathway in numerous regenerative processes, like fin and liver regeneration, I aimed to clarify the role of Wnt/ β -catenin signaling in zebrafish heart regeneration (Clevers 2006, Ueno et al 2007, Klaus et al 2007, Stoick-Copper et al 2007, Goessling et al 2008). Stoick-Cooper et al (2007) showed the activation of canonical Wnt signaling at the amputation plane early in heart regeneration using a transgenic fish line that contains the Wnt/ β -catenin responsive TOPdGFP reporter (Stoick-Cooper et al 2007).

During my analysis I did not detect published *gfp* presence at the amputation plane using the same transgenic fish line. Only faint *gfp* staining was detectable at the outermost surface of whole mount hearts representing the epicardial layer that displays possibly overstained background due to very long staining times. In situ hybridization on sections did not show an epicardial *gfp* staining neither at the wound edges nor as faint signal in the epicardial layer. Instead, I verified reporter activity in the pericardial sac of uninjured and injured hearts on sections suggesting active Wnt/ β -catenin signaling in this cardiac layer. However, since the wound area adheres strongly to the pericardial sac after amputation it is possible that extracted amputated hearts still have remaining pericardial tissue (positive for TOPdGFP activity) attached especially at the wound site. At the same time extracted control hearts do not have pericardial tissue attached because uninjured hearts do not adhere to the pericardial sac. These technical reasons could be causative for the published positive staining of the reporter TOPdGFP at the wound site but not in the control heart as shown by Stoick-Cooper et al (2007). Alternatively, it is possible that the TOPdGFP transgenic fish stock used in our lab for these experiments differs in its expression pattern from the one used by Stoick-Cooper et al at the University of Washington. Epigenetic

modification resulting in silencing of transgenes can occur and might depend on the genetic background and the generation of fish. While I detected expression of TopdGFP in the adult pericardium and brain, excluding complete silencing of the transgene, it is still possible that tissue-specific silencing has occurred in our line. To conclude, I could not confirm an amputation specific activation of Wnt signaling using transgenic TOPdGFP (Tg(*TOP:GFP*)w25) fish.

Several target genes of the Wnt/ β -catenin pathway such as the general targets *axin2* or *lef1* (Kagermeier-Schenk in revision, Jho et al 2002, Skokowa et al 2007), which are themselves pathway components, are expressed in brain areas known to exhibit active Wnt/ β -catenin signaling (Nyholm et al 2007; unpublished observation of J. Kaslin). However, an amputation specific expression of *axin2* and *lef1* was not detectable in the injured heart suggesting that active Wnt signaling is not present early in heart regeneration. Nevertheless, the techniques used to assay expression of these genes have detection limits and very low expression levels and thus activity of Wnt/ β -catenin signaling cannot be excluded. The TOPdGFP reporter has limitations as well for the GFP protein detection since a destabilized GFP variant is expressed, which displays a high turnover (Dorsky et al 2001). Additionally, although reporter lines can serve as readout for active signaling, these can also fail to report true signaling due to the artificial construction of promoter regions, which might not respond to endogenous signaling in some tissues or result in false positive expression. *gfp* positive staining in the pericardial sac of TOPdGFP transgenic fish could not be confirmed using *axin2* and *lef1* expression suggesting either very low expression levels of endogenous Wnt/ β -catenin target genes or false positive *gfp* staining in that layer.

In summary, I did not detect an amputation specific activation of the Wnt/ β -catenin targets *axin2* and *lef1* or the Wnt/ β -catenin responsive reporter in the early phase of heart regeneration, suggesting that the pathway is not active early during cardiac regeneration.

4.1.2 Overexpression of Wnt/ β -catenin pathway inhibitors has no influence on gene expression in early heart regeneration

Since the tested Wnt/ β -catenin targets *axin2* and *lef1* were not detectable in heart regeneration I looked for other Wnt/ β -catenin pathway target genes regulated in a regeneration specific manner. Using microarray analysis, Kagermeier-Schenk and colleagues revealed the downregulation of Wnt/ β -catenin target genes during zebrafish

embryonic development after inhibition of the pathway with certain transgenic fish lines (Kagermeier-Schenk - in revision). In contrast, using a similar approach to identify direct Wnt/ β -catenin targets after induction of Wnt pathway inhibitors Dkk1 and Axin1 during heart regeneration, I found few regulated transcripts only after applying filtering criteria with very low stringency. Bona fide Wnt/ β -catenin regulated genes should be regulated by Dkk1 and Axin1 overexpression. Since the sets of transcripts obtained in both lines however were not overlapping, I considered the respective genes to appear regulated rather due to unspecific background than actually regulated by Wnt signaling, indicating that direct Wnt target genes were not detectable using oligoexpression microarrays.

The early phase of heart regeneration is characterized by an upregulation of embryonic markers such as *hand2*, *nkx2.5*, *raldh2*, and *tbx18* suggesting that the embryonic gene expression program is reactivated in response to injury (Lepilina et al 2006, Kim et al. 2010). Some cardiac progenitor genes like *hand2* and *nkx2.5* have been shown to be positively regulated by Wnt/ β -catenin signaling in mouse embryonic stem cells (Kwon et al 2007; Ueno et al 2007). While the microarray gene expression profiling did not reveal *hand2* as Dkk1 target, qPCR indicated that Dkk1 overexpression significantly downregulated *hand2* expression. However, this could not be confirmed by influencing Wnt signaling via Axin1 induction. Furthermore, other early cardiac markers were neither identified as Wnt targets in the microarray or by direct PCR-based assays.

Since Wnt/ β -catenin targets were not detected using oligoexpression microarray, I tested the reliability of applied protocols by assaying for amputation specific genes. Transcripts known to be upregulated in heart regeneration at 7 dpa were detected and suggesting the accuracy of the microarray results.

In conclusion, amputation specific direct or indirect Wnt/ β -catenin target genes could not be identified within early (first 7 days of) heart regeneration indicating that the Wnt/ β -catenin pathway, if active, does not regulate gene expression during this early phase of heart regeneration.

However, all these results rely on the functionality of the used transgenic fish lines. The Dkk1 or Axin1 inducible transgenic fish lines are well established for functional studies of Wnt/ β -catenin signaling in zebrafish embryonic development and adult fin regeneration and were recently used to identify new Wnt/ β -catenin targets in zebrafish embryonic development (Stoick-Cooper et al 2007, Kagermeier-Schenk – in revision). Although

transgene expression in the heart was verified it is not clear whether induced transgene levels were sufficient to influence signaling.

In summary, a functional role of Wnt/ β -catenin signaling during the first days of heart regeneration was not detectable, which, with respect to possible restrictions, suggests that the canonical Wnt pathway has no influence on that early phase in regeneration.

4.1.3 Wnt/ β -catenin signaling does not influence cardiomyocyte proliferation

During heart regeneration proliferating cardiomyocytes are detectable starting at 7 dpa and the peak of proliferative cardiomyocytes occurs at 14 dpa (Poss et al 2002). Recently Kikuchi et al (2010) and others showed that differentiated cardiomyocytes loose sarcomeric structures upon ventricular resection, reenter the cell cycle and thus are presumably the source for new cardiomyocytes (Kikuchi et al 2010, Jopling et al 2010). However, signaling pathways regulating proliferation of cardiomyocytes and other cell types during zebrafish heart regeneration are unknown so far.

Wnt/ β -catenin signaling is described to positively regulate proliferation of cardiac precursors and cardiac cells that had initiated differentiation *in vivo* and *in vitro* in mouse (Kwon et al 2007). However, I did not detect any significant influence of Wnt signaling on proliferating cells during heart regeneration. Proliferation of cardiomyocytes is not influenced by Dkk1 induction and, likewise, Dkk1 overexpression has no reproducible effect on non-myocardial proliferating cells, which indicates that proliferation during heart regeneration is not influenced by Dkk1 overexpression and therefore not regulated by Wnt/ β -catenin signaling.

On the other hand, as mentioned before, the functionality of the used transgenic fish line and appropriate expression levels of the transgene are critical for influencing putative Wnt/ β -catenin signaling processes.

In summary, I did not detect an altered proliferative response to injury after Dkk1 induction indicating that canonical Wnt signaling does not influence cell proliferation during heart regeneration; yet possible limitations of the transgenic fish line have to be considered.

4.1.4 Wnt/ β -catenin signaling does not influence the overall extent of heart regeneration

Regarding the role of Wnt signaling on morphological zebrafish heart regeneration as evidenced by removal of wound tissue, I could not detect differences in the progress of regeneration, neither by enhancement of Wnt/ β -catenin signaling nor by expression of pathway inhibitors suggesting that Wnt signaling does not influence important cellular or molecular processes during heart regeneration.

Nevertheless, as mentioned, these analyses rely strongly on the functionality of the transgenic and mutant fish lines. Due to lethality of homozygous *masterblind* mutants (*axin1^{tm13/tm13}*) that are deficient for *axin1* (Heisenberg et al 2001), I used heterozygous adult mutant fish to enhance Wnt/ β -catenin signaling, which did not display specific phenotypes in adults implicating that effects on Wnt signaling, if present, are just of minor character. The use of hypomorphs could be causative for the lack of detectable influences on regeneration. Additionally, as mentioned earlier, it is unclear whether the transgene levels in heat-shock inducible transgenic fish lines are sufficient to enhance or inhibit Wnt/ β -catenin signaling in the adult zebrafish heart. The induction of heat-shocks twice daily for a long time in order to provide high transgene levels caused reduced regenerative capability even of wild-type siblings, implicating that the heat-shock itself can impair regeneration (data not shown). A reduction of the frequency to one heat-shock per day resulted in better regenerative outcome of the wild-type control group but also of the transgenic group. Although continuous expression of the transgene was provided as assayed by fluorescence, reduced levels of the transgene are likely, due to reduced heat-shock frequency, which might result in transgene expression levels that cannot influence signaling processes.

Wnt/ β -catenin signaling is essential in controlling homeostasis of the gut epithelium and influences self-renewal of haematopoietic stem cells and haematopoietic progenitor cells in mammals (Reya and Clevers 2005). Thus it is possible that inhibition of Wnt signaling for a long timeframe causes problems in these organ systems leading to impaired health of transgenic fish, which was, however, not observed in the transgenic fish lines. This observation could indicate that transgene levels are insufficient to influence Wnt/ β -catenin signaling in several tissues. Additionally, it is possible that Wnt/ β -catenin signaling is acting at different time windows, similar to heart development (Ueno et al 2007), and thus effects are not detected after a long manipulation period and phenotypes possibly vanish.

In summary, I conclude that detection of an important role of Wnt/ β -catenin signaling in heart regeneration with the used examination methods was not possible.

4.1.5 Wnt/ β -catenin signaling influences mammalian and zebrafish heart development and mammalian cardiac hypertrophy – but does not influence zebrafish heart regeneration

Although Wnt signaling might not have a role in zebrafish heart regeneration (see remarks above), I would like to compare my results with what is known about the role of Wnt signaling in heart development and during pathological changes after heart infarction in mammalian systems. Since another prominent signaling pathway namely FGF signaling has an important role in both heart development (Marques et al 2008) and heart regeneration in zebrafish (Lepilina et al 2006) it was tempting to speculate that the Wnt/ β -catenin pathway, which is clearly critical in heart development (Eisenberg and Eisenberg 2006, Ueno et al 2007), also has a functional role in zebrafish heart regeneration.

Although resident progenitor cells are presumably not the source for new cardiomyocytes, there are, however, early cardiac genes like *hand2*, *nkx2.5*, *tbx5* upregulated after surgery (Lepilina et al 2006, Kikuchi et al 2010, Jopling et al 2010). Positive influences of Wnt/ β -catenin signaling expression on some of these gene such as *hand2* and *nkx2.5* during mammalian development (Kwon et al 2007), were not reproducibly detectable during zebrafish heart regeneration. Additionally Wnt/ β -catenin target genes, either as reporter or endogenous genes, were not identified during the early regeneration period which is in contrast to the activation of a Wnt/ β -catenin responsive reporter expressed in progenitors of the second heart field (SHF) in mouse (Klaus A et al 2007).

Dedifferentiating and proliferating cardiomyocytes are likely responsible for regeneration of new cardiomyocytes (Kikuchi et al 2010, Jopling et al 2010). Thus, although Wnt/ β -catenin signaling can positively regulate proliferation of cardiac precursors and of early committed ventricular cardiomyocytes in heart development (Klaus et al 2007, Kwon et al 2007) this promoting function is not detectable in myocardial or other cells during zebrafish heart regeneration.

During the entire process of cardiac regeneration I detected neither any inhibitory nor any promoting role of the canonical Wnt pathway after inhibiting or enhancing the signaling. Although Wnt/ β -catenin signaling, like FGF signaling, has been shown to be critical for

heart development (Eisenberg and Eisenberg 2006, Eisenberg and Eisenberg 2007; Ueno et al; Klaus A et al), interestingly my data did not show an important role for the Wnt pathway in zebrafish heart regeneration while FGF signaling functions in revascularization during cardiac regeneration (Lepilina et al 2006). Thus, I speculate that zebrafish heart regeneration might not only be a recapitulation of cardiac development, since not all crucial molecular signals in development seem to play a role in heart regeneration.

Wnt/ β -catenin signaling is also implicated in pathological cardiac hypertrophy after mammalian heart infarction, which can lead to cardiac failure (van de Schans et al 2008). Interfering with Wnt signaling, however, results in improved cardiac function, reduced infarct size (Barandon et al 2003) in mammals but has no effect on zebrafish heart regeneration, which is an interesting difference between teleosts and mammals in reaction on a heart injury event.

4.2 Sox9a in zebrafish heart regeneration

4.2.1 The transcription factor Sox9a is expressed in epicardial, myocardial and endocardial/endothelial cells during early stages of cardiac regeneration

Screening for amputation specific signals revealed the upregulation of the transcription factor Sox9a during the early phase of heart regeneration, while hearts of sham amputated fish did not show Sox9a expression, indicating that Sox9a induction in the zebrafish heart is truly injury specific. Interestingly, during heart development Sox9 function is restricted to mammalian septum development and valvulogenesis and Sox9 mouse mutants have defects in cardiac valve development (Lincoln et al 2007, Akiyama et al 2004, Rahkonen et al 2003); yet, valve structures are not removed or injured in surgical resection of the zebrafish ventricle.

Reports concerning Sox9 expression in cardiomyocytes during cardiac development are contradictory, since Sox9 positive cardiomyocytes are shown by Rahkonen et al (2003) whereas Sox9 is not present in developing myocardium at different stages according to Lincoln et al (2007). Thus due to the questionable expression in developing cardiomyocytes, but the definitive Sox9 requirement for valve structures, Sox9a upregulation in regenerating heart tissue in zebrafish, which does not include cardiac valves, is presumably not the reactivation of a developmental gene expression program.

Using transgenic reporter fish lines labeling the respective cardiac layers, I could show that Sox9a is expressed in a subset of epicardial, myocardial and endothelial/endocardial cells at the wound edges.

The entire epicardial layer responds to cardiac injury by reactivation of developmental genes such as *tbx18* and *raldh2* and by thickening of the epicardium at the wound edges (Lepilina et al 2006). Wt1 is expressed in the developing epicardium as well (Männer et al 2001, Martinez Estrada et al 2010, Serluca 2008) and the transgenic reporter fish line wt1b:GFP (Tg(*wt1b*:eGFP)^{li1}) (Perner et al 2007) reactivates GFP expression in response to heart injury in the epicardial layer. The expression of Wt1 has also been shown for most leukemias and in a small portion of hematopoietic progenitors during development (Menssen et al 1997, Vidovic et al 2010), while it is not clear whether Wt1b is expressed in normal hematopoietic cells in adult zebrafish.

According to the expression pattern of *wt1b*:GFP transgenic fish, *wt1b*, however, was identified as another transcription factor presumably upregulated in epicardial cells after heart injury. Thus the transgenic fish line *wt1b*:GFP represents a new useful tool to label activated epicardial cells during heart regeneration.

Using this reporter line I revealed Sox9a expression very early after amputation (3 dpa) in activated epicardial cells especially in the lateral wound edges. A transcriptional regulatory link between Sox9 and Wt1 expression is shown during testes development and it is suggested that Wt1 is required for Sox9 expression in mouse (Gao et al 2006). Whether Wt1b regulates Sox9a expression in activated epicardial cells remains to be determined.

Sox9a expression was also detectable close to the wound area in differentiated myocardial cells, marked by activity of the *cardiac myosin light chain 2 (cmlc2)* promoter. Others have shown that myocardial cells initiate proliferation during heart regeneration and thus produce new cardiomyocytes (Kikuchi et al 2010, Jopling et al 2010). I detected proliferating Sox9a⁺ cardiomyocytes, suggesting that Sox9a is expressed in cardiomyocytes that are actively involved in regeneration. Whether this myocardial Sox9a expression resembles developmental processes is not clear. As mentioned before, it is unclear whether Sox9 is expressed in cardiomyocytes during cardiac development, since Sox9 positive cardiomyocytes are shown by Rahkonen et al (2003) whereas Sox9 is not present in developing myocardium at different stages according to Lincoln et al (2007).

Endothelial cells, reported by the activity of the *fli1* promoter (Lawson and Weinstein 2002), express Sox9a already very early (at 3 and 7 dpa) during heart regeneration. Sox9a⁺/Fli1⁺ cells are present in the lateral wound edges and in endothelial cells surrounding the trabecular myocardium indicating that Sox9a is expressed in endothelial cells of coronary vessels and in endocardial cells respectively. Sox9a was detected in proliferating endothelial cells, suggesting its expression in newly generated endothelial/endocardial cells that actively take part in the cardiac regeneration process.

The transcription factor Fli1 is involved in very early development of endothelial and hematopoietic progenitor cells, which are also labeled in *fli*:eGFP (*Tg(fli1:eGFP)^{y1}*) transgenic fish during early development in zebrafish. Whether the *fli1*:eGFP reporter displays eGFP expression in hematopoietic cells in adult zebrafish as well is not clear. However, as development proceeds the reporter is downregulated in the erythroid lineage (Lawson and Weinstein 2002). Fli1 precedes the expression of the vascular markers such as Flk1/KDR (KDRL in zebrafish) (Ellensdottir et al 2010) in endothelial development,

which thus represents a later vascular marker. Endothelial expression of Sox9a was verified with the transgenic reporter fish line *kdr1:GFP* (*Tg(kdr1:GFP)^{la116}*) (Jin et al 2005).

My data revealed the upregulation of Sox9a in epicardial, myocardial and endothelial/endocardial cells close to the wound area after ventricular resection, suggesting an important role of Sox9a very early during heart regeneration. However, the Sox9a expression pattern in a subset of each cardiac lineage and in only few proliferating Sox9a+ endothelial or myocardial cells implies that Sox9a is presumably not responsible for regeneration of all epicardial, myocardial or endothelial/endocardial cells. The proportion/fraction of each lineage that is dependent on Sox9a expression remains to be determined.

4.2.2 Sox9a is important for endothelial and myocardial regeneration

To assess the role of Sox9a transcription factor during heart regeneration I used mutant and transgenic fish lines to interfere with Sox9a function.

Only heterozygous *sox9a* mutant (*jellyfish^{hw37}*) fish grow to adulthood, which did not show a different capacity in heart regeneration compared to injured wild-type siblings. However, heterozygous mutants presumably have a hypomorphic Sox9a mutant phenotype and it might thus be that influences of Sox9a on heart regeneration were phenotypically not detectable.

The transcription factor Sox9a is a transcriptional activator for certain target genes like *col2a1a* and *col11a2* (Yan et al 2002, Yokoi et al 2009, Yan et al 2005). To examine Sox9a function during heart regeneration, a Sox9a repressor construct was designed containing a Sox9a deletion construct that included the HMG DNA binding domain but lacked the C-terminus (Kamachi et al 1999, Hsiao et al 2003, Chiang et al 2001). This Sox9a deletion construct was fused to the Engrailed repressor domain to generate a repressor that competes with Sox9a binding to target genes and represses target gene transcription. A similar approach showed the inhibitory function of a Sox9-Eng construct on target gene expression in quail development and cell culture (Sakai et al 2006).

Tests in zebrafish embryos for Sox9aEng repressor function revealed that injection of Sox9aEng did not resemble *sox9a*^{-/-} or *sox9a*^{-/-},*sox9b*^{-/-} mutant phenotypes but caused more severe defects in embryos.

Sox9a mutant embryos (*sox9a*^{-/-}) mostly showed missing or reduced cartilage replacement bones whereas double homozygous *sox9a*^{-/-},*sox9b*^{-/-} embryos displayed for instance more severe skeletal malformations also present in Campomelic dysplasia patients (Yan et al 2002, Yan et al 2005, Mansour et al 2002). In contrast, *sox9aEng* injected embryos showed phenotypes such as reduction of anterior and posterior structures and an open neural tube in early development indicating that Sox9aEng interferes not only with Sox9a target gene expression. This assumption was confirmed by coinjection experiments showing that Sox9aEng phenotypes in embryos can be rescued by Sox9a, Sox9b and Sox10 suggesting that Sox9aEng interferes with the target gene expression of these three subgroup E transcription factors. Moreover, I cannot exclude an interference of Sox9aEng with Sox transcription factors of other subgroups because other factors than subgroup E proteins were not examined. Thus, Sox9aEng induced phenotypes might be very severe due to the accumulation of defects caused by inhibition of several Sox target genes.

Using the transgenic fish line hsSox9aEng (Tg(hsp70l:dTomato p2a Sox9aΔCEngrailed)), which is inducible for *sox9aEng* expression via heat-shock application, I reproduced the same phenotypic classes in embryos and detected a dose dependent downregulation of Sox9a (and Sox9b) target genes *col11a2* and *col2a1a* (Yokoi et al 2009, Yan et al 2005) after induction of *sox9aEng* expression in transgenic embryos. Thus these results indicated that Sox9aEng presumably works as transcriptional repressor of several target genes.

Hence, Sox9aEng can interfere with Sox9a target gene expression; yet its interference is not specifically confined to Sox9a target genes, since effects can also be rescued by Sox9b and Sox10. However, Sox9a is the only member of the subgroup E that is expressed during heart regeneration. Therefore I expect Sox9aEng to mainly influence Sox9a target genes during cardiac regeneration.

Using the inducible transgenic fish line hsSox9aEng, I revealed that the myocardial and endothelial cell layer are impaired in regeneration after *sox9aEng* expression, suggesting that Sox9a target gene expression is important for regeneration of these cardiac cell layers. However, the influence of Sox9aEng on epicardial regeneration was so far not examined. Furthermore, the Sox9aEng function in myocardial and endothelial/endocardial regeneration needs to be confirmed, for instance by tissue specific expression of the repressor in the respective lineages. So far *sox9aEng* expression was induced ubiquitously via the heat-shock promoter in all cells.

More importantly, the functional role of Sox9a in myocardial and endothelial regeneration also needs to be confirmed using for instance *in vivo* morpholinos to interfere with endogenous Sox9a function, an approach which is independent of the construct Sox9aEng.

4.2.3 Possible role of Sox9a during heart regeneration

Recent publications demonstrated Sox9 expression in embryonic progenitors of the intestine and pancreas and its requirement for generation and maintenance of neural stem cells in embryonic development of the central nervous system (CNS) (Furuyama et al 2010, Kopp et al 2010, Seymour et al 2007, Scott et al 2010). Moreover Sox9 marks progenitor cells of the CNS, exocrine pancreas, intestine and liver in adults (Scott et al 2010, Furuyama et al 2010) and Sox9 positive precursor cells are suggested to function as source for regenerating cells after certain types of liver injury (Furuyama et al 2010). Thus, different tissue types harbor Sox9+ progenitor cells that serve as a source for new cells during homeostasis or regeneration. A similar role for Sox9a+ cells during heart regeneration is likely. Sox9a presumably functions in progenitor-like cells, which might include partially dedifferentiated cardiomyocytes, but not in resident stem cells as suggested by literature. Recent publications suggest that new cardiomyocytes in the regenerating zebrafish heart are presumably derived from existing differentiated cardiomyocytes that undergo dedifferentiation and proliferation (Kikuchi et al 2010, Jopling et al 2010). The vast majority of new cardiomyocytes is therefore generated by proliferating myocardial cells and thus a role of resident stem cells seems to be unlikely (Kikuchi et al 2010, Jopling et al 2010). So far, it is not entirely clear how endothelial or epicardial cells are replaced.

Concluding from the above, I suggest that Sox9a+ cells represent progenitor-like cells of each analyzed cell type (epicardial, myocardial, endothelial cells) during heart regeneration. These progenitor-like cell types could be derived from dedifferentiated existing cells, such as myocardial cells, or precursor cells of other lineages, which start to express Sox9a upon activation after heart amputation. A function of Sox9 in adult progenitor cells is further supported by observations showing Sox9 expression in cardiac myxomas, the most frequent tumor of the heart, which implicates its contribution to the stem cell like properties of tumor cells (Orlandi et al 2006).

Furthermore, Sox9 is implicated in epithelial-to-mesenchymal transformation/transition (EMT) of neural crest cells and endocardial cushion cells, the precursors of the heart

valves during development (Sakai et al 2010, Lincoln et al 2007, Akiyama et al 2004). In addition, EMT is important during cardiac development since epicardial cells undergo EMT leading to epicardial derived cells (EPDCs), which invade the subepicardial matrix and the myocardium to form coronary arteries, fibroblast and endocardial cushions (Lie-Venema et al 2007). EPDCs have been also suggested to function as myocardial progenitor cells in the developing heart (van Wijk and van den Hoff 2010, Martinez-Estrada et al 2010). Thus Sox9a expression in the regenerating zebrafish heart could also point to EMT processes that might lead to formation of new coronary arteries derived from epicardial cells. Whether epicardial cells are a source for myocardial cells in the adult fish remains questionable.

To summarize, Sox9a⁺ cells presumably have different interesting roles during heart regeneration. The function of Sox9a in epicardial, myocardial and endothelial/endocardial cells can be different, representing possibly EMT processes in one cardiac lineage, like e.g. in epicardial cells, and the progenitor status in myocardial and/or endothelial cells. However, whether Sox9a⁺ cells contribute a significant amount to the regenerated heart tissue remains to be determined. Lineage tracing experiments, which label Sox9a⁺ cells to follow their fate in regeneration, will elucidate the contribution of Sox9a⁺ cells to the process of heart regeneration. Together with tissue specific inhibition of Sox9a function by Sox9aEng expression, induced at different time points, Sox9a function for each cellular lineage in the regenerating heart could be revealed.

Several pathways, like FGF signaling, BMP signaling or Hh signaling, are described to regulate Sox9 expression during embryonic development, cancer or during regeneration of the caudal fin in zebrafish (Turner and Grose 2010, Park et al 2010, Smith et al 2006). Identification of the signaling pathway that regulates Sox9a expression could be helpful to confirm Sox9a function in regeneration and give more insight in the process of heart regeneration.

4.3 Cryoinjury – an alternative heart injury model in zebrafish

Zebrafish have the impressive competence to effectively regenerate heart tissue after a massive injury (Poss et al 2002). In contrast, mammals heal a cardiac injury by scarring followed by functional limitations that mostly results in cardiac failure (van de Schans et al 2008). The features of the wound area after ventricular resection in zebrafish are different from those of the lesioned area after a mammalian heart infarction, which is tissue death typically due to ischemia (Cleutjens et al 1999, Abarbanell et al 2010). I developed a simple method using dry-ice to cause cryoinjuries, which led to massive cell death and thus to lesions in the zebrafish heart. Cryoinjuries in zebrafish heart cause widespread tissue death since wound morphology and TUNEL analysis suggests the presence of necrotic and apoptotic tissue, accompanied by an inflammatory response, which is similar to mammalian cryoinjury models (van Amerongen et al 2008). Histological analyses and expression analysis of *cardiac myosin light chain 2 (cmlc2)* mRNA via in situ hybridization in cryoinjured heart sections strongly indicated the loss of cardiomyocytes in the affected wound area. Strikingly, cryoinjured hearts displayed a robust regenerative response with extensive removal of lesioned tissue and finally little scar formation. Notably, ventricular resection can also result in little scar formation (Poss et al 2002) indicating that cryoinjury and ventricular resection are comparable regarding the overall extent of regenerative capability.

4.3.1 Epicardium and myocardium respond similarly to cryoinjury and ventricular resection

Similar cellular mechanisms were induced in the regenerative response following ventricular resection and cryoinjury. For example, the entire epicardium activated the expression of developmental genes such as *tbx18* (Lepilina et al 2006) and *Wt1b* as reported in *wt1b:GFP* transgenic fish very early during regeneration. Soon after injury, activated epicardial cells covered the lesioned area. Proliferation of epicardial cells and morphological changes including thickening of the epicardial layer at the wound edges were detectable after both types of injury (Lepilina et al 2006). The epicardial wound coverage is completed earlier after cryoinjury than after resection. Thus, to some extent epicardial cells respond differently to cryoinjury than to ventricular resection.

Nevertheless, no significant differences were detectable in timing or level of epicardial gene expression or in upregulation of epicardial proliferation after either type of injury. Hence, these reasons are less likely to be causative for the difference in epicardial coverage of the lesion. Interestingly, wound tissue adhered more strongly to the pericardial sac after ventricular resection than after cryoinjury, presumably impairing the epicardial coverage of the wound due to this tissue adherence in resected hearts.

Mature cardiomyocytes, labeled in the transgenic fish line *cmlc2:GFP*, proliferate in response to ventricular resection (Poss et al 2002, Kikuchi et al 2010) and, likewise, I detected proliferating myocardial cells and cardiomyocytes invading the lesion after cryoinjury. Proliferating cardiomyocytes were detectable already 3 days after cryoinjury, which seems, however, earlier than after ventricular resection (Poss et al 2002, Kikuchi et al 2010). There, proliferating myocardial cells have been detected at 7 dpa, but it remains unclear whether this is the earliest time point for detection of myocardial proliferation after ventricular resection.

In addition to early activation of the epicardial layer and the presence of proliferating cardiomyocytes in response to cryoinjury or ventricular resection, Sox9 expression was induced in either injury model. This suggests that similar molecular mechanisms might regulate cardiac regeneration after both injury types.

In summary, I showed that zebrafish regenerates the heart after cardiac lesions with massive cell death caused by cryoinjury similar to the injury caused by surgical removal of heart tissue. Despite very few temporal differences, I detected similar cellular and molecular responses during the regeneration process after resection and after cryoinjury. However, lesions caused by cryoinjury better reflect the damage of heart tissue seen in humans, which is associated with massive cell death (Cleutjens et al 1999). Thus, cryoinjury will be a useful method for future examination of cellular and molecular mechanisms of heart regeneration and can help to improve therapies in humans after heart infarction.

4.4 Gene expression profiling of zebrafish heart regeneration verifies known and identifies novel regulated genes

Systematic gene expression profiling of the first 14 days of zebrafish heart regeneration was performed using oligoexpression microarray analysis. Other transcription profiling approaches and analysis using in situ hybridization on sections of regenerating hearts revealed the upregulation of several transcripts such as *mdka* or *tbx18* during zebrafish cardiac regeneration (Lepilina et al 2006, Lien et al 2006). In the presented gene expression analysis I identified genes that are known to be expressed and novel genes that are upregulated during zebrafish heart regeneration. Interestingly, most transcripts are upregulated during early heart regeneration (4 dpa), indicating that cellular responses are initiated especially very early after ventricular resection, although the complete regeneration process of the zebrafish heart lasts around 60 days (Poss et al 2002).

Genes such as the transcription factors *tbx1*, *sox4b* or *nkx2a*, are implicated in embryonic heart development, suggesting a reactivation of an embryonic gene expression program. Thus *tbx1*, belonging to the T-box family of transcription factors, is expressed throughout different stages in heart development and is moreover suggested to be the critical factor for cardiovascular anomalies in the mouse model of the rare DiGeorge syndrome (Kochilas et al 2003). *sox4b* is, like *sox4a*, an orthologue of the human *SOX4* and implicated in zebrafish pancreas development (Mavropoulos et al 2005), while, in mouse, the conditional null allele of *sox4* causes severe heart malformations leading to death, which thus indicates a critical role for Sox4 for vertebrate heart development (Pendoz-Mendez et al 2007). Tbx2a is as well implicated in zebrafish heart development since misexpression leads to incomplete cardiac looping and impaired atrioventricular canal (AVC) constriction, which is normally preceding valve formation (Ribeiro et al 2007). It is suggested that Tbx2 regulates together with other Tbx factors cell proliferation during heart remodeling processes (Ribeiro et al 2007).

Other transcripts like *gli2a* and *pea3* even indicate the activation of signaling pathways like Hedgehog signaling and Fgf signaling respectively. The transcription factor *gli2* is implicated in mediating Hh signaling in zebrafish (Karlstrom et al 1999). In mammals, Hh signaling influences secondary heart field (SHF) formation during heart development and is furthermore suggested to positively regulate angiogenesis after myocardial infarction in mammals (Dyer et al 2010, Ueda et al 2010).

Fgf signaling is crucial for embryonic heart development and is implicated in revascularization of the new myocardial wall during zebrafish heart regeneration (Marques et al 2008, Lepilina et al 2006). The amputation specific expression pattern of the Fgf target genes *pea3* (Roel and Nüsslein-Volhard 2001, Raible and Brand 2001) and *dusp6* (dual-specificity phosphatase 6)/MKP3 (MAPK phosphatase 3) (Ekerot et al 2008), reported by TG(*dusp6:d2eGFP*) transgenic fish line (Molina et al 2007), suggested active Fgf signaling very early during heart regeneration. The upregulation of Fgf pathway components as shown by Lepilina and colleagues and FGF target genes strongly suggest a functional role of Fgf signaling very early during heart regeneration (Lepilina et al 2006). Whether this function is restricted to the process of revascularization remains to be determined.

The upregulation of the transcription factors *snai1a* and *snai2* suggested that epithelial-to-mesenchymal transition/transformation (EMT) occurs during cardiac regeneration. *snai1a*, an orthologue of the *snail1* gene, and *snai2* have been described to be required for EMT processes in embryonic development (Blanco et al 2007, Dave et al 2001, Sakai et al 2006, Nieto 2002). In cardiac development, EMT leads to epicardial derived cells (EPDCs), which can invade the myocardium to form for instance coronary vessels in the developing myocardial wall (Lie-Venema et al 2007). EMT of epicardial cells might be also important for formation of new coronary vessels during heart regeneration (Lepilina et al 2006, Kim et al 2010), which is supported by upregulation of *snail2* mRNA, as EMT marker, at 7 and 10 dpa in regenerating zebrafish hearts (Kim et al 2010). Beside an amputation specific upregulation of *snai2* and *snai1b* in the performed microarray, I detected cells presumably of epicardial origin that are expressing VE - Cadherin, a marker of mature endothelial cells, in regenerating hearts at 7 dpa (Montero-Balaguer et al 2009). This result might suggest that epicardial cells or cells of epicardial origin display possibly endothelial characteristics during heart regeneration. Thus I speculate that epicardial cells might undergo EMT contribute to new endothelial cells during zebrafish cardiac regeneration; this theorie, however, is also suggested by others (Kim et al 2010, Lepilina et al 2006).

In summary, using oligoexpression microarray analysis, I identified novel transcription factors and pathways that are implicated in cardiac development and expressed/reactivated during heart regeneration supporting the assumption that developmental signals are reactivated during cardiac regeneration. The identification of EMT markers and antibody stainings of sectioned regenerating hearts might suggests a role of epicardial cells for

regeneration of vascular structures after resection (Lepilina et al 2006, Kim et al 2010). The establishment of transgenic fish lines to lineage trace epicardial cells will elucidate whether epicardial EMT processes are present and necessary to generate new vasculature during heart regeneration. However, results of the oligoexpression microarray provide a starting point for further analysis of transcription factors, the functional role of pathways or cellular processes such as EMT in zebrafish heart regeneration.

4.5 General conclusion

In this thesis, I aimed at identifying and understanding the functionality of signaling pathways and transcription factors during cardiac regeneration in zebrafish. The regeneration process is presumably initiated by activated epicardial and endocardial/endothelial cells (Lepilina et al 2006, Kikuchi et al 2011). The activity of *wt1b* promoter elements and the initiation of epicardial proliferation, shown in this work and by others, further support the impression of an epicardial cell layer that is active early in zebrafish heart regeneration (Lepilina et al 2006). Presumably, activated epicardial cells migrate from the wound edges into the wound area and cover the wound (Lepilina et al 2006). So far it is not clear how endocardial/endothelial cells and epicardial cells are regenerated, although theories for endothelial regeneration exist, as explained below. In contrast, it was shown that mature cardiomyocytes dedifferentiate and induce proliferation to generate new myocardial cells (Kikuchi et al 2010). The epicardial and endocardial layer, which are activated very early in regeneration, presumably provide signals that are important for cardiomyocyte proliferation (Kikuchi et al 2011). It might be possible that endocardial/endothelial and epicardial cells also dedifferentiate to a more immature or progenitor – like state in order to proliferate and generate new endocardial/endothelial and epicardial cells. Furthermore, epicardial cells might undergo EMT thereby contributing new cells to coronary vessels, a mechanism already present during heart development (Lepilina et al 2006, Kim et al 2010).

Regulators of cardiac development could be involved in these mechanisms. A functional role of Wnt/ β -catenin signaling, which is crucial for heart development, however, was not detectable at several stages of heart regeneration. In contrast, the transcription factor Sox9a is expressed during early stages of heart regeneration in activated cells of the epicardial, endocardial/endothelial and myocardial lineage. Using transgenic fish that inducibly interfere with Sox9a target gene expression, I could detect that Sox9a target genes are presumably important for endothelial and myocardial regeneration. Sox9 is so far described for heart valve and septum development (Lincoln et al 2007); data concerning Sox9 expression in myocardial cells are contradictory (Rahkonen et al 2003, Lincoln et al 2007). The expression of Sox9a in regeneration is seen in epicardial, endocardial/endothelial and myocardial cells, which might not suggest the reactivation of a developmental gene program. Since Sox9 is required for maintenance of stem/progenitor cells in several tissues like the CNS (Scott et al 2010), it is possible that Sox9a is expressed

in progenitor cells of cardiac lineages, possibly including partially dedifferentiated myocardial cells, during heart regeneration. Alternatively, it might be implicated in epicardial EMT processes to generate new vasculature in the regenerating tissue, a theory that is supported by my microarray results and the work of others (Lepilina et al 2006, Kim et al 2010).

The oligoexpression microarray analyzing the first 14 dpa identified new signals including transcription factors that are upregulated during cardiac regeneration. The FGF signaling pathway, which is important during cardiac development, is one of the pathways that was detected on the microarray. Expression of transcription factors of the Snai protein family further indicated that EMT processes are involved in heart regeneration.

In addition to ventricular resection, I aimed at developing an injury model that closer resembles the situation after human infarction. I established a cryoinjury model, which recapitulates general hallmarks of infarctions like massive tissue death. Importantly, zebrafish are able to regenerate heart tissue after cryoinjury to a similar extent and by the same cellular mechanisms when compared with ventricular resection. This injury model therefore provides a useful procedure to further study principles of zebrafish heart regeneration, which can be compared to cellular events that are activated after mammalian cardiac injury.

Parts of the results “cryoinjury – an alternative heart injury model in zebrafish” were published (Schnabel et al 2011). At the same time, others also showed regeneration of the zebrafish heart after cryoinjury/cryocauterization (González-Rosa et al 2011, Chablais et al 2011).

References

- Abarbanell, A.M., Herrmann, J.L., Weil, B.R., Wang, Y., Tan, J., Moberly, S.P., Fiege, J.W., Meldrum, D.R.** (2010). Animal models of myocardial and vascular injury. *J Surg Res* 162(2):239-49.
- Akiyama, H., Chaboissier, M.C., Behringer, R.R., Rowitch, D.H., Schedl, A., Epstein, J.A., de Crombrughe, B.** (2004). Essential role of Sox9 in the pathway that controls formation of cardiac valves and septa. *Proc Natl Acad Sci U S A* 101(17):6502-7.
- Altschul, S.F., Gish, W., Miller, W., Myers, E.W., Lipman, D.J.** (1990). Basic local alignment search tool. *J Mol Biol* 215(3):403-10.
- Ausoni, S., Sartore, S.** (2009). From fish to amphibians to mammals: in search of novel strategies to optimize cardiac regeneration. *J Cell Biol* 184(3):357-64.
- Bafico, A., Liu, G., Yaniv, A., Gazit, A., Aaronson, S.A.** (2001). Novel mechanism of Wnt signalling inhibition mediated by Dickkopf-1 interaction with LRP6/Arrow. *Nat Cell Biol* 3(7):683-6.
- Balakumar, P., Jagadeesh, G.** (2010). Multifarious molecular signaling cascades of cardiac hypertrophy: can the muddy waters be cleared? *Pharmacol Res* 62(5):365-83.
- Barandon, L., Couffinhal, T., Ezan, J., Dufourcq, P., Costet, P., Alzieu, P., Leroux, L., Moreau, C., Dare, D., Dupl a, C.** (2003). Reduction of infarct size and prevention of cardiac rupture in transgenic mice overexpressing FrzA. *Circulation* 108(18):2282-9.
- Blanco, M.J., Barrallo-Gimeno, A., Acloque, H., Reyes, A.E., Tada, M., Allende, M.L., Mayor, R., Nieto, M.A.** (2007). Snail1a and Snail1b cooperate in the anterior migration of the axial mesendoderm in the zebrafish embryo. *Development* 134(22):4073-81.
- Blankesteijn, W.M., van de Schans, V.A., ter Horst, P., Smits, J.F.** (2008). The Wnt/frizzled/GSK-3 beta pathway: a novel therapeutic target for cardiac hypertrophy. *Trends Pharmacol Sci* 29(4):175-80.
- Bollig, F., Mehringer, R., Perner, B., Hartung, C., Sch fer, M., Scharl, M., Volf, J.N., Winkler, C., Englert, C.** (2006). Identification and comparative expression analysis of a second wt1 gene in zebrafish. *Dev Dyn* 235(2):554-61.
- Brand, T.** (2003). Heart development: molecular insights into cardiac specification and early morphogenesis. *Dev Biol* 258(1):1-19.

- Campbell, N.A.** (1997). *Biologie. Spectrum Akademischer Verlag GmbH Heidelberg-Berlin.Oxford.* 902
- Chablais, F., Veit, J., Rainer, G., Jazwińska, A.** (2011). The zebrafish heart regenerates after cryoinjury-induced myocardial infarction. *BMC Dev Biol* 11:21.
- Chiang, E.F., Pai, C.I., Wyatt, M., Yan, Y.L., Postlethwait, J., Chung, B.** (2001). Two sox9 genes on duplicated zebrafish chromosomes: expression of similar transcription activators in distinct sites. *Dev Biol* 231(1):149-63.
- Chien, K.R., Domian, I.J., Parker, K.K.** (2008). Cardiogenesis and the complex biology of regenerative cardiovascular medicine. *Science* 322(5907):1494-7.
- Cleutjens, J.P., Blankesteyn, W.M., Daemen, M.J., Smits, J.F.** (1999). The infarcted myocardium: simply dead tissue, or a lively target for therapeutic interventions. *Cardiovasc Res* 44(2):232-41.
- Clevers, H.** (2006). Wnt/beta-catenin signaling in development and disease. *Cell* 127(3):469-80.
- Dave, N., Guaita-Esteruelas, S., Gutarra, S., Frias, À., Beltran, M., Peiró, S., de Herreros, A.G.** (2011). Functional cooperation between Snail1 and twist in the regulation of ZEB1 expression during epithelial to mesenchymal transition. *J Biol Chem* 286(14):12024-32.
- de Pater, E., Clijsters, L., Marques, S.R., Lin, Y.F., Garavito-Aguilar, Z.V., Yelon, D., Bakkers, J.** (2009). Distinct phases of cardiomyocyte differentiation regulate growth of the zebrafish heart. *Development* 136(10):1633-41.
- Dorsky, R.I., Sheldahl, L.C., Moon, R.T.** (2002). A transgenic Lef1/beta-catenin-dependent reporter is expressed in spatially restricted domains throughout zebrafish development. *Dev Biol* 241(2):229-37.
- Dorsky, R.I., Moon, R.T., Raible, D.W.** (1998). Control of neural crest cell fate by the Wnt signalling pathway. *Nature* 396(6709):370-3.
- Dyer, L.A., Makadia, F.A., Scott, A., Pegram, K., Hutson, M.R., Kirby, M.L.** (2010). BMP signaling modulates hedgehog-induced secondary heart field proliferation. *Dev Biol* 348(2):167-76.
- Ellertsdóttir, E., Lenard, A., Blum, Y., Krudewig, A., Herwig, L., Affolter, M., Belting, H.G.** (2010). Vascular morphogenesis in the zebrafish embryo. *Dev Biol* 341(1):56-65.
- Eisenberg LM, Eisenberg CA.** (2006). Wnt signal transduction and the formation of the myocardium. *Dev Biol* 293(2):305-15.

- Eisenberg, L.M., Eisenberg, C.A.** (2007). Evaluating the role of Wnt signal transduction in promoting the development of the heart. *ScientificWorldJournal* 7:161-76.
- Eisenhart, C.** (1947). The assumptions underlying the analysis of variance. *Biometrics* 3, 1-21.
- Ekerot, M., Stavridis, M.P., Delavaine, L., Mitchell, M.P., Staples, C., Owens, D.M., Keenan, I.D., Dickinson, R.J., Storey, K.G., Keyse, S.M.** (2008). Negative-feedback regulation of FGF signalling by DUSP6/MKP-3 is driven by ERK1/2 and mediated by Ets factor binding to a conserved site within the DUSP6/MKP-3 gene promoter. *Biochem J* 412(2):287-98.
- Engel, F.B., Schebesta, M., Duong, M.T., Lu, G., Ren, S., Madwed, J.B., Jiang, H., Wang, Y., Keating, M.T.** (2005). p38 MAP kinase inhibition enables proliferation of adult mammalian cardiomyocytes. *Genes Dev* 19(10):1175-87.
- Furuyama, K., Kawaguchi, Y., Akiyama, H., Horiguchi, M., Kodama, S., Kuhara, T., Hosokawa, S., Elbahrawy, A., Soeda, T., Koizumi, M., Masui, T., Kawaguchi, M., Takaori, K., Doi, R., Nishi, E., Kakinoki, R., Deng, J.M., Behringer, R.R., Nakamura, T., Uemoto, S.** (2011). Continuous cell supply from a Sox9-expressing progenitor zone in adult liver, exocrine pancreas and intestine. *Nat Genet* 43(1):34-41.
- Gao, F., Maiti, S., Alam, N., Zhang, Z., Deng, J.M., Behringer, R.R., Lécureuil, C., Guillou, F., Huff, V.** (2006). The Wilms tumor gene, *Wt1*, is required for Sox9 expression and maintenance of tubular architecture in the developing testis. *Proc Natl Acad Sci U S A* 103(32):11987-92.
- Glickman, N.S., Yelon, D.** (2002). Cardiac development in zebrafish: coordination of form and function. *Semin Cell Dev Biol* 13(6):507-13.
- Goessling, W., North, T.E., Lord, A.M., Ceol, C., Lee, S., Weidinger, G., Bourque, C., Strijbosch, R., Haramis, A.P., Puder, M., Clevers, H., Moon, R.T., Zon, L.I.** (2008). APC mutant zebrafish uncover a changing temporal requirement for wnt signaling in liver development. *Dev Biol* 320(1):161-74.
- González-Rosa, J.M., Martín, V., Peralta, M., Torres, M., Mercader, N.** (2011). Extensive scar formation and regression during heart regeneration after cryoinjury in zebrafish. *Development* 138(9):1663-74.
- Halloran, M.C., Sato-Maeda, M., Warren, J.T., Su, F., Lele, Z., Krone, P.H., Kuwada, J.Y., Shoji, W.** (2000). Laser-induced gene expression in specific cells of transgenic zebrafish. *Development* 127(9):1953-60.

- Hardt, S.E., Sadoshima, J.** (2002). Glycogen synthase kinase-3beta: a novel regulator of cardiac hypertrophy and development. *Circ Res* 90(10):1055-63.
- Heisenberg, C.P., Houart, C., Take-Uchi, M., Rauch, G.J., Young, N., Coutinho, P., Masai, I., Caneparo, L., Concha, M.L., Geisler, R., Dale, T.C., Wilson, S.W., Stemple, D.L.** (2001). A mutation in the Gsk3-binding domain of zebrafish Masterblind/Axin1 leads to a fate transformation of telencephalon and eyes to diencephalon. *Genes Dev* 15(11):1427-34.
- Hsiao, N.W., Samuel, D., Liu, Y.N., Chen, L.C., Yang, T.Y., Jayaraman, G., Lyu, P.C.** (2003). Mutagenesis study on the zebra fish SOX9 high-mobility group: comparison of sequence and non-sequence specific HMG domains. *Biochemistry* 42(38):11183-93.
- Hu, N., Yost, H.J., Clark, E.B.** (2001). Cardiac morphology and blood pressure in the adult zebrafish. *Anat Rec* 264(1):1-12.
- Huang, C.J., Tu, C.T., Hsiao, C.D., Hsieh, F.J., Tsai, H.J.** (2003). Germ-line transmission of a myocardium-specific GFP transgene reveals critical regulatory elements in the cardiac myosin light chain 2 promoter of zebrafish. *Dev Dyn* 228(1):30-40.
- Hurlstone, A.F., Haramis, A.P., Wienholds, E., Begthel, H., Korving, J., Van Eeden, F., Cuppen, E., Zivkovic, D., Plasterk, R.H., Clevers, H.** (2003). The Wnt/beta-catenin pathway regulates cardiac valve formation. *Nature* 425(6958):633-7.
- Jho, E.H., Zhang, T., Domon, C., Joo, C.K., Freund, J.N., Costantini, F.** (2002). Wnt/beta-catenin/Tcf signaling induces the transcription of Axin2, a negative regulator of the signaling pathway. *Mol Cell Biol* 22(4):1172-83.
- Jin, S.W., Beis, D., Mitchell, T., Chen, J.N., Stainier, D.Y.** (2005). Cellular and molecular analyses of vascular tube and lumen formation in zebrafish. *Development* 132(23):5199-209.
- Jopling, C., Sleep, E., Raya, M., Martí, M., Raya, A., Belmonte, J.C.** (2010). Zebrafish heart regeneration occurs by cardiomyocyte dedifferentiation and proliferation. *Nature* 464(7288):606-9.
- Kamachi, Y., Cheah, K.S., Kondoh, H.** (1999). Mechanism of regulatory target selection by the SOX high-mobility-group domain proteins as revealed by comparison of SOX1/2/3 and SOX9. *Mol Cell Biol* 19(1):107-20.
- Kan NG, Junghans D, Izpisua Belmonte JC.** (2009). Compensatory growth mechanisms regulated by BMP and FGF signaling mediate liver regeneration in zebrafish after partial hepatectomy. *FASEB J* 23(10):3516-25.

Karlstrom, R.O., Talbot, W.S., Schier, A.F. (1999). Comparative synteny cloning of zebrafish you-too: mutations in the Hedgehog target *gli2* affect ventral forebrain patterning. *Genes Dev* 13(4):388-93.

Karnovsky, M.J. (1965). A formaldehyde-glutaraldehyde fixative of high osmolality for use in electron microscopy. *J Cell Biol* 27: 137A.

Kiefer, J.C. (2007). Back to basics: Sox genes. *Dev Dyn* 236(8):2356-66.

Kikuchi, K., Holdway, J.E., Major, R.J., Blum, N., Dahn, R.D., Begemann, G., Poss, K.D. (2011). Retinoic acid production by endocardium and epicardium is an injury response essential for zebrafish heart regeneration. *Dev Cell* 20(3):397-404.

Kikuchi, K., Holdway, J.E., Werdich, A.A., Anderson, R.M., Fang, Y., Egnaczyk, G.F., Evans, T., Macrae, C.A., Stainier, D.Y., Poss, K.D. (2010). Primary contribution to zebrafish heart regeneration by *gata4(+)* cardiomyocytes. *Nature* 464(7288):601-5.

Kim, J., Wu, Q., Zhang, Y., Wiens, K.M., Huang, Y., Rubin, N., Shimada, H., Handin, R.I., Chao, M.Y., Tuan, T.L., Starnes, V.A., Lien, C.L. (2010). PDGF signaling is required for epicardial function and blood vessel formation in regenerating zebrafish hearts. *Proc Natl Acad Sci U S A* 107(40):17206-10.

Knopf, F., Hammond, C., Chekuru, A., Kurth, T., Hans, S., Weber, C.W., Mahatma, G., Fisher, S., Brand, M., Schulte-Merker, S., Weidinger, G. (2011). Bone Regenerates via Dedifferentiation of Osteoblasts in the Zebrafish Fin. *Dev Cell* 20(5):713-24.

Knopf, F., Schnabel, K., Haase, C., Pfeifer, K., Anastassiadis, K., Weidinger, G. (2010). Dually inducible TetON systems for tissue-specific conditional gene expression in zebrafish. *Proc Natl Acad Sci U S A* 107(46):19933-8.

Kochilas, L.K., Potluri, V., Gitler, A., Balasubramanian, K., Chin, A.J. (2003). Cloning and characterization of zebrafish *tbx1*. *Gene Expr Patterns* 3(5):645-51.

Kopp, J.L., Dubois, C.L., Schaffer, A.E., Hao, E., Shih, H.P., Seymour, P.A., Ma, J., Sander, M. (2011). Sox9⁺ ductal cells are multipotent progenitors throughout development but do not produce new endocrine cells in the normal or injured adult pancreas. *Development* 138(4):653-65.

Kraus, F., Haenig, B., Kispert, A. (2001). Cloning and expression analysis of the mouse T-box gene *Tbx18*. *Mech Dev* 100(1):83-6.

Kurth, T., Berger, J., Wilsch-Bräuninger, M., Kretschmar, S., Cerny, R., Schwarz, H., Löffberg, J., Piendl, T., Epperlein, H.H. (2010). Electron microscopy of the

amphibian model systems *Xenopus laevis* and *Ambystoma mexicanum*. *Methods Cell Biol* 96:395-423.

Kwon, C., Cordes, K.R., Srivastava, D. (2008). Wnt/beta-catenin signaling acts at multiple developmental stages to promote mammalian cardiogenesis. *Cell Cycle* 7(24):3815-8.

Kwon C, Arnold J, Hsiao EC, Taketo MM, Conklin BR, Srivastava D. (2007). Canonical Wnt signaling is a positive regulator of mammalian cardiac progenitors. *Proc Natl Acad Sci U S A* 104(26):10894-9.

Laflamme, M.A., Murry, C.E. (2011). Heart regeneration. *Nature* 473(7347):326-35.

Lawson, N.D., Weinstein, B.M. (2002). In vivo imaging of embryonic vascular development using transgenic zebrafish. *Dev Biol* 248(2):307-18.

Lepilina, A., Coon, A.N., Kikuchi, K., Holdway, J.E., Roberts, R.W., Burns, C.G., Poss, K.D. (2006). A dynamic epicardial injury response supports progenitor cell activity during zebrafish heart regeneration. *Cell* 127(3):607-19.

Leri, A., Kajstura, J., Anversa, P., Frishman, W.H. (2008). Myocardial regeneration and stem cell repair. *Curr Probl Cardiol* 33(3):91-153.

Leung, T., Bischof, J., Söll, I., Niessing, D., Zhang, D., Ma, J., Jäckle, H., Driever, W. (2003). *bozozok* directly represses *bmp2b* transcription and mediates the earliest dorsoventral asymmetry of *bmp2b* expression in zebrafish. *Development* 130(16):3639-49.

Lien, C.L., Schebesta, M., Makino, S., Weber, G.J., Keating, M.T. (2006). Gene expression analysis of zebrafish heart regeneration. *PLoS Bio* 4(8):e260.

Lie-Venema, H., van den Akker, N.M., Bax, N.A., Winter, E.M., Maas, S., Kekarainen, T., Hoeben, R.C., deRuiter, M.C., Poelmann, R.E., Gittenberger-de Groot, A.C. (2007). Origin, fate, and function of epicardium-derived cells (EPDCs) in normal and abnormal cardiac development. *ScientificWorldJournal* 7:1777-98.

Lincoln, J., Kist, R., Scherer, G., Yutzey, K.E. (2007). Sox9 is required for precursor cell expansion and extracellular matrix organization during mouse heart valve development. *Dev Biol* 305(1):120-32.

Mably, J.D., Mohideen, M.A., Burns, C.G., Chen, J.N., Fishman, M.C. (2003). Heart of glass regulates the concentric growth of the heart in zebrafish. *Curr Biol* 13(24):2138-47.

- MacDonald, B.T., Tamai, K., He, X.** (2009). Wnt/beta-catenin signaling: components, mechanisms, and diseases. *Dev Cell* 17(1):9-26.
- Männer, J., Pérez-Pomares, J.M., Macías, D., Muñoz-Chápuli, R.** (2001). The origin, formation and developmental significance of the epicardium: a review. *Cells Tissues Organs* 169(2):89-103.
- Mansour, S., Offiah, A.C., McDowall, S., Sim, P., Tolmie, J., Hall, C.** (2002). The phenotype of survivors of campomelic dysplasia. *J Med Genet* 39(8):597-602.
- Mansour, S., Hall, C.M., Pembrey, M.E., Young, I.D.** (1995). A clinical and genetic study of campomelic dysplasia. *J Med Genet* 32(6):415-20.
- Mao, B., Wu, W., Davidson, G., Marhold, J., Li, M., Mechler, B.M., Delius, H., Hoppe, D., Stannek, P., Walter, C., Glinka, A., Niehrs, C.** (2002). Kremen proteins are Dickkopf receptors that regulate Wnt/beta-catenin signalling. *Nature* 417(6889):664-7.
- Marques, S.R., Lee, Y., Poss, K.D., Yelon, D.** (2008). Reiterative roles for FGF signaling in the establishment of size and proportion of the zebrafish heart. *Dev Biol* 321(2):397-406.
- Martínez-Estrada, O.M., Lettice, L.A., Essafi, A., Guadix, J.A., Slight, J., Velecela, V., Hall, E., Reichmann, J., Devenney, P.S., Hohenstein, P., Hosen, N., Hill, R.E., Muñoz-Chapuli, R., Hastie, N.D.** (2010). Wt1 is required for cardiovascular progenitor cell formation through transcriptional control of Snail and E-cadherin. *Nat Genet* 42(1):89-93.
- Mavropoulos, A., Devos, N., Biemar, F., Zecchin, E., Argenton, F., Edlund, H., Motte, P., Martial, J.A., Peers, B.** (2005). sox4b is a key player of pancreatic alpha cell differentiation in zebrafish. *Dev Biol* 285(1):211-23.
- Menssen, H.D., Renkl, H.J., Entezami, M., Thiel, E.** (1997). Wilms' tumor gene expression in human CD34+ hematopoietic progenitors during fetal development and early clonogenic growth. *Blood* 89(9):3486-7.
- Molina, G.A., Watkins, S.C., Tsang, M.** (2007). Generation of FGF reporter transgenic zebrafish and their utility in chemical screens. *BMC Dev Biol* 7:62.
- Montero-Balaguer, M., Swirsding, K., Orsenigo, F., Cotelli, F., Mione, M., Dejana, E.** (2009). Stable vascular connections and remodeling require full expression of VE-cadherin in zebrafish embryos. *PLoS One* 4(6):e5772.
- Moon, R.T., Kohn, A.D., De Ferrari, G.V., Kaykas, A.** (2004). WNT and beta-catenin signalling: diseases and therapies. *Nat Rev Genet* 5(9):691-701.

- Nieto, M.A.** (2002). The snail superfamily of zinc-finger transcription factors. *Nat Rev Mol Cell Biol* 3(3):155-66.
- Nyholm, M.K., Wu, S.F., Dorsky, R.I., Grinblat, Y.** (2007). The zebrafish *zic2a-zic5* gene pair acts downstream of canonical Wnt signaling to control cell proliferation in the developing tectum. *Development* 134(4):735-46.
- Oh, C.D., Maity, S.N., Lu, J.F., Zhang, J., Liang, S., Coustry, F., de Crombrughe, B., Yasuda, H.** (2010). Identification of SOX9 interaction sites in the genome of chondrocytes. *PLoS One* 5(4):e10113.
- Orlandi, A., Ciucci, A., Ferlosio, A., Genta, R., Spagnoli, L.G., Gabbiani, G.** (2006). Cardiac myxoma cells exhibit embryonic endocardial stem cell features. *J Pathol* 209(2):231-9.
- Park, J., Zhang, J.J., Moro, A., Kushida, M., Wegner, M., Kim, P.C.** (2010). Regulation of Sox9 by Sonic Hedgehog (Shh) is essential for patterning and formation of tracheal cartilage. *Dev Dyn* 239(2):514-26.
- Penzo-Méndez, A., Dy, P., Pallavi, B., Lefebvre, V.** (2007). Generation of mice harboring a Sox4 conditional null allele. *Genesis* 45(12):776-80.
- Pérez-Pomares, J.M., González-Rosa, J.M., Muñoz-Chápuli, R.** (2009). Building the vertebrate heart - an evolutionary approach to cardiac development. *Int J Dev Biol* 53(8-10):1427-43.
- Perner, B., Englert, C., Bollig, F.** (2007). The Wilms tumor genes *wt1a* and *wt1b* control different steps during formation of the zebrafish pronephros. *Dev Biol* 309(1):87-96.
- Porrello, E.R., Mahmoud, A.I., Simpson, E., Hill, J.A., Richardson, J.A., Olson, E.N., Sadek, H.A.** (2011). Transient regenerative potential of the neonatal mouse heart. *Science* 331(6020):1078-80.
- Poss, K.D., Wilson, L.G., Keating, M.T.** (2002). Heart regeneration in zebrafish. *Science* 298(5601):2188-90.
- Provost, E., Rhee, J., Leach, S.D.** (2007). Viral 2A peptides allow expression of multiple proteins from a single ORF in transgenic zebrafish embryos. *Genesis* 45(10):625-9.
- Qin, Z., Barthel, L.K., Raymond, P.A.** (2009). Genetic evidence for shared mechanisms of epimorphic regeneration in zebrafish. *Proc Natl Acad Sci U S A* 106(23):9310-5.

- Qu, J., Zhou, J., Yi, X.P., Dong, B., Zheng, H., Miller, L.M., Wang, X., Schneider, M.D., Li, F.** (2007). Cardiac-specific haploinsufficiency of beta-catenin attenuates cardiac hypertrophy but enhances fetal gene expression in response to aortic constriction. *J Mol Cell Cardiol* 43(3):319-26.
- Rahkonen, O., Savontaus, M., Abdelwahid, E., Vuorio, E., Jokinen, E.** (2003). Expression patterns of cartilage collagens and Sox9 during mouse heart development. *Histochem Cell Biol* 120(2):103-10.
- Raible, F., Brand, M.** (2001). Tight transcriptional control of the ETS domain factors Erm and Pea3 by Fgf signaling during early zebrafish development. *Mech Dev* 107(1-2):105-17.
- Red-Horse, K., Ueno, H., Weissman, I.L., Krasnow, M.A.** (2010). Coronary arteries form by developmental reprogramming of venous cells. *Nature* 464(7288):549-53.
- Remm, M., Storm, C.E., Sonnhammer, E.L.** (2001). Automatic clustering of orthologs and in-paralogs from pairwise species comparisons. *J Mol Biol* 314(5):1041-52.
- Reya, T., Clevers, H.** (2005). Wnt signalling in stem cells and cancer. *Nature* 434(7035):843-50.
- Ribeiro, I., Kawakami, Y., Büscher, D., Raya, A., Rodríguez-León, J., Morita, M., Rodríguez Esteban, C., Izpisua Belmonte, J.C.** (2007). Tbx2 and Tbx3 regulate the dynamics of cell proliferation during heart remodeling. *PLoS One* 2(4):e398.
- Roehl, H., Nüsslein-Volhard, C.** (2001). Zebrafish pea3 and erm are general targets of FGF8 signaling. *Curr Biol* 11(7):503-7.
- Sakai, D., Suzuki, T., Osumi, N., Wakamatsu, Y.** (2006). Cooperative action of Sox9, Snail2 and PKA signaling in early neural crest development. *Development* 133(7):1323-33.
- Sambrook, J., Russel, D.W., Sambrook, J.** (2001). Molecular cloning: A laboratory manual. *Cold Spring Harbor Laboratory Press*, New York
- Schnabel, K., Wu, C.C., Kurth, T., Weidinger, G.** (2011). Regeneration of cryoinjury induced necrotic heart lesions in zebrafish is associated with epicardial activation and cardiomyocyte proliferation. *PLoS One* 6(4):e18503.
- Scott, C.E., Wynn, S.L., Sesay, A., Cruz, C., Cheung, M., Gomez Gaviro, M.V., Booth, S., Gao, B., Cheah, K.S., Lovell-Badge, R., Briscoe, J.** (2010). SOX9 induces and maintains neural stem cells. *Nat Neurosci* 13(10):1181-9.
- Semënov, M.V., Zhang, X., He X.** (2008). DKK1 antagonizes Wnt signaling without promotion of LRP6 internalization and degradation. *J Biol Chem* 283(31):21427-32.

- Serluca, F.C.** (2008). Development of the proepicardial organ in the zebrafish. *Dev Biol* 315(1):18-27.
- Seymour, P.A., Freude, K.K., Tran, M.N., Mayes, E.E., Jensen, J., Kist, R., Scherer, G., Sander, M.** (2007). SOX9 is required for maintenance of the pancreatic progenitor cell pool. *Proc Natl Acad Sci U S A* 104(6):1865-70.
- Skokowa, J., Welte, K.** (2007). LEF-1 is a decisive transcription factor in neutrophil granulopoiesis. *Ann N Y Acad Sci* 1106:143-51.
- Smith, A., Avaron, F., Guay, D., Padhi, B.K., Akimenko, M.A.** (2006). Inhibition of BMP signaling during zebrafish fin regeneration disrupts fin growth and scleroblasts differentiation and function. *Dev Biol* 299(2):438-54.
- Sprague, J., Bayraktaroglu, L., Clements, D., Conlin, T., Fashena, D., Frazer, K., Haendel, M., Howe, D.G., Mani, P., Ramachandran, S., Schaper, K., Segerdell, E., Song, P., Sprunger, B., Taylor, S., Van Slyke, C.E., Westerfield, M.** (2006). The Zebrafish Information Network: the zebrafish model organism database. *Nucleic Acids Res* 34:D581-5.
- Stainier, D.Y.** (2001). Zebrafish genetics and vertebrate heart formation. *Nat Rev Genet* 2(1):39-48.
- Statistisches Bundesamt Deutschland** “Sterbefälle insgesamt 2009 nach den 10 häufigsten Todesursachen der International Statistical Classification of Diseases and Related Health Problems (ICD-10)”
- Stoick-Cooper, C.L., Weidinger, G., Riehle, K.J., Hubbert, C., Major, M.B., Fausto, N., Moon, R.T.** (2007). Distinct Wnt signaling pathways have opposing roles in appendage regeneration. *Development* 134(3):479-89.
- Stoick-Cooper, C.L., Moon, R.T., Weidinger, G.** (2007). Advances in signaling in vertebrate regeneration as a prelude to regenerative medicine. *Genes Dev* 21(11):1292-315.
- Tamhane, Ajit C., & Dunlop, Dorothy D.** (2000). Statistics and Data Analysis from Elementary to Intermediate. *Prentice Hall* 473-474.
- Turner, N., Grose, R.** (2010). Fibroblast growth factor signalling: from development to cancer. *Nat Rev Cancer* 10(2):116-29.
- Ueda, K., Takano, H., Niitsuma, Y., Hasegawa, H., Uchiyama, R., Oka, T., Miyazaki, M., Nakaya, H., Komuro, I.** (2010). Sonic hedgehog is a critical mediator of erythropoietin-induced cardiac protection in mice. *J Clin Invest* 120(6):2016-29.
- Ueno, S., Weidinger, G., Osugi, T., Kohn, A.D., Golob, J.L., Pabon, L., Reinecke, H., Moon, R.T., Murry, C.E.** (2007). Biphasic role for Wnt/beta-catenin

signaling in cardiac specification in zebrafish and embryonic stem cells. *Proc Natl Acad Sci U S A* 104(23):9685-90.

van Amerongen, M.J., Engel, F.B. (2008). Features of cardiomyocyte proliferation and its potential for cardiac regeneration. *J Cell Mol Med* 12(6A):2233-44.

van Amerongen, M.J., Harmsen, M.C., Petersen, A.H., Popa, E.R., van Luyn, M.J. (2008). Cryoinjury: a model of myocardial regeneration. *Cardiovasc Pathol* 17(1):23-31.

van de Schans, V.A., Smits, J.F., Blankesteyn, W.M. (2008). The Wnt/frizzled pathway in cardiovascular development and disease: friend or foe? *Eur J Pharmacol* 585(2-3):338-45.

van Wijk, B., van den Hoff, M. (2010). Epicardium and myocardium originate from a common cardiogenic precursor pool. *Trends Cardiovasc Med* 20(1):1-7.

VENABLE, J.H., COGGESHALL, R. (1965). A SIMPLIFIED LEAD CITRATE STAIN FOR USE IN ELECTRON MICROSCOPY. *J Cell Biol* 25:407-8.

Vidovic, K., Svensson, E., Nilsson, B., Thuresson, B., Olofsson, T., Lennartsson, A., Gullberg, U. (2010). Wilms' tumor gene 1 protein represses the expression of the tumor suppressor interferon regulatory factor 8 in human hematopoietic progenitors and in leukemic cells. *Leukemia* 24(5):992-1000.

Wang, J., Greene, S.B., Bonilla-Claudio, M., Tao, Y., Zhang, J., Bai, Y., Huang, Z., Black, B.L., Wang, F., Martin, J.F. (2010). Bmp signaling regulates myocardial differentiation from cardiac progenitors through a MicroRNA-mediated mechanism. *Dev Cell* 19(6):903-12.

Wang Y, Kaiser MS, Larson JD, Nasevicius A, Clark KJ, Wadman SA, Roberg-Perez SE, Ekker SC, Hackett PB, McGrail M, Essner JJ. (2010). Moesin1 and Ve-cadherin are required in endothelial cells during in vivo tubulogenesis. *Development* 137(18):3119-28.

Wegner, M. (2010). All purpose Sox: The many roles of Sox proteins in gene expression. *Int J Biochem Cell Biol* 42(3):381-90.

Wheelan SJ, Church DM, Ostell JM. (2001). Spidey: a tool for mRNA-to-genomic alignments. *Genome Res* 11(11):1952-7.

Wheeler, D.L., Barrett, T., Benson, D.A., Bryant, S.H., Canese, K., Church, D.M., DiCuccio, M., Edgar, R., Federhen, S., Helmberg, W., Kenton, D.L., Khovayko, O., Lipman, D.J., Madden, T.L., Maglott, D.R., Ostell, J., Pontius, J.U., Pruitt, K.D., Schuler, G.D., Schriml, L.M., Sequeira, E., Sherry, S.T., Sirotkin, K., Starchenko, G.,

- Suzek, T.O., Tatusov, R., Tatusova, T.A., Wagner, L., Yaschenko, E.** (2005). Database resources of the National Center for Biotechnology Information. *Nucleic Acids Res* 33:D39-45.
- Wills, A.A., Holdway, J.E., Major, R.J., Poss, K.D.** (2008). Regulated addition of new myocardial and epicardial cells fosters homeostatic cardiac growth and maintenance in adult zebrafish. *Development* 135(1):183-92.
- Wixon, J.** (2000). Featured organism: Danio rerio, the zebrafish. *Yeast* 17(3):225-31.
- Wolke, U., Weidinger, G., Köprunner, M., Raz, E.** (2002). Multiple levels of posttranscriptional control lead to germ line-specific gene expression in the zebrafish. *Curr Biol* 12(4):289-94.
- Wu, S.M., Chien, K.R., Mummery, C.** (2008). Origins and fates of cardiovascular progenitor cells. *Cell* 132(4):537-43.
- Yamagishi, T., Ando, K., Nakamura, H.** (2009). Roles of TGFbeta and BMP during valvulo-septal endocardial cushion formation. *Anat Sci Int* 84(3):77-87.
- Yan Y.L., Willoughby, J., Liu, D., Crump, J.G., Wilson, C., Miller, C.T., Singer, A., Kimmel, C., Westerfield, M., Postlethwait, J.H.** (2005). A pair of Sox: distinct and overlapping functions of zebrafish sox9 co-orthologs in craniofacial and pectoral fin development. *Development* 132(5):1069-83.
- Yan, Y.L., Miller, C.T., Nissen, R.M., Singer, A., Liu, D., Kirn, A., Draper, B., Willoughby, J., Morcos, P.A., Amsterdam, A., Chung, B.C., Westerfield, M., Haffter, P., Hopkins, N., Kimmel, C., Postlethwait, J.H.** (2002). A zebrafish sox9 gene required for cartilage morphogenesis. *Development* 129(21):5065-79.
- Yi, B.A., Wernet, O., Chien, K.R.** (2010). Regenerative medicine: developmental paradigms in the biology of cardiovascular regeneration. *J Clin Invest* 120(1):20-8. doi: 10.1172/JCI40820.
- Yokoi, H., Yan, Y.L., Miller, M.R., BreMiller, R.A., Catchen, J.M., Johnson, E.A., Postlethwait, J.H.** (2009). Expression profiling of zebrafish sox9 mutants reveals that Sox9 is required for retinal differentiation. *Dev Biol* 329(1):1-15.
- Zdobnov, E.M., Apweiler, R.** (2001). InterProScan--an integration platform for the signature-recognition methods in InterPro. *Bioinformatics* 17(9):847-8.
- Zelarayan, L., Gehrke, C., Bergmann, M.W.** (2007). Role of beta-catenin in adult cardiac remodeling. *Cell Cycle* 6(17):2120-6.

List of Publications

Schnabel, K. €, **Wu, C.C. €**, **Kurth, T.**, **Weidinger, G.** (2011) Regeneration of cryoinjury induced necrotic heart lesions in zebrafish is associated with epicardial activation and cardiomyocyte proliferation. *PLoS One* 6(4):e18503.*

*Parts of this publication were presented in the thesis

Knopf, F. €, **Schnabel, K. €**, **Haase, C.**, **Pfeifer, K.**, **Anastassiadis, K.**, **Weidinger, G.** (2010) Dually inducible TetON systems for tissue-specific conditional gene expression in zebrafish. *Proc Natl Acad Sci U S A* 107(46):19933-8.

€Authors contributed equally to this work.

Erklärung entsprechend §5.5 der Promotionsordnung

Hiermit versichere ich, dass ich die vorliegende Arbeit ohne unzulässige Hilfe Dritter und ohne Benutzung anderer als der angegebenen Hilfsmittel angefertigt habe; die aus fremden Quellen direkt oder indirekt übernommenen Gedanken sind als solche kenntlich gemacht. Die Arbeit wurde bisher weder im Inland noch im Ausland in gleicher oder ähnlicher Form einer anderen Prüfungsbehörde vorgelegt.

Die Dissertation wurde von Prof. Dr. Michael Brand, Molekulare Entwicklungsgenetik, Biotechnologisches Zentrum, Technische Universität Dresden, in der Arbeitsgruppe von Dr. Gilbert Weidinger am Biotechnologischen Zentrum, Technische Universität Dresden, betreut und im Zeitraum vom 01/07 bis 04/11 verfasst.

Meine Person betreffend erkläre ich hiermit, dass keine früheren erfolglosen Promotionsverfahren stattgefunden haben.

Ich erkenne die Promotionsordnung der Fakultät für Mathematik und Naturwissenschaften, Technische Universität Dresden an.

.....

Datum, Unterschrift

Acknowledgements

In first place, I would like to thank my supervisor Dr. Gilbert Weidinger for the opportunity to work on this very interesting heart project, for supporting me throughout the time of my PhD thesis also with helpful discussions, the possibility to attend conferences and to learn in Ken Poss' laboratory (Duke University; USA).

I am very thankful to Prof. Dr. Michael Brand and Prof. Dr. Evelin Schröck for reviewing my thesis.

Special thanks go to our collaboration partners Herman Spaink from the University of Leiden (Netherlands) for creation of customized zebrafish microarrays, Bianca Habermann and Charles Richard Bradshaw from the MPI Bioinformatics Facility for help with statistical analysis of gene expression and to Julia Jarrells and Britta Schilling from the microarray DNA facility (MPI-CBG Dresden) for their help with microarray analysis. I would also like to thank Ramu Chenna from the Biotec bioinformatics facility for statistical analysis of certain long term heart regeneration experiments and Thomas Kurth for electron microscopy experiments.

Many thanks also to the Biotec facilities: the microscopy facility for technical advice, the fish facility for great fish care and the histology facility for great work – all facilities were a great help on the way to the results!

Furthermore, I would like to thank the present and former members of the Brand laboratory for helpful discussions, material and for their help with methods. In particular, I would like to thank Jan Kaslin for the Sox9 project, Stefan Hans, Anja Machate, Nadine Galfe, Julia Ganz for in situ hybridization probes – and all of you for having always time and patience to answer my questions and for useful discussions! Many thanks also to Christian Bökel for great antibody-staining discussions.

Thanks to the present and former members of the Weidinger lab for a great working atmosphere, comments and help. Especially, I would like to thank Chi Chung Wu for working with me on the cryoinjury project and for useful discussions. Many thanks to Günes, Franzi and Gilbert for critically reading my manuscript! Thanks to Christa and Katja, who did a great job in organizing the lab and to the students Franziska, Kathleen and Jule for help with lab work. Special thanks go Franzi for being a great friend and motivating discussions during the last years!

Ich danke meiner Familie und der Familie meines Partners für ihre Unterstützung und Zuspruch während der letzten Jahre.

Im Besonderen möchte ich meinem lieben Partner Björn Fischer für seine fortwährende Unterstützung, seine große Geduld und sein Verständnis - einfach für Alles - von ganzem Herzen danken!